Plasmas-Laser et applications vers le biomédical

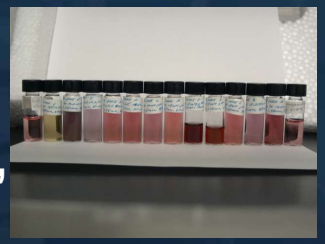

M. Sentis

LP3 : J. Herman, S. Noel, L. Mercadier, A. Kabashin, P. Blandin, ...

CiNAM : W. Marine

LHuC : T. Itina

INRS (Canada) : JC Kieffer and co-authors

INFLPR (Roumanie) : I. Mihalescu, M. Dinescu

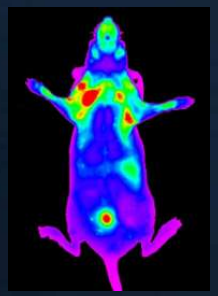

Et beaucoup d'autres!

Aix-Marseille University, CNRS, LP3 UMR 7341, 13288 Marseille, France

Summary

~10^{10} W/cm^2

✓Few words on pulsed laser matter interaction.

✓Laser Plasma produced at moderate intensity

- Bio thin films produced by PLD
- Nanoclusters for imaging and therapy
- LIBS for biomedical applications

✓Laser Plasma : X-ray source

- Phase contrast imaging

✓Laser Plasma : Proton source

- Proton therapy
- Isotopes for TEP

~10^{22} W/cm^2

Parameters of laser matter interaction

Important issues:

☞ laser beam

*** wavelength
*** intensity
*** pulse duration, τ_L
** beam quality
* time and spatial fluctuations

☞ material parameters

absorption coefficient, α
heat conductivity, D
heat capacity
heat of melting
heat of evaporation
roughness

☞ ambient environment

Air, inert or reactive gas, liquid

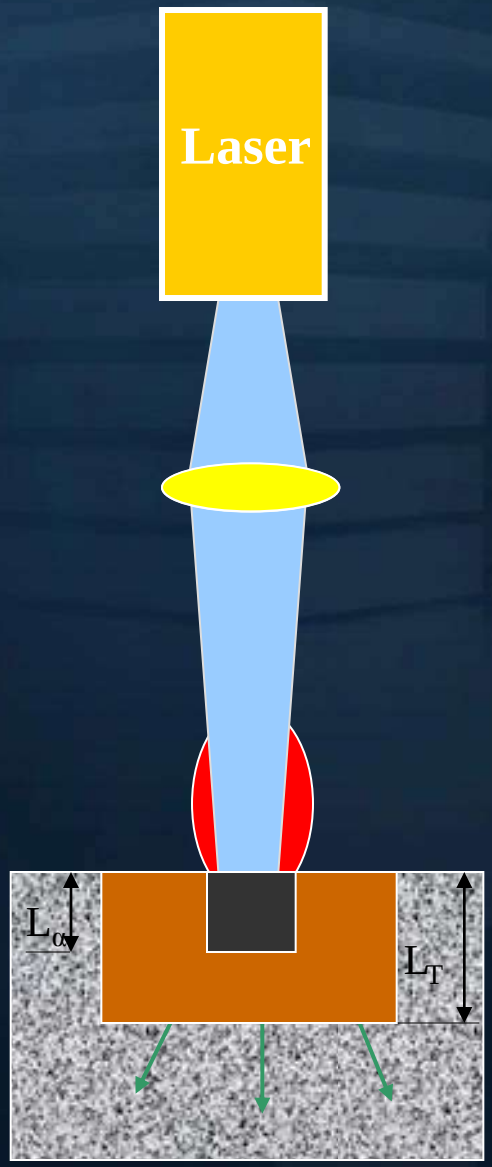

$L_\alpha = \alpha^{-1}$ optical penetration depth

$L_T \sim (D\,\tau_L)^{1/2}$ thermal diffusion length ($\tau_L > 1$ps)

dynamic processes

non-equilibrium phase transformations
liquid phase
surface tension
viscosity
vapor phase
vapor density
electron density
temperature gradient
plasma absorption
scattering

Les régimes d'interaction laser-matière

$$I = E/(S \times \tau)$$

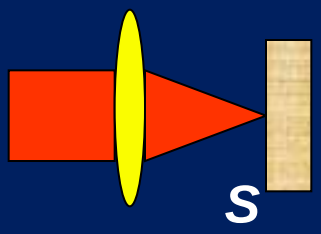

E = energie

τ= durée de l'impulsion

S = tache focale

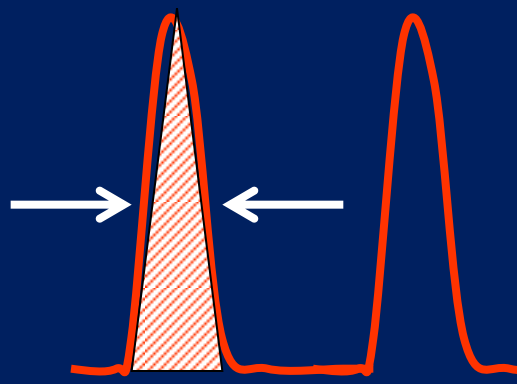

Diffusion

10^3 W/cm^2

Ablation

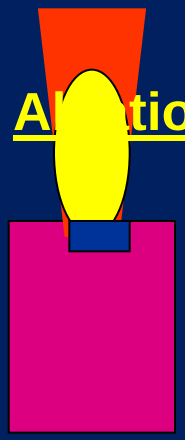

Production X

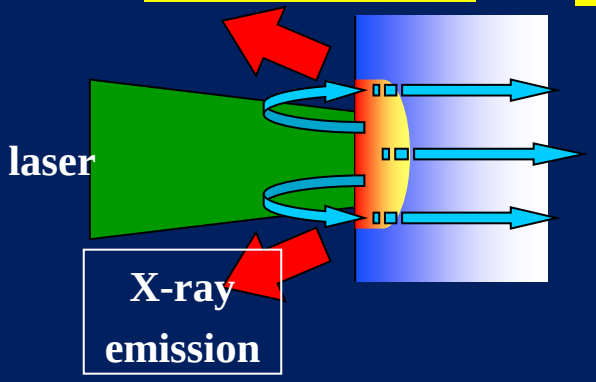

Production de proton

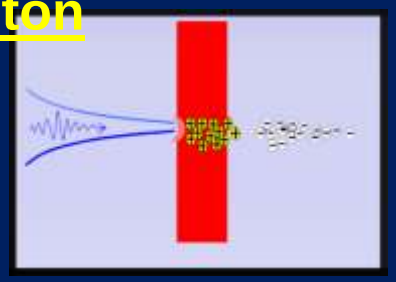

10^{22} W/cm^2

1 fs = 10^{-15}s - 1 ps = 10^{-12}s

Propriété de focalisation de l'émission LASER

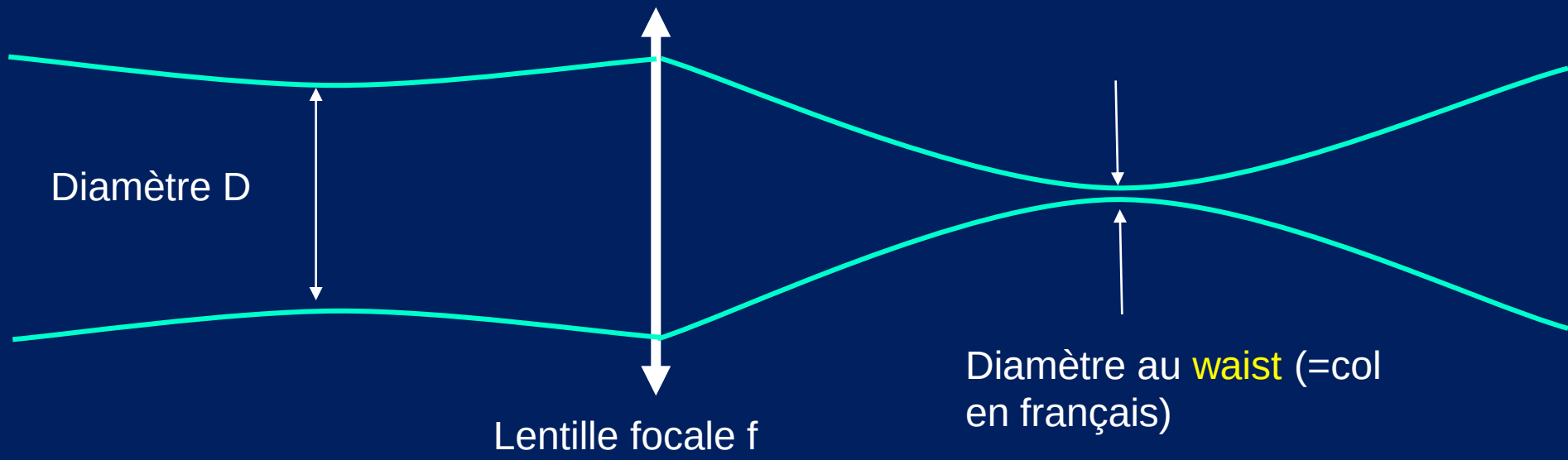

$$\Phi \approx \lambda f / \pi D$$

<u>Ordre de grandeur</u> : si f ~ D → Φ ~ λ

Focalisation sur des très petites dimensions (surface min ~ λ^2)

→ Conséquence de cette concentration dans l'espace : **Densités de Puissance énormes** !

<u>Ordre de grandeur</u> : laser 10 W à λ = 500 nm (vert) : densité de puissance max au waist (=Puissance/surface) = $10/(0{,}5.10^{-6})^2$ = **4 GW/cm²**

Les Lasers une course vers les très hautes intensités

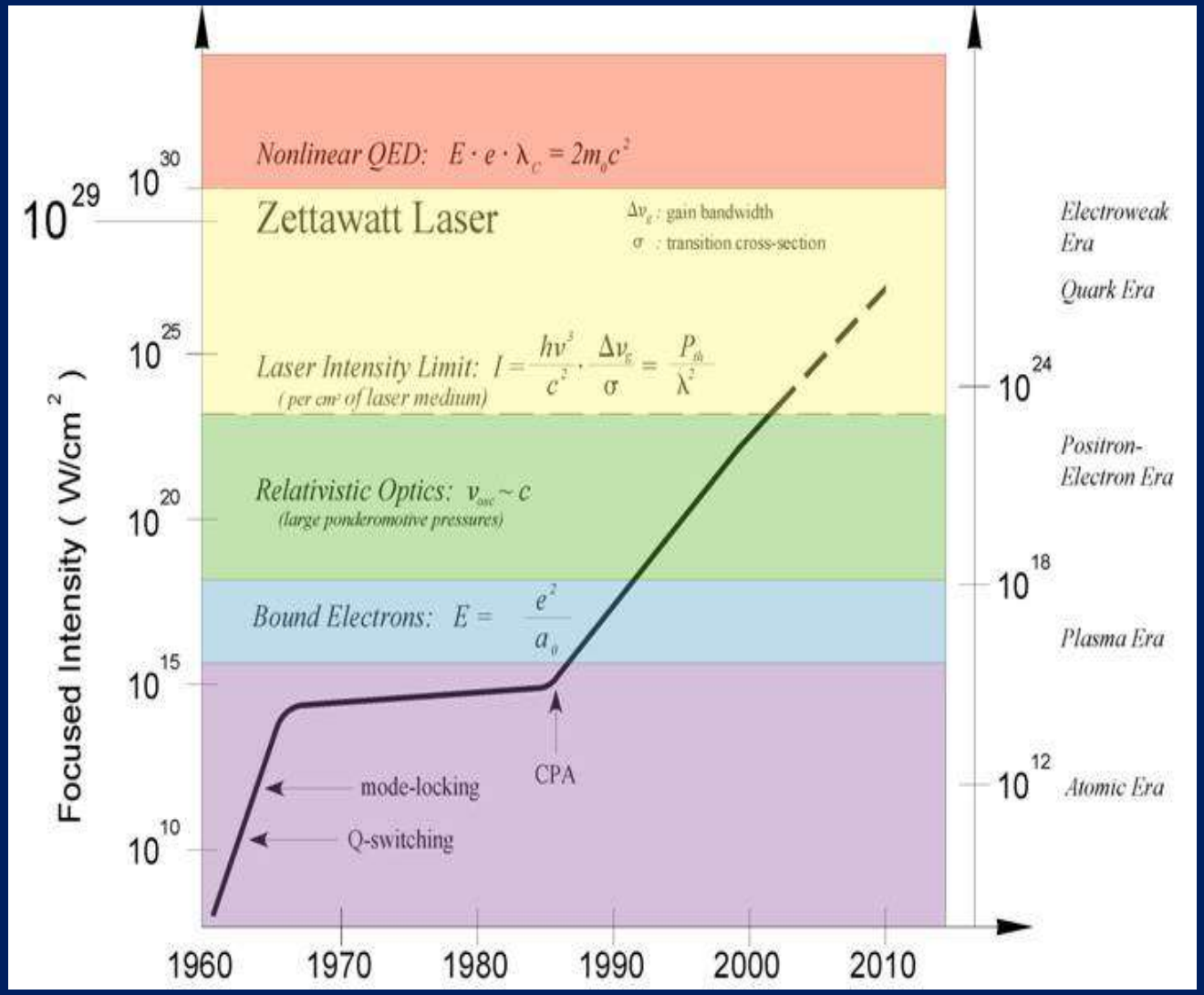

Zetta : 10^{21}

Exa : 10^{18}

Peta : 10^{15}

Tera:10^{12}

Giga : 10^{9}

1985 Le concept

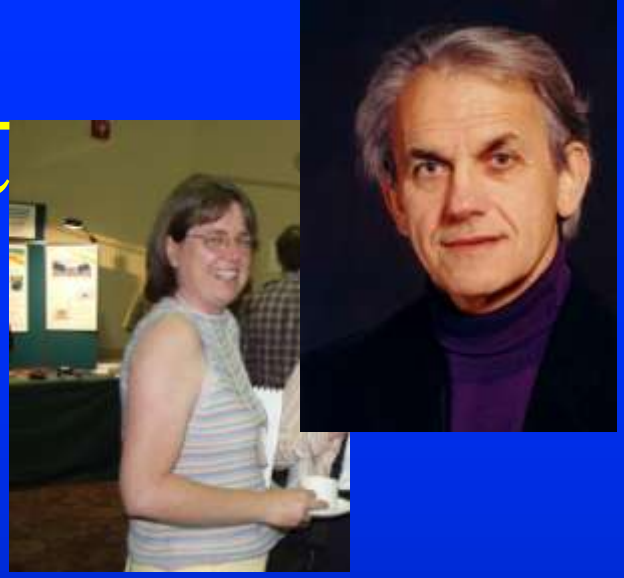

fs oscillateur

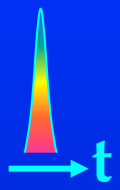

étireur

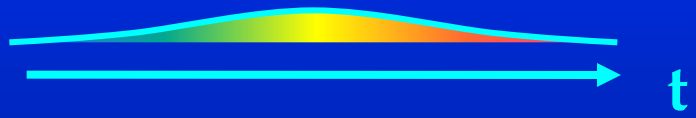

amplificateur

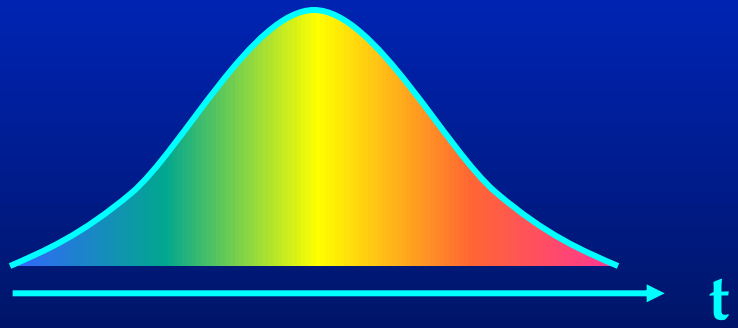

compresseur

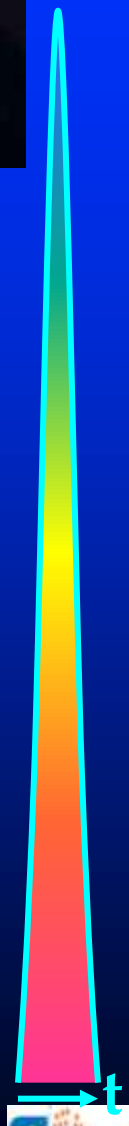

Strickland & Mourou, Opt. Comm. 56, 219, (1985)

Quelques grandeurs caractéristiques

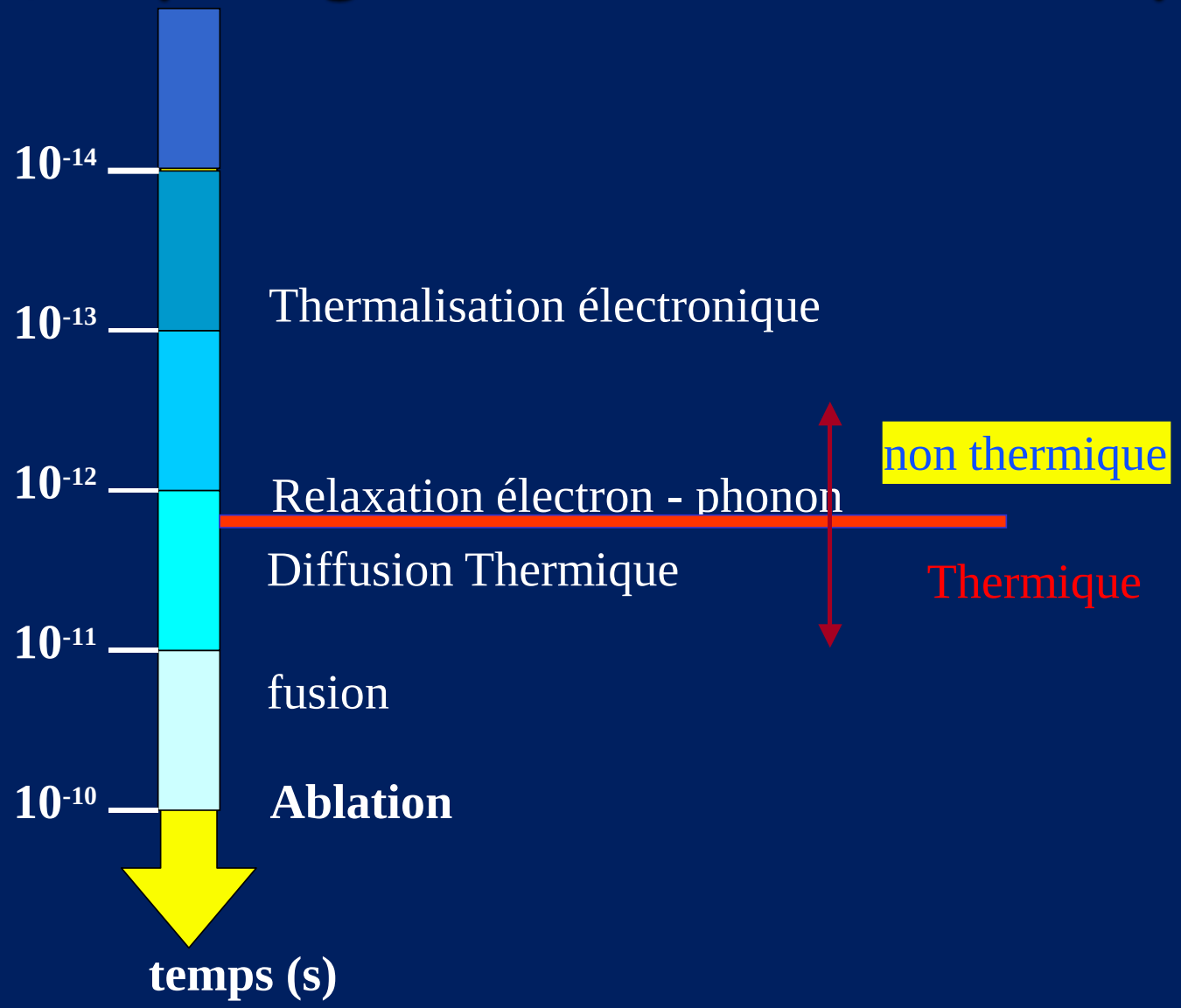

Zepto : 10^{-21}

Atto : 10^{-18}

Femto : 10^{-15}

Pico : 10^{-12}

Nano : 10^{-9}

Sources laser : cw, impulsionnels (ms, µs), courts (ns),ultra-courts (ps,fs, as)

How is a laser plasma formed ?

A wide range of physics is involved in laser-matter interactions:

- Absorption, reflection
- Heat transfer
- Thermodynamics (phase change)
- Plasma breakdown
- Shock waves (gas)
- Stress waves (solid)
- Laser-plasma interactions
- Gas dynamic expansion
- Atomic & molecular processes

$$\omega_P = (4\pi e^2 n_e / m_e)^{1/2},$$

$$n_c\ (\mathrm{cm}^{-3}) = 1.1 \times 10^{21}\ (1\ \mu\mathrm{m}/\lambda_{Laser})^2$$

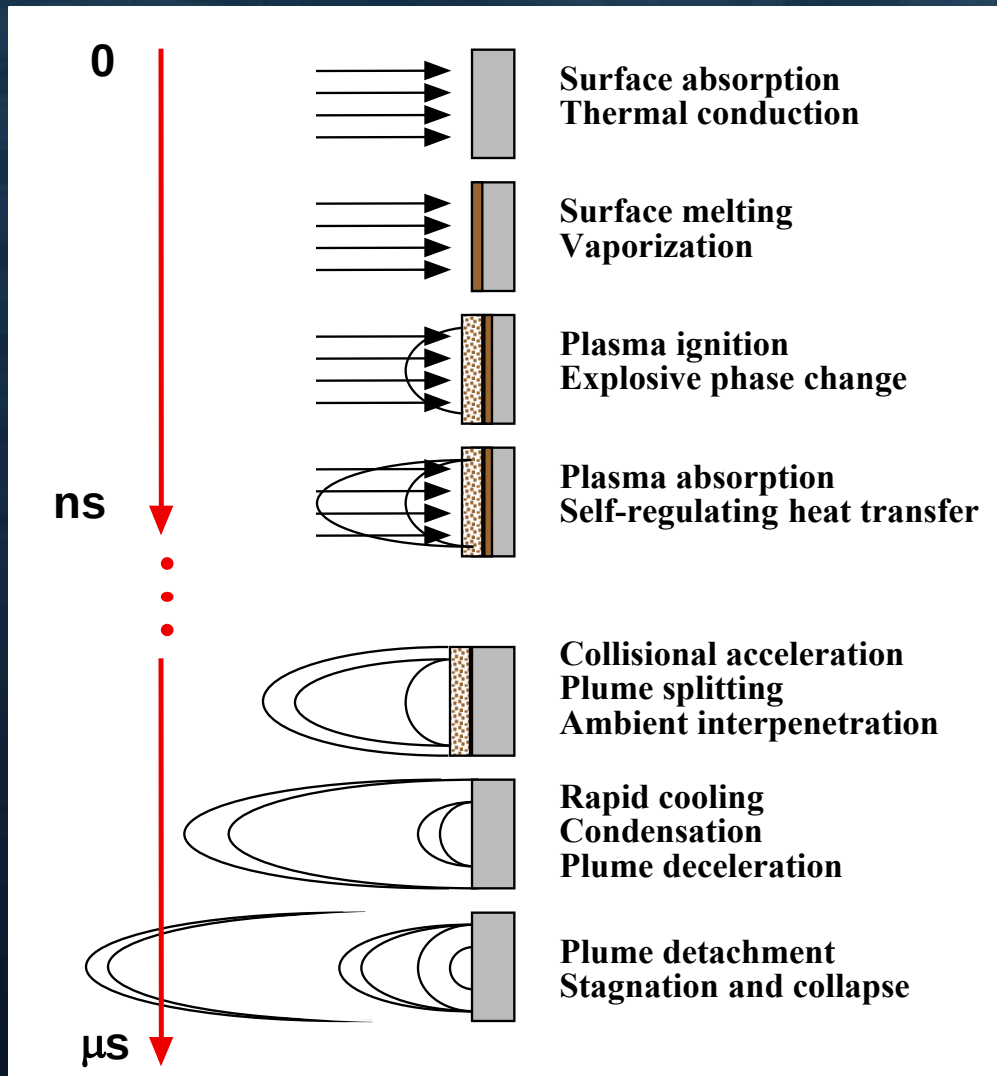

Laser Induced Plasma in gas and liquids at moderate intensities $I = 10^{11}$ to 10^{14} W/cm^2

- Biomedical thin films by P LD in gaseous media
- Nanoclusters produced by laser ablation for medical imaging and therapy
- LIBS for biomedical applications

Laser Induced Plasma in Gas : PLD

ns to fs laser pulse duration

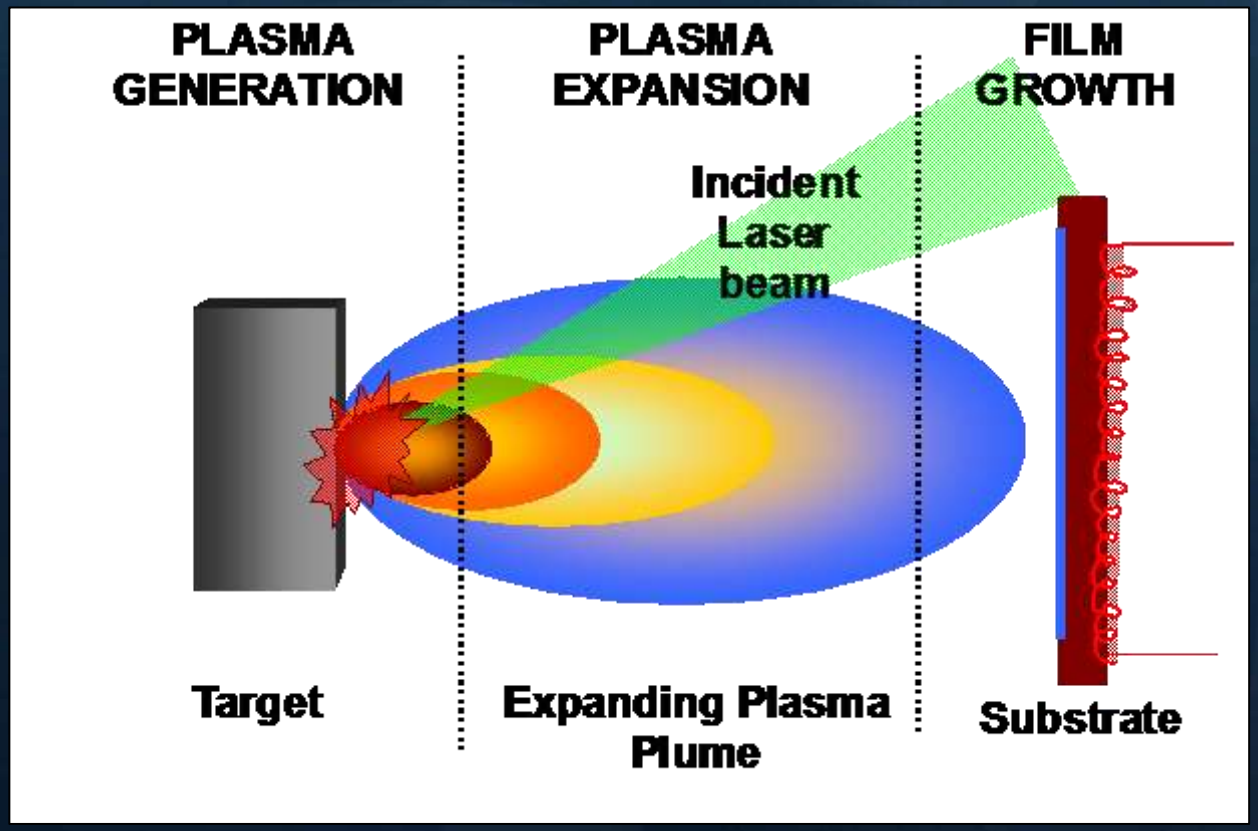

Pulsed Laser Deposition

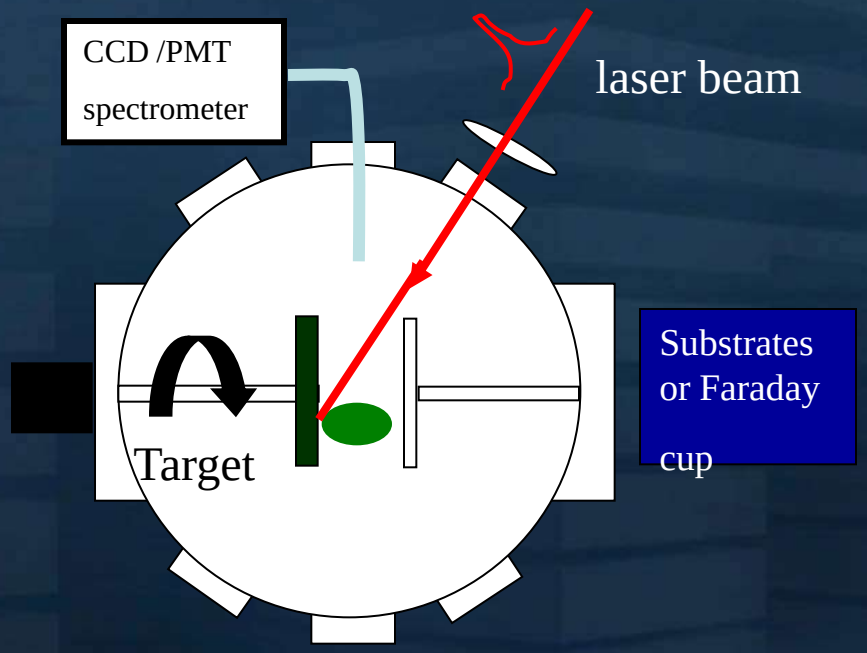

Pulsed Laser Deposition

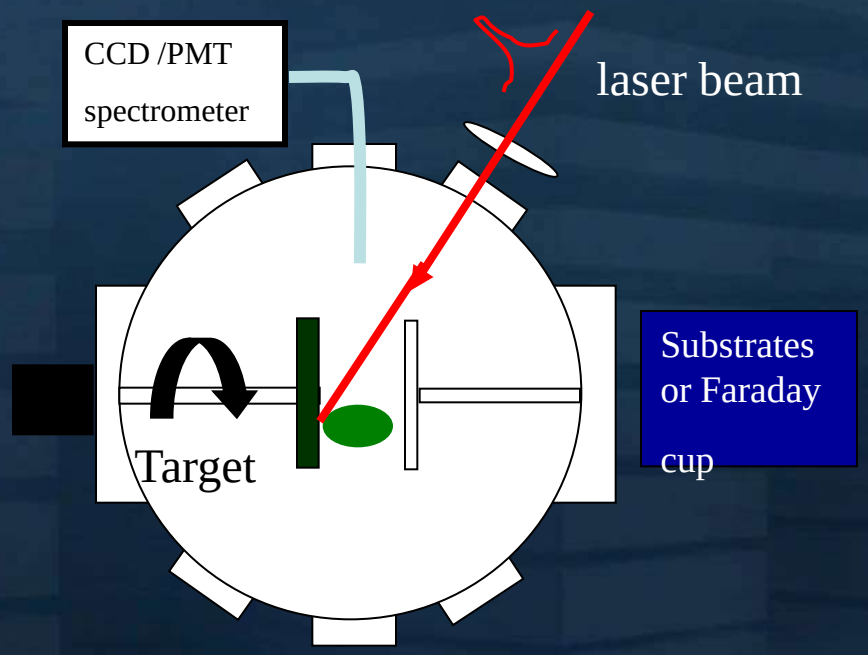

Target: Just about anything! (metals, semiconductors…)

Laser: Typically excimer (UV, 10 nanosecond pulses)

Vacuum: Atmospheres to ultrahigh vacuum

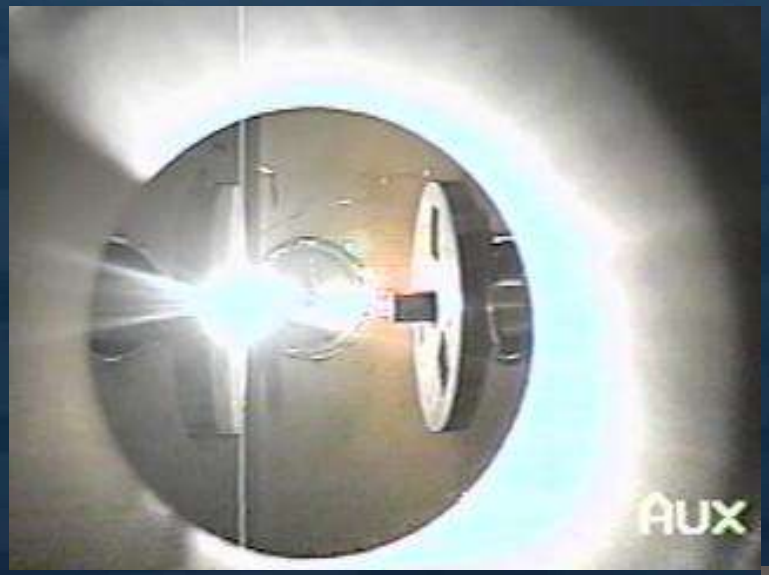
AUX

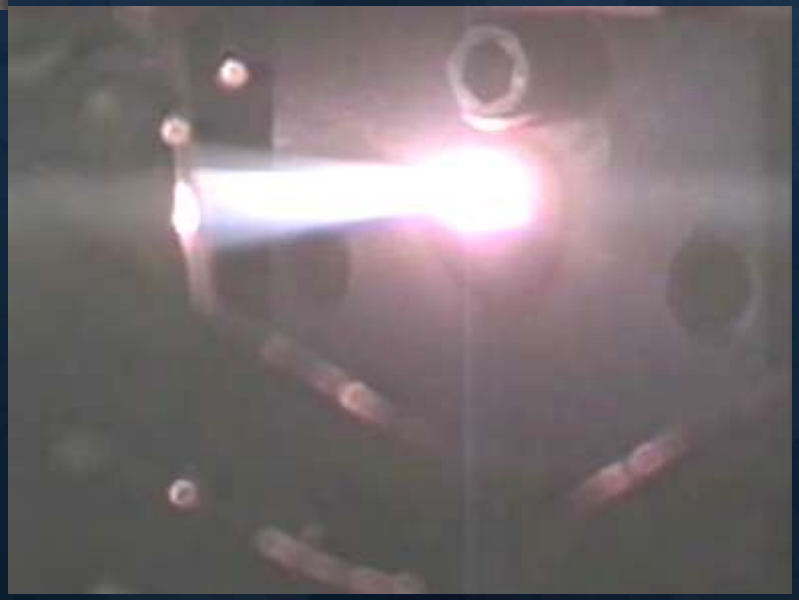

Processes in PLD

Processes in PLD

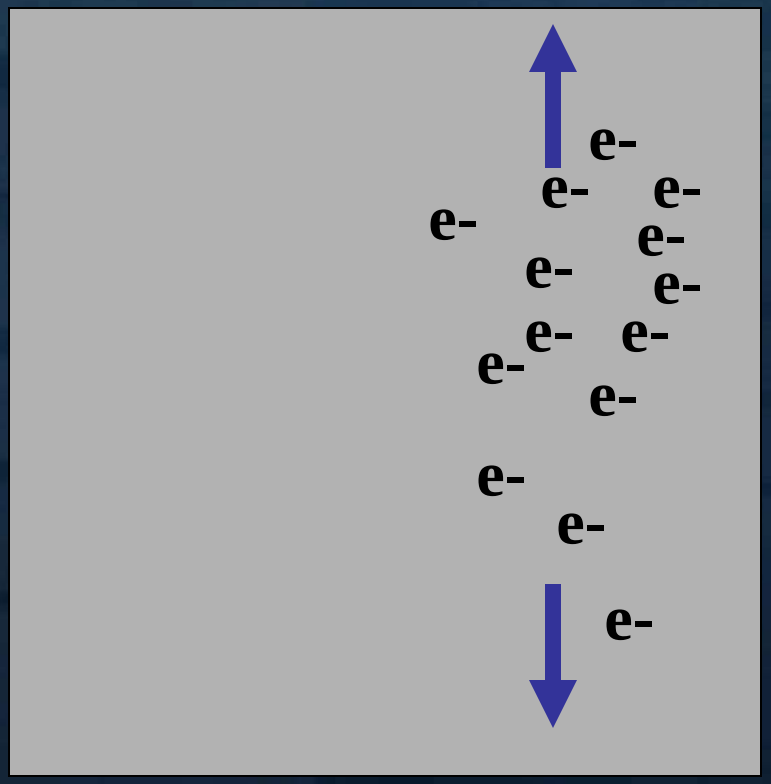

Electronic excitation

Processes in PLD

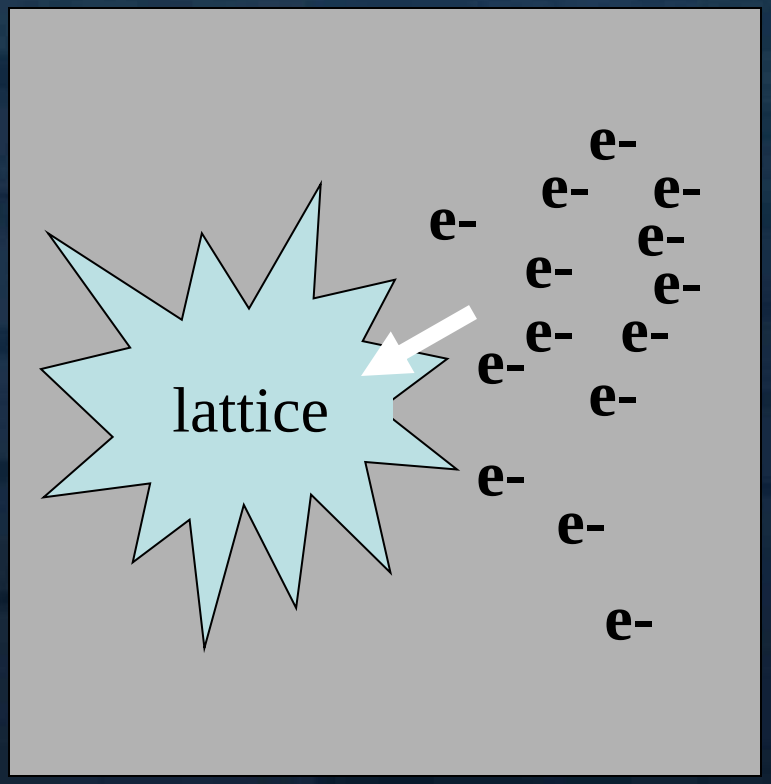

Energy relaxation to lattice (~1 ps)

Processes in PLD

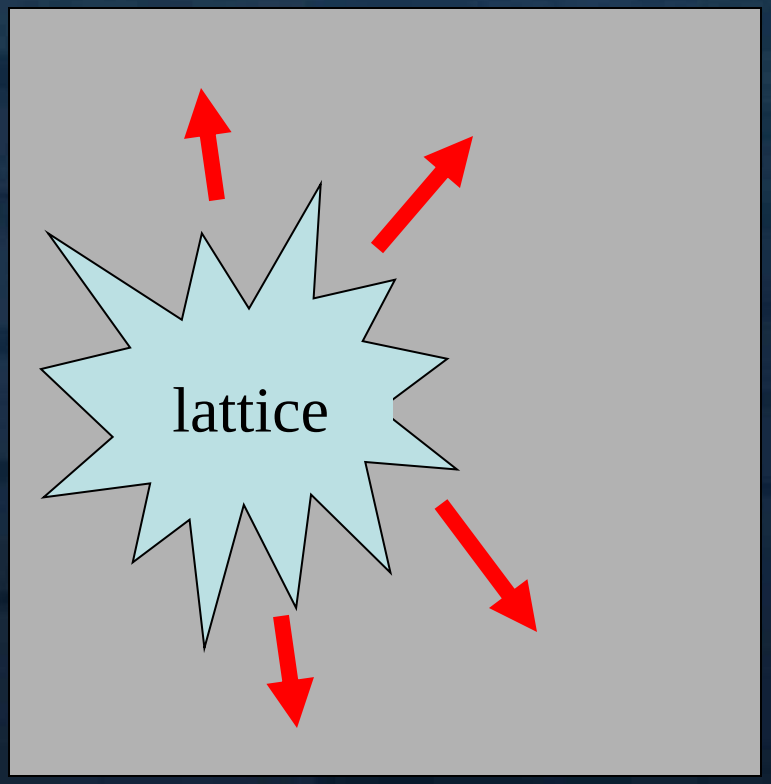

Heat diffusion (over microseconds)

Processes in PLD

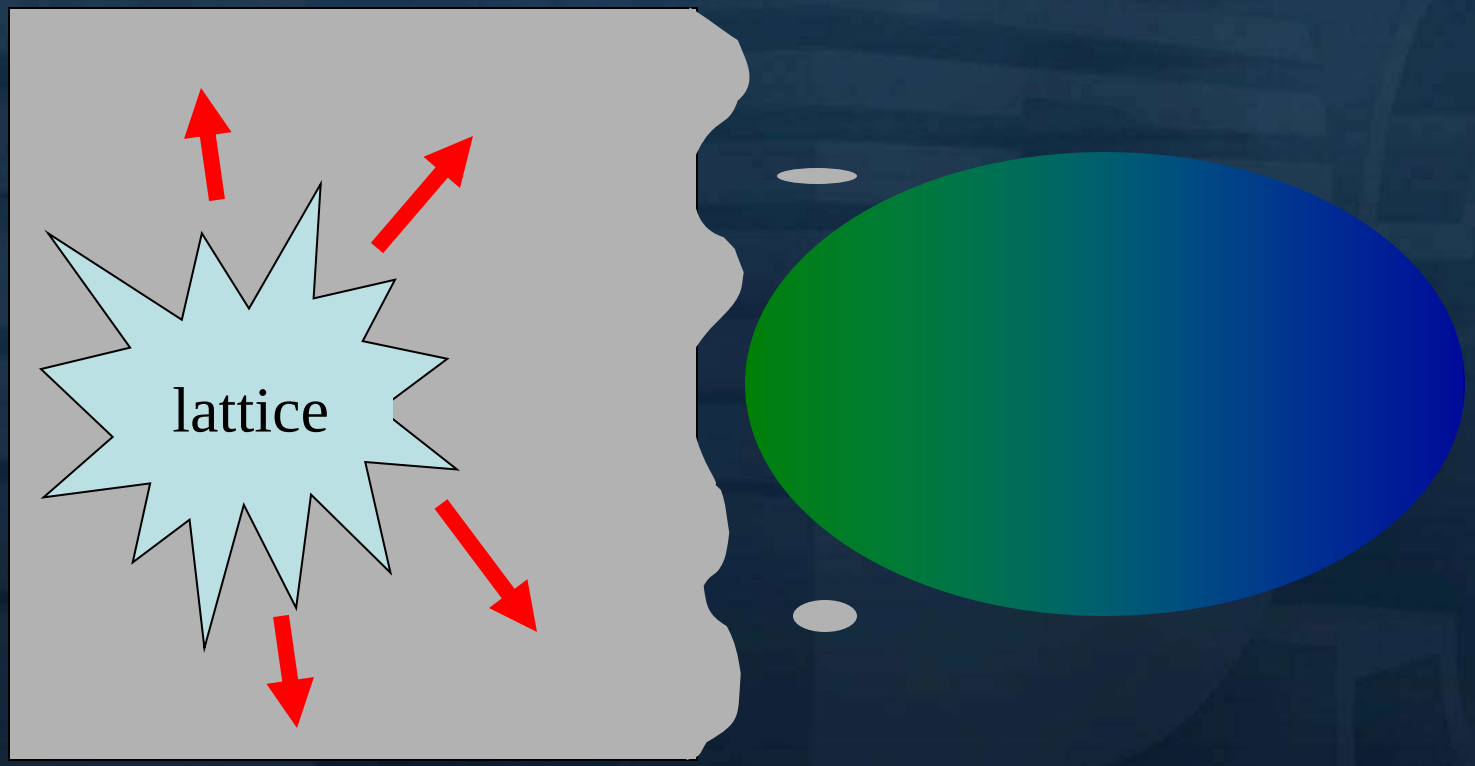

Melting (tens of ns), Evaporation, Plasma Formation (microseconds), Resolidification

Processes in PLD

If laser pulse is long (ns) or repetition rate is high, laser may continue interactions

Processes in Pulsed Laser Deposition

1. ***Absorption of laser pulse in material***

$Q_{ab}=(1-R)I_o e^{-\alpha L}$

(metals, absorption depths ~ 10 nm, depends on λ)

2. ***Relaxation of energy*** (~ 1 ps) (electron-phonon interaction)

3. ***Heat transfer, Melting and Evaporation***

when electrons and lattice at thermal equilibrium (long pulses) use heat conduction equation:

$$\rho C_p \frac{\partial T}{\partial t} = \nabla \cdot (K \nabla T) + Q_{ab}$$

(or heat diffusion model)

Initially Incredibly Non-Equilibrium!!!

- At peak of laser pulse, temperatures on target can reach $>10^5$ K (> 40 eV!)
- Electric Fields > 10^5 V/cm, also high magnetic fields
- Plasma Temperatures 3000-5000 K
- Ablated Species with energies 1 –100 eV

Why biomaterials?

- repair and reconstruction of parts of the musculo-skeletal system of vertebrates.

- minimal biological requirement: biocompatibility associated with the absence of any adverse effect (non-toxic and non-allergic).

Other requests:

- resistance to physiological fluids;

- should not interfere with the body's natural immunity system;

- withstand mechanical stress during whole lifetime;

- manufacturability in any appropriate shape.

Possible classification:

-a) *biologically inactive (inert)*: alumina, zirconia, stainless steel, CoCrNi, CoCrMo, titanium, titanium alloys, carbon, latex, PE, PMMA, …

-b) *porous*: Calcium Phosphates (CaPs), CaP-coated metal

-c) *bioactive*: dense calcium phosphate ceramics, bioactive glasses, bioactive glass-ceramics, bioactive composites, …

-d) *Resorbable*: tricalcium phosphate, calciumaliminate, polylactic acid, poly-L-acetate

Our option: biocompatible, porous and bioactive CaP

Acronym	Chemical formula	Compound name	Ca/P ratio
HA	$Ca_{10}(PO_4)_6(OH)_2$	Hydroxylapatite	1.67
FA	$Ca_{10}(PO_4)_6F_2$	Fluorapatite	1.67
CDHA	$Ca_{10-x}(HPO_4)_x(PO_4)_{6-x}(OH)_{2-x}$ $(0<x<2)$	Calcium-deficient Hydroxylapatite	1.33-1.67
BA	$Ca_{8.3}(PO_4)_{4.3}(CO_3\text{-}HPO_4)_{1.7}(OH)_{0.3}$ BA=carbonated CDHA (x=1.7)	Biological apatite	1.38-1.93
Mn-CHA	HA with (0.4-2)% Mn^{2+} and (2-6)% CO_3^{2-}	Mn^{2+} doped carbonated hydroxylapatite	1.51- 1,65
OHA	$Ca_{10}(PO_4)_6(OH)_{2-2x}O_x\square_x$ $(0<x<1)$	Oxyhydroxylapatite	1.67
OA	$Ca_{10}O(PO_4)_6$	Oxyapatite	1.67
MCPM	$Ca(H_2PO_4)_2\cdot H_2O$	Monocalcium phosphate monohydrate	0.5
MCPA	$Ca(H_2PO_4)_2$	Monocalcium phosphate anhydrate	0.5
DCPD	$CaHPO_4\cdot 2H_2O$	Dicalcium phosphate dihydrate (Brushite)	1
DCPA	$CaHPO_4$	Dicalcium phosphate anhydrate	1
OCP	$Ca_8(HPO_4)_2(PO_4)_4\cdot 5H_2O$	Octacalcium phosphate	1.33
α-TCP	$Ca_3(PO_4)_2$ (monoclinic)	Tricalcium phosphate (phase α)	1.5
β-TCP	$Ca_3(PO_4)_2$ (rhombohedral)	Tricalcium phosphate (phase β, Whitlockite)	1.5
TTCP	$Ca_4O(PO_4)_2$	Tetracalcium phosphate	2
α-DCP	$Ca_2P_2O_7$ (orthorhombic)	Dicalcium phosphate (phase α)	1
β-DCP	$Ca_2P_2O_7$ (tetragonal)	Dicalcium phosphate (phase β)	1
ACP	$Ca_x(PO_4)_y\, nH_2O$	(Amorphous Calcium pyrophosphate)	1.2-2.2

Main deficiency of CaPs : brittle in bulk

Alternative solution: Biomimetic coatings for metallic implants

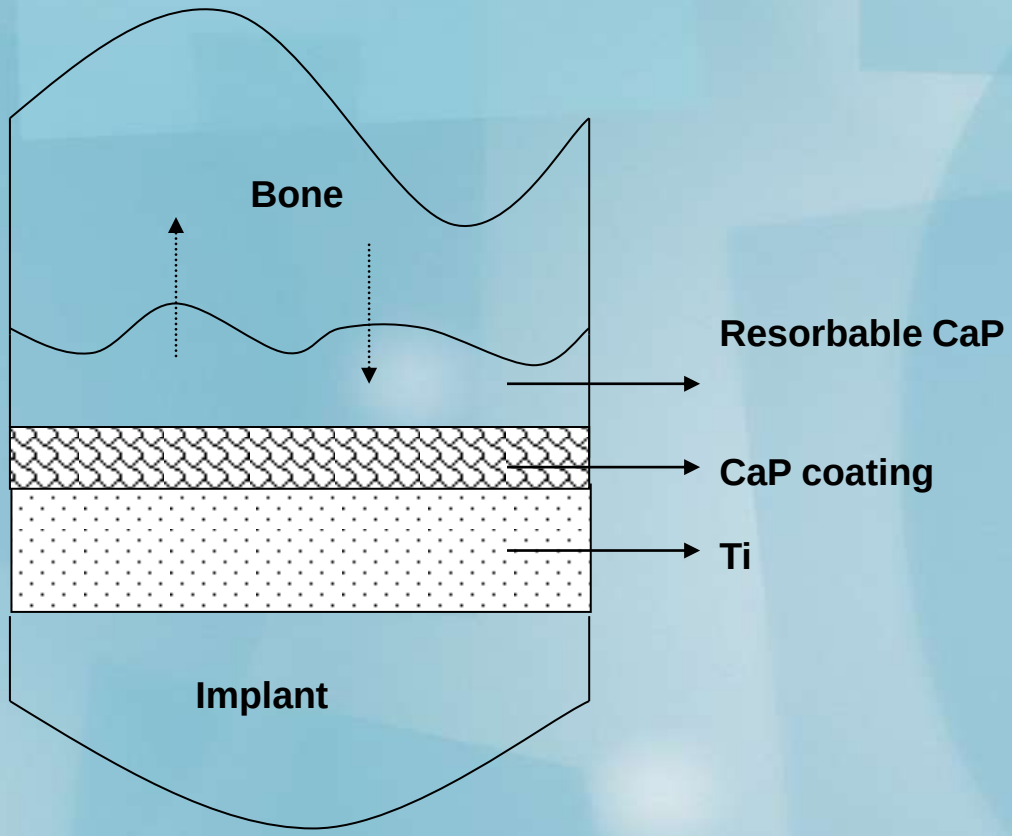

How difficult is to deposit CaPs? (1)

- very complex molecules

HA molecule : $Ca_{10}(PO_4)_6OH_2$

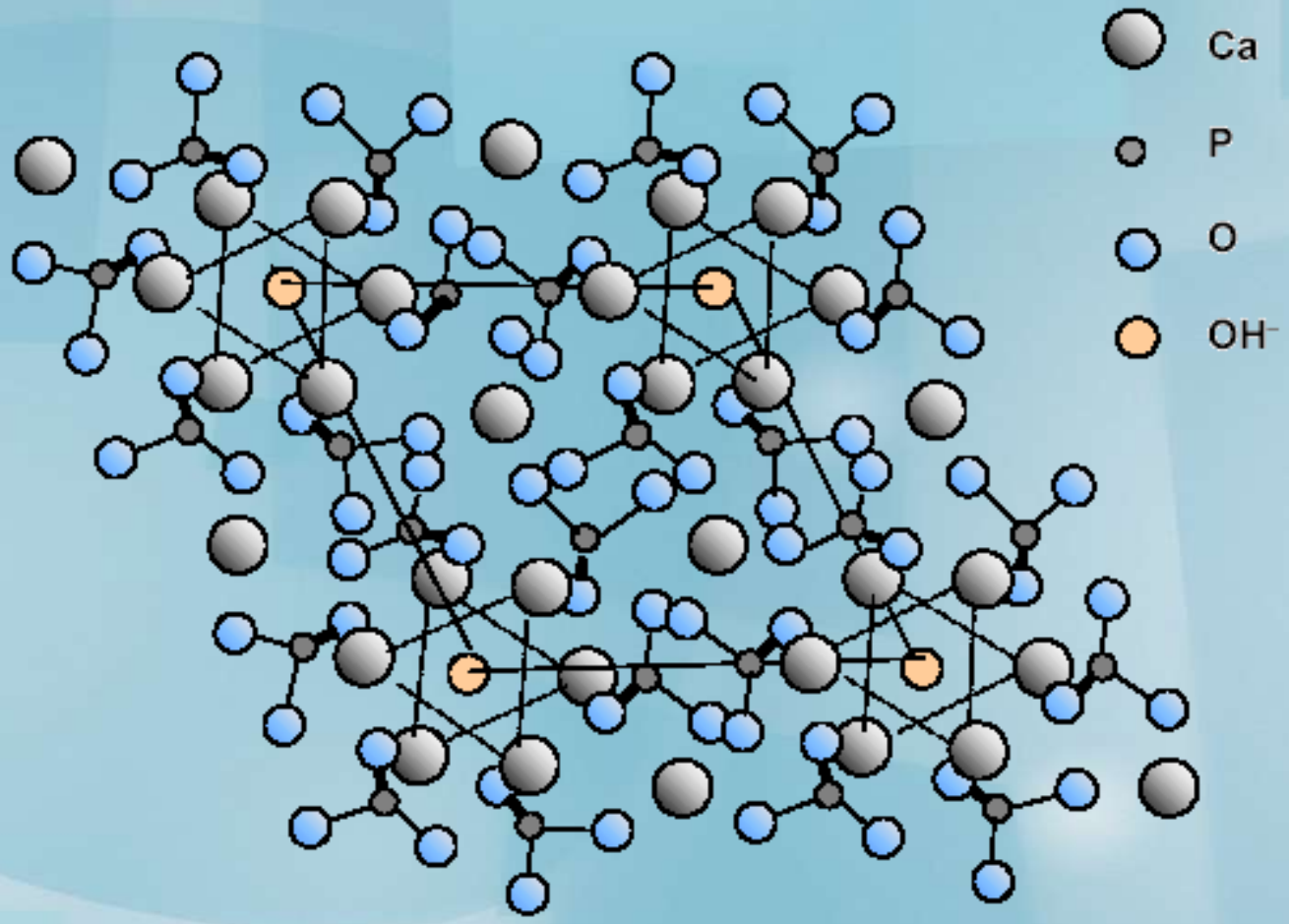

Projection in the (001) base plan of the hydroxyapatite unit cell (hexagonal structure)

How difficult is to deposit CaPs? (2)

Crystal structure of OCP projected down the c-axis

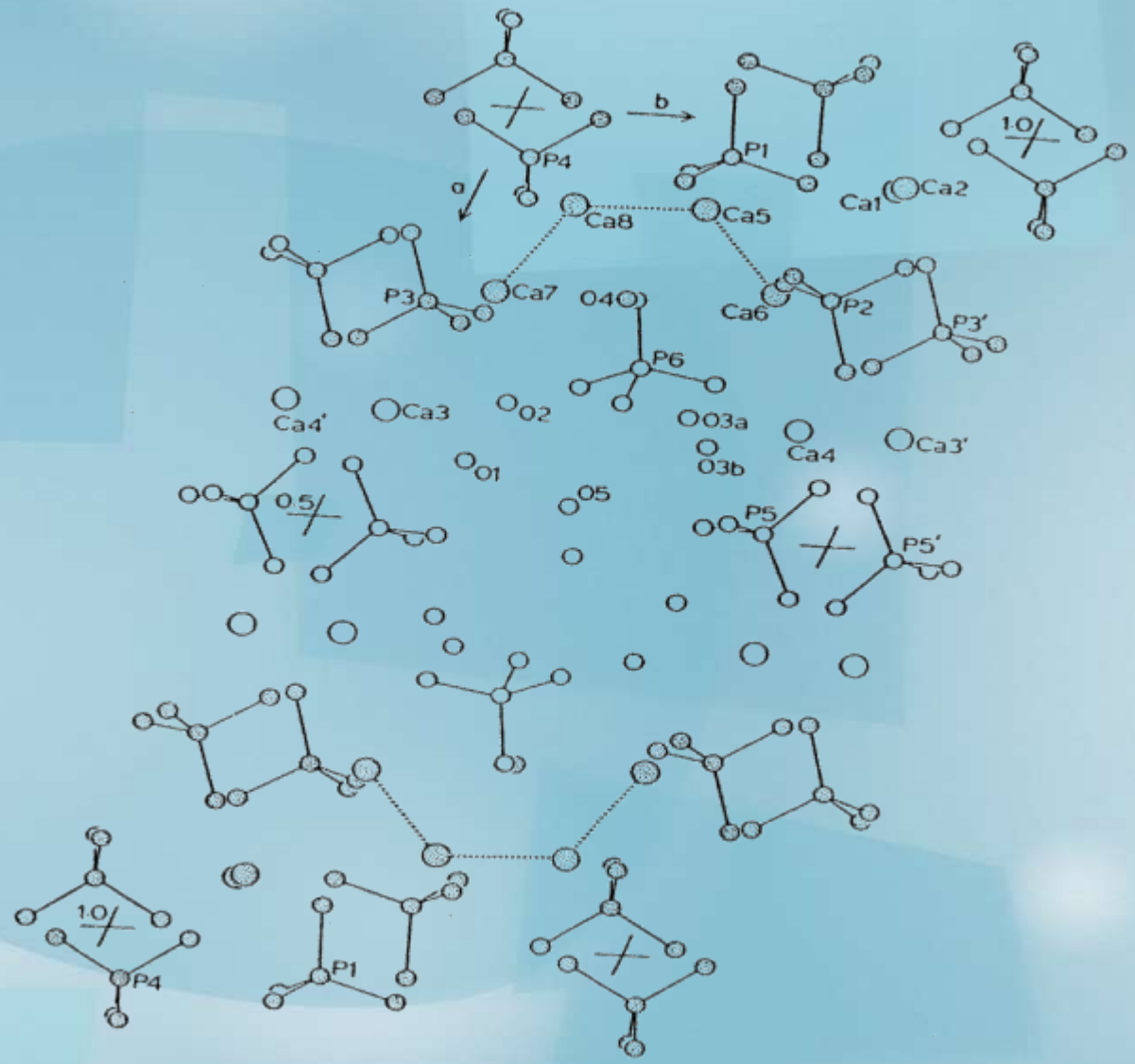

Octacalcium phosphate ($Ca_8(HPO_4)_2(PO_4)_4 \cdot 5H_2O$)

Alternating apatite- and hydrated- layers, ‖(100) planes.

The region with shaded atoms, the "**apatitic layer**", is very similar to HA.
The zone containing 10 water molecules is the "**hydrated layer**".

H atoms are omitted for clarity

Mesures par spectroscopie optique d'emission sur le plasma issu de l'irradiation laser 248 nm d'une cible d'HA pure

Présence des ions de

- calcium (Ca I et Ca II),
- oxygène (O I et O II) et
- phosphore (P II).

Émissions dues à des espèces moléculaires présentes dans le plasma.

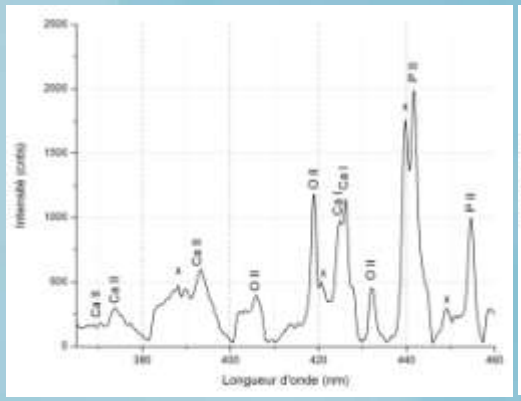

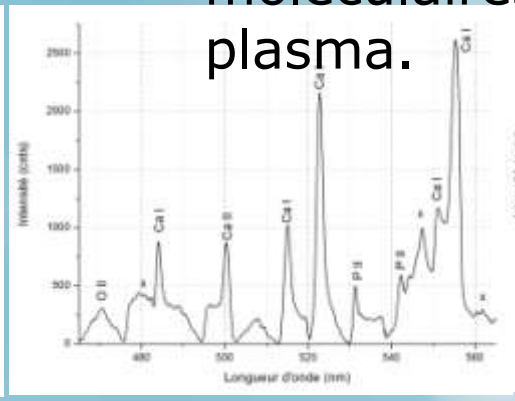

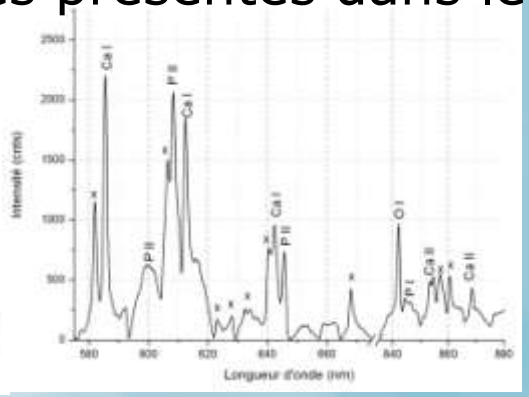

Croissance impulsion par impulsion !

Couche mince d'hydroxyapatite obtenue par ablation laser

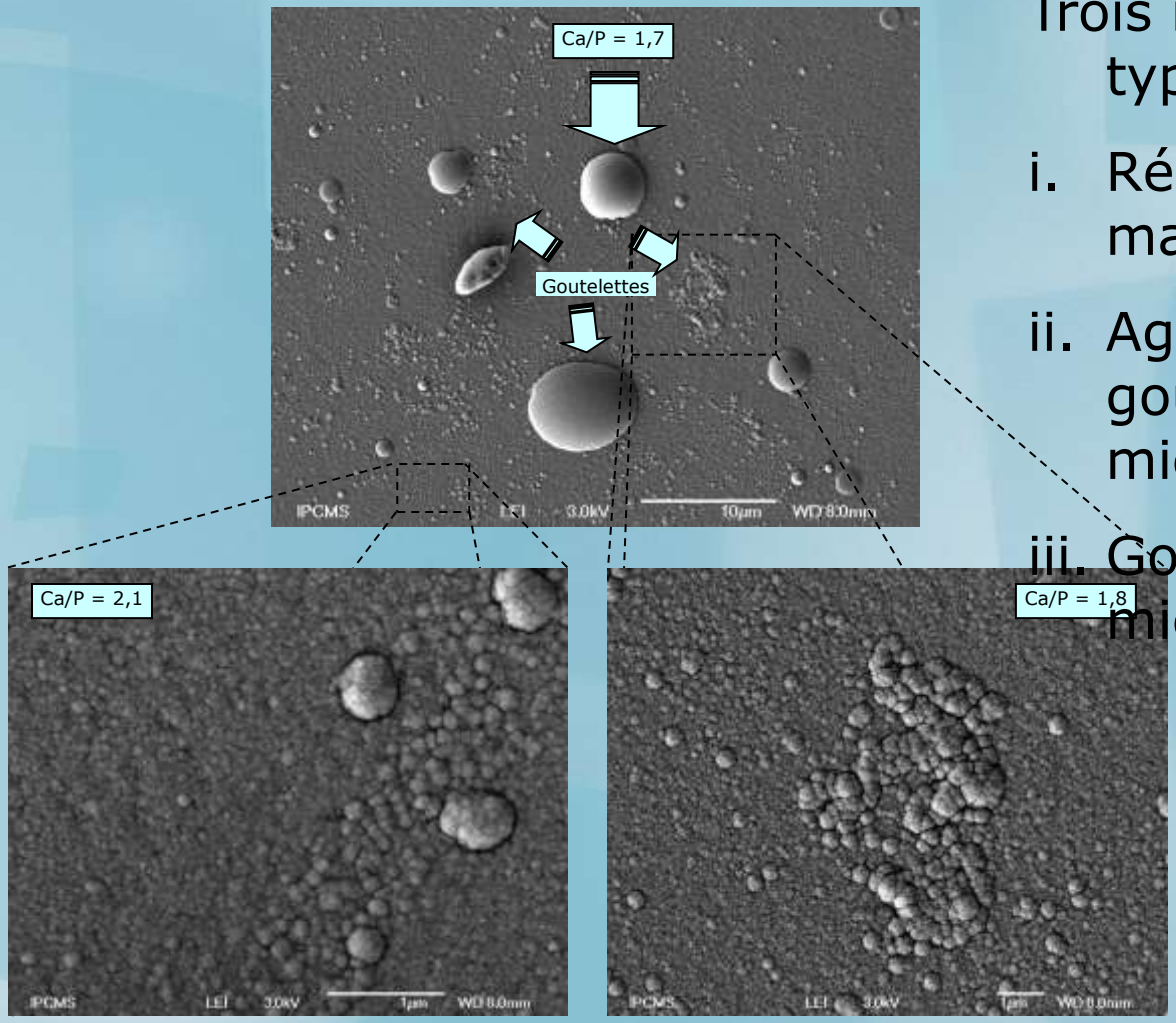

Trois régions typiques:

i. Région majoritaire lisse

ii. Agglomération de gouttelettes sub-micrométriques

iii. Gouttelettes micrométriques

Bioactivity tests

Human primary osteoblasts (hOB) were cultured on OCP coated-Ti, Mn-CHA coated–Ti, HA coated-Ti, Ti, control (polystyrene).

hOB response: SEM micrographs

- on bare Ti: (a) after 7 days, (b) after 21 days

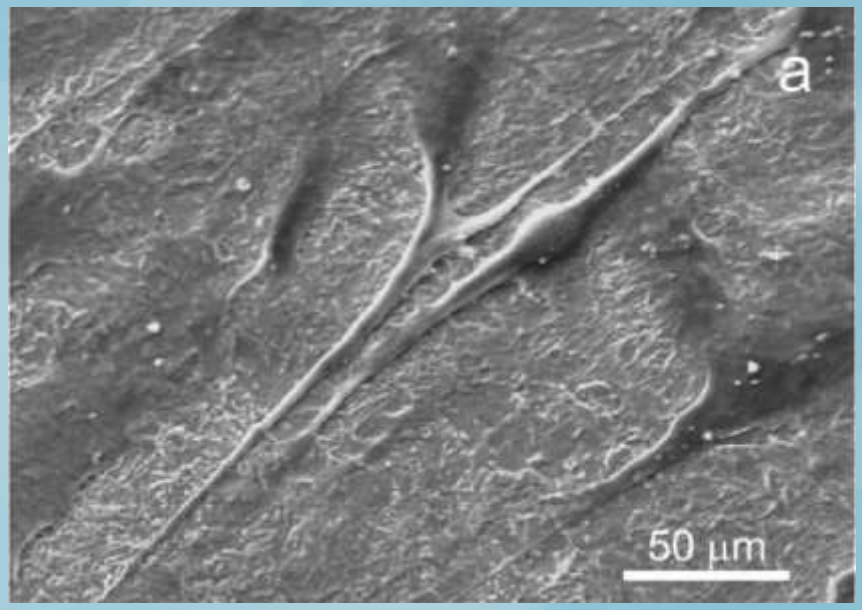

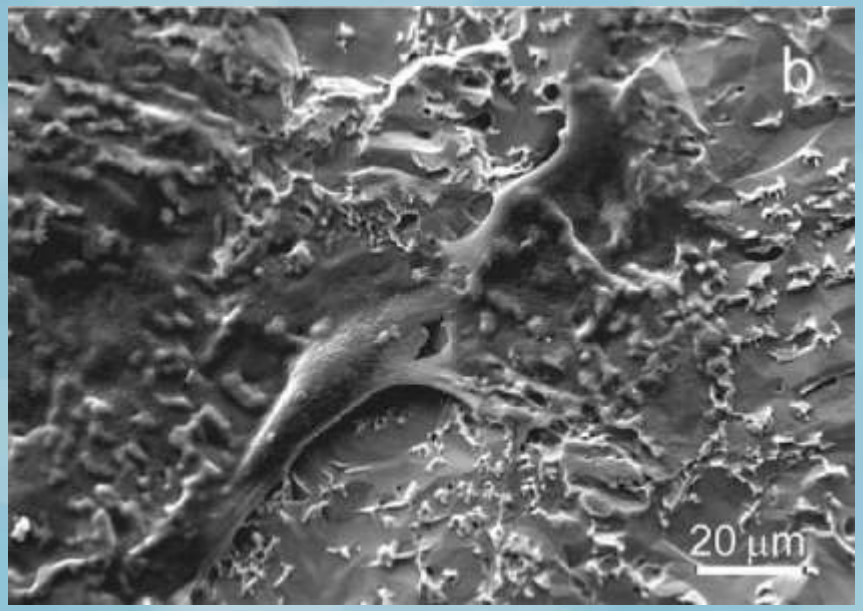

Elongated, rod-like morphology

hOB response: SEM micrographs

- **OCP coatings**: (c) after 7 days, (d) after 21 days

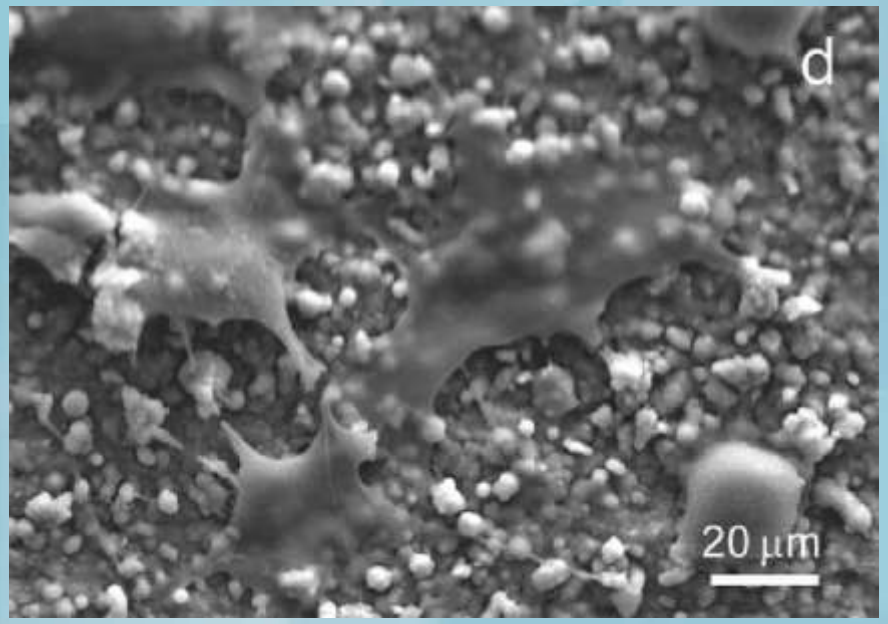

- In time cells spread and expand with flattened, polyhedral-morphology.
- Numerous cytoplasmatic extensions.

hOB response: SEM micrographs

- **Mn-CHA coatings**: (e) after 7 days, (f) after 21 days

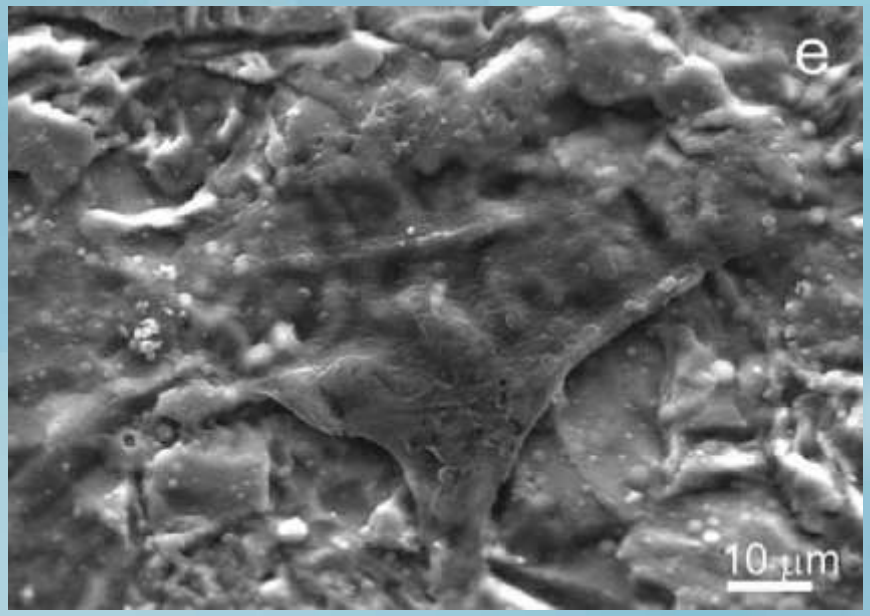

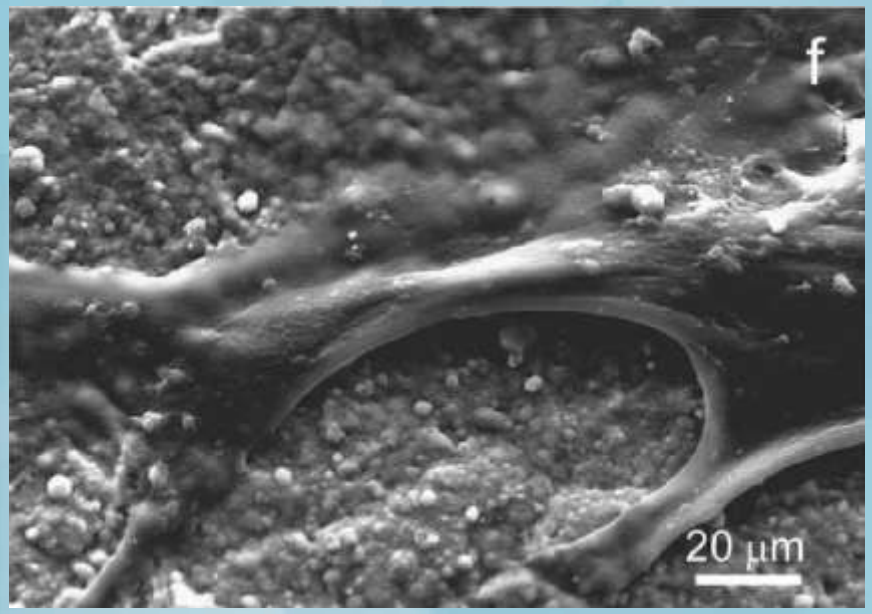

- In time cells spread and expand, with flattened, polyhedral-morphology.
- Less cytoplasmatic extensions

Dépôt de DLC par PLD femtoseconde

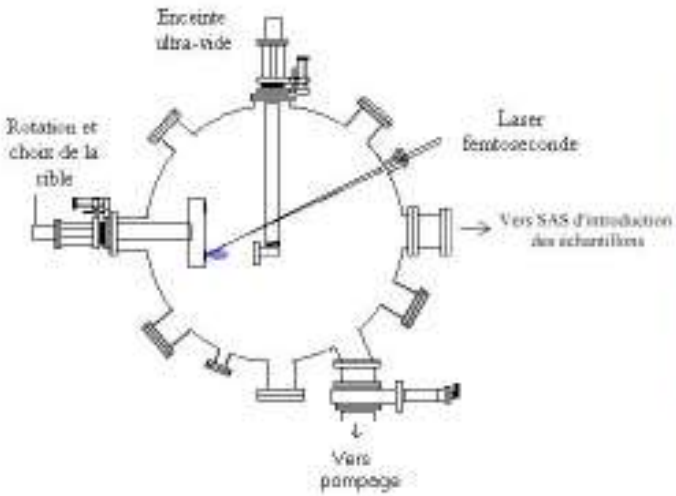

Revêtement d 'implants orthopédiques

Tête sphérique vierge

Tête sphérique revêtue d'un film de DLC après décapage ionique *in situ*

Thèse de A.-S. Loir, Saint Etienne (2004).

Biocompatible metallic thin films by PLD
Alloys: NiTinol NiTi

NiTi characteristics

- Super-Elastic Property
- Radiopaque
- Shape-Memory Effect

NiTi biomedical applications

- Tweezers for removing foreign objects via small incisions
- Anchors for tendon fixation
- Stents for cardiovascular applications
- Dentistry - Orthodontic wires, which no not need to be retightened and adjusted

PULSED LASER DEPOSITION (PLD)

Deposition chamber

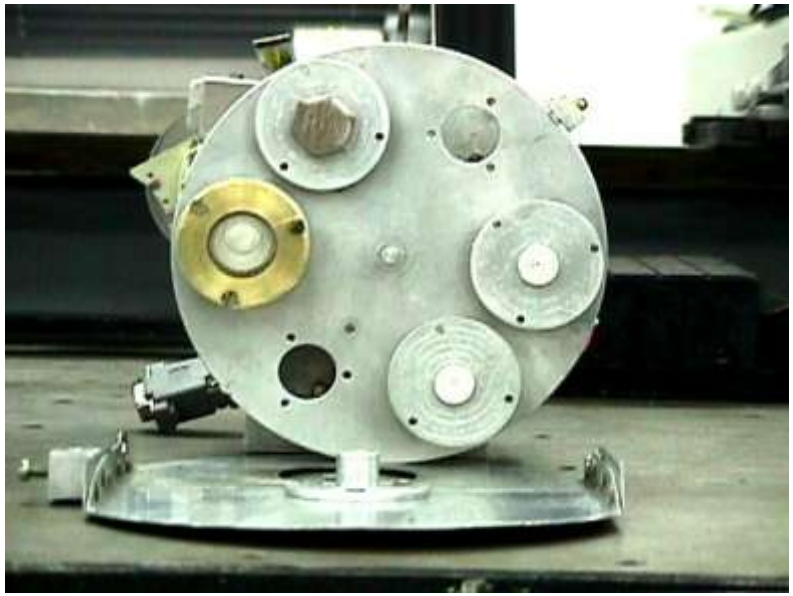

Multitarget system

SEM

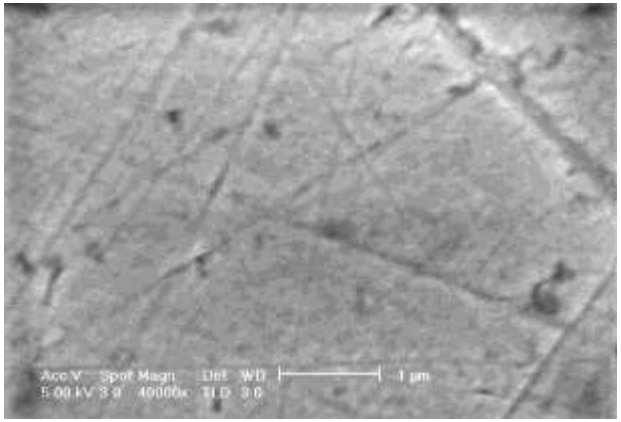

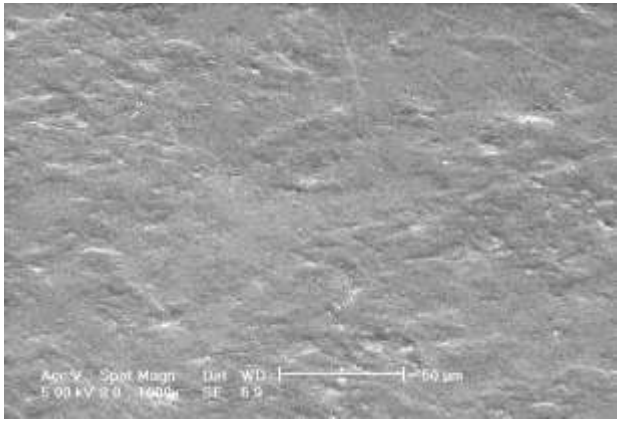

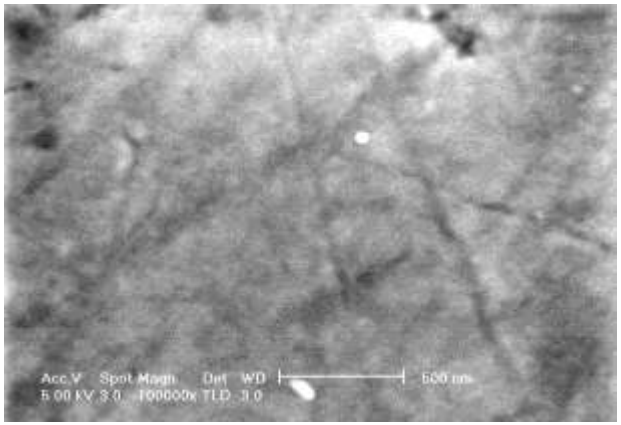

Nitinol, 30 sequences

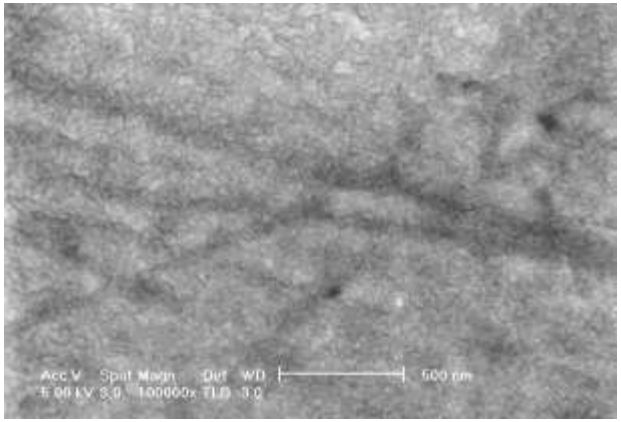

Nitinol, 20 sequences

Cytotoxicity evaluation on microorganism culture

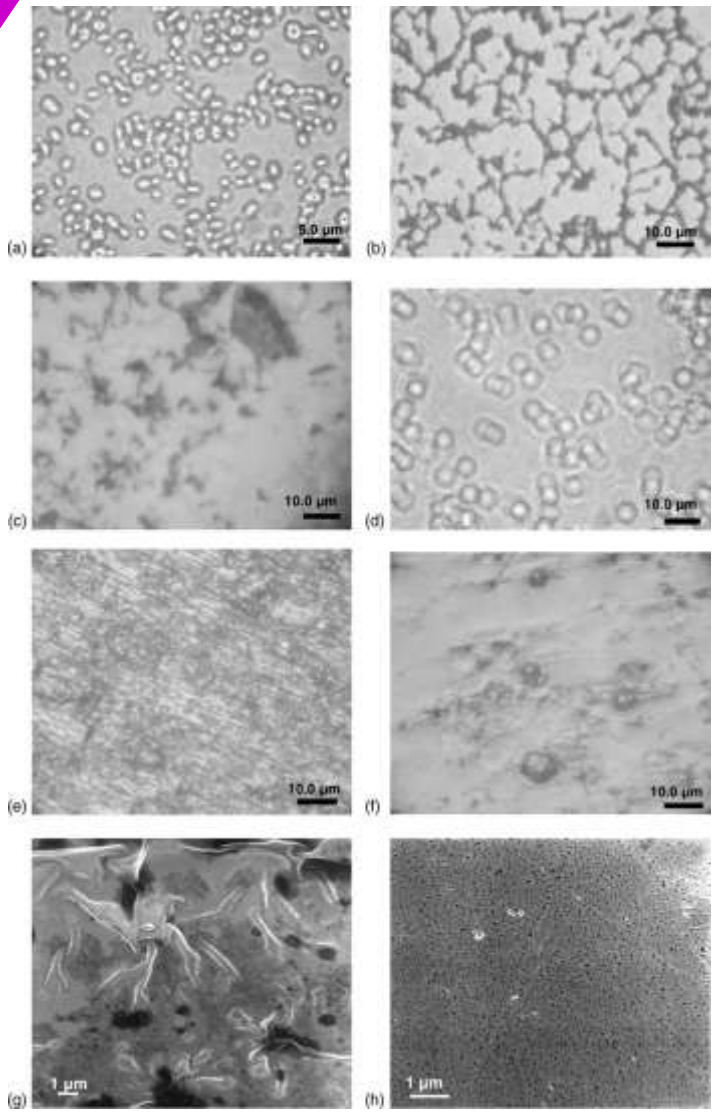

E. coli and S. cerevisiae cell cultures on the nitinol thin films.

(a) E. coli reference cell culture

(b) E. coli cell culture on Ti surface

(c) E. coli cell culture on NiTi surface

(d) S. cerevisiae references cell culture

(e) S. cerevisiae cell culture Ti surface

(f) S. cerevisiae cell culture on NiTi surface

(g) SEM on E. coli cell culture on NiTi surface

(h) SEM on S. cerevisiae cell culture on NiTi surface.

CONCLUSIONS

- **Biocompatible**
- **Low adherence of microorganism on NiTi surface:** NiTi alloy does not stimulate the development at genetic level for specific genes which are involved in adhesion processes for microorganism cells.

- **Low release of Ni ions in solutions**

MAPLE

Matrix Assisted Pulsed Laser Evaporation

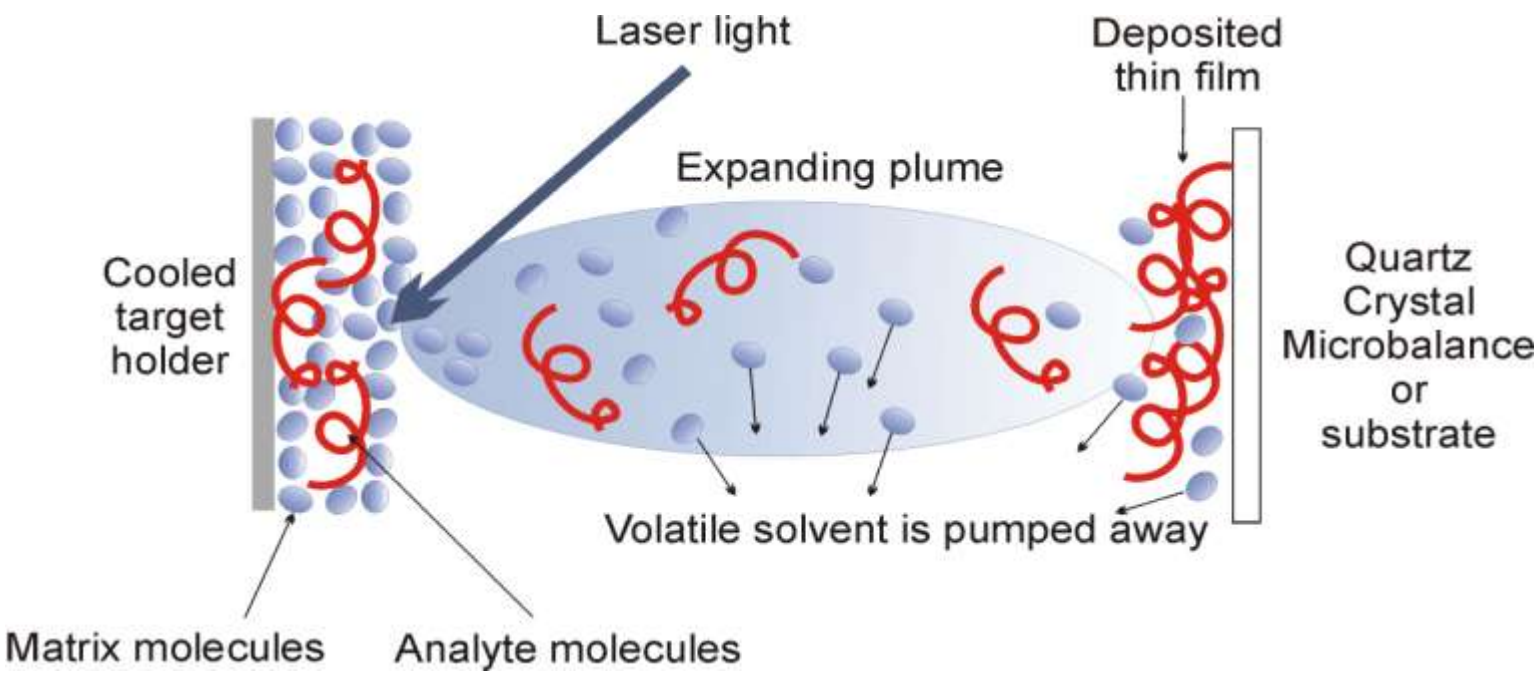

- No need for UHV
- Matrix prepared outside the chamber
- High flexibility

You can use everything you can dissolve in a solvent!

MAPLE of polymers blends with Ag nanoparticles

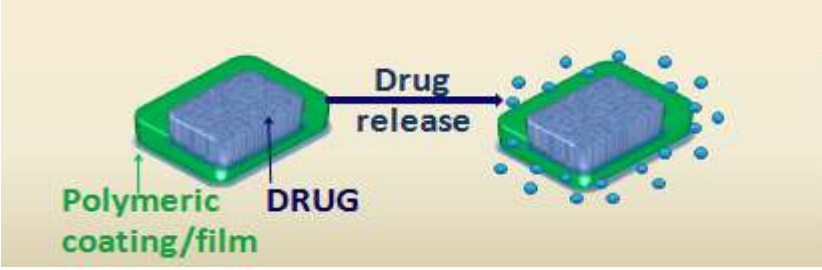

Controlled release of antibacterial agents
MAPLE deposition of PEG:PLGA films with incorporated silver nanoparticles (AgNPs)

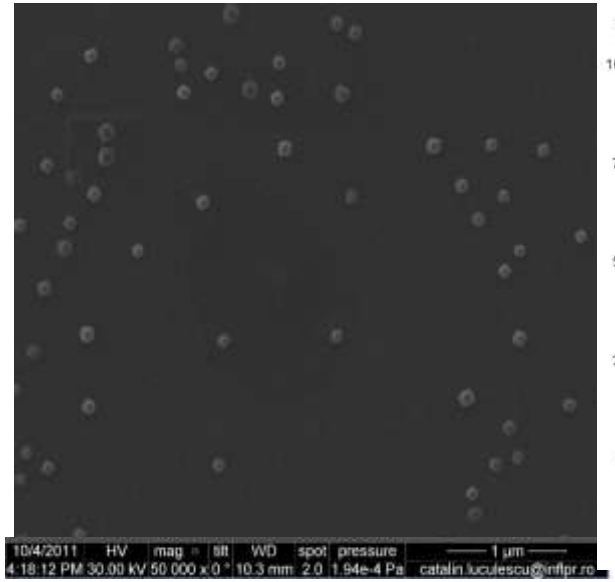

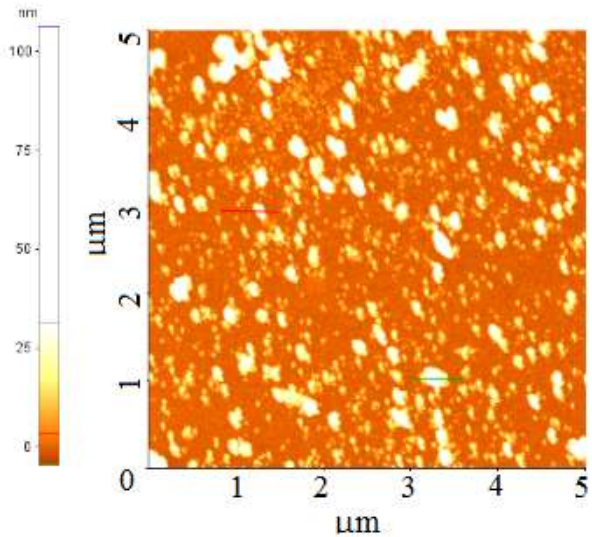

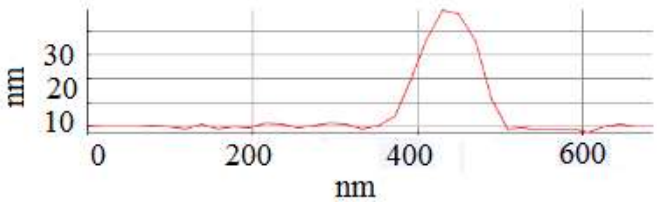

Antibacterial efficiency against E. Coli

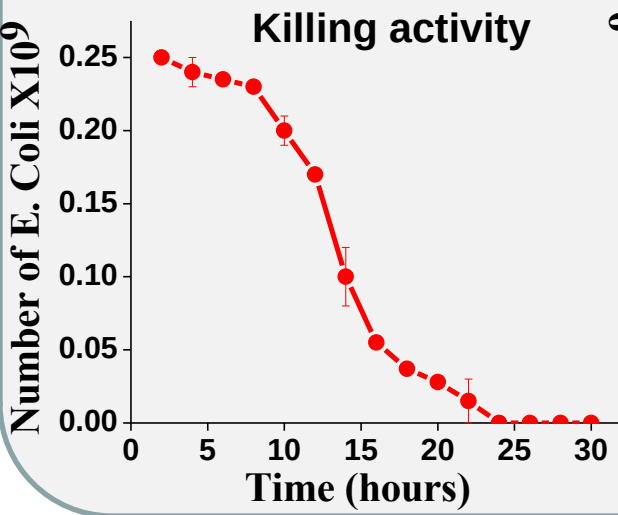

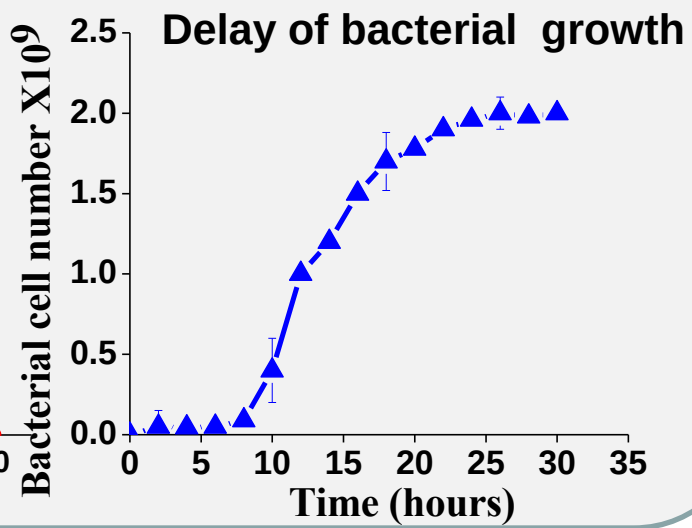

Direct writing by femtosecond laser pulses

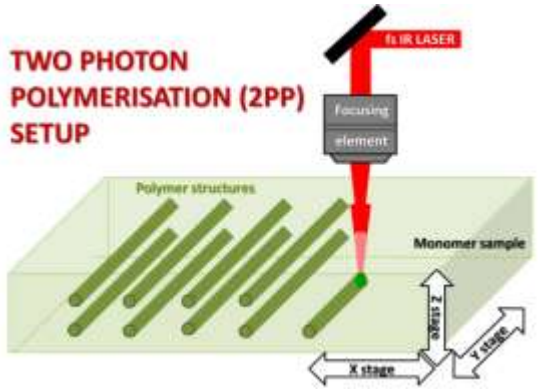

Ormosil scaffolds for tissue engineering

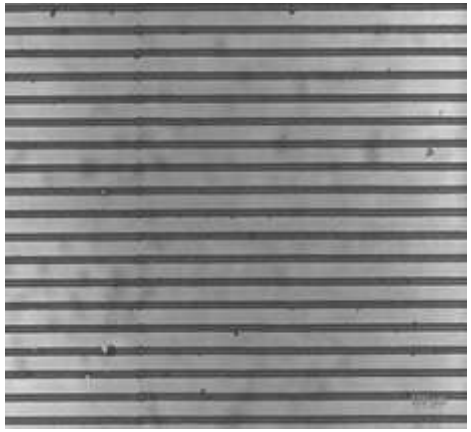

50 lines ormosil sample. Distance between lines = 100 μm

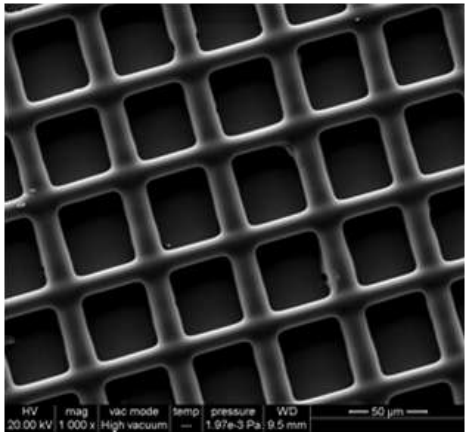

30x30 lines ormosil sample. Distance between lines = 50 μm

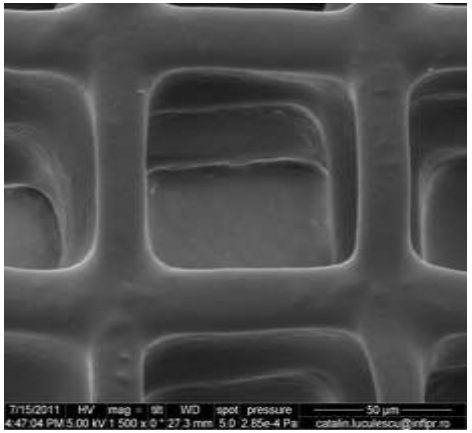

3 layers 30x30 lines ormosil sample. Distance between lines = 100 μm

Scaffold functionalization

Protein deposition on the scaffolds by MAPLE

- Lysozyme: antibacterial/ antitumor uses
- Fibrinogen: biocompatible protein

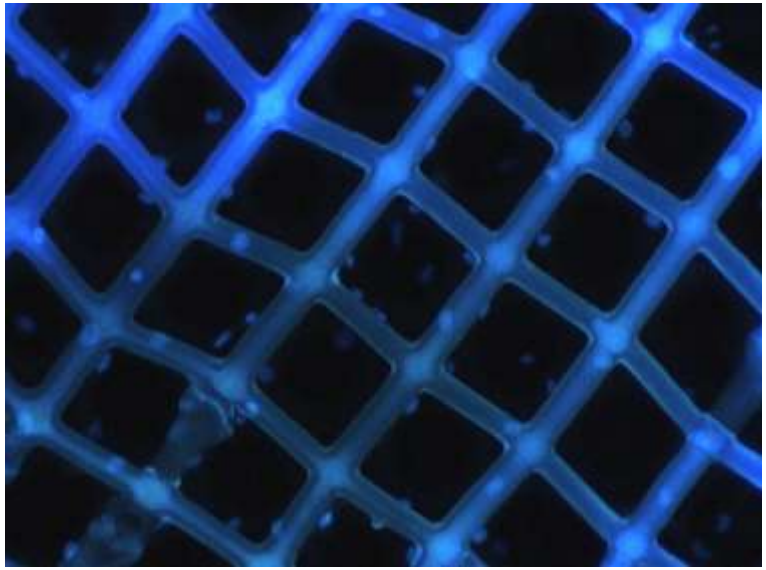

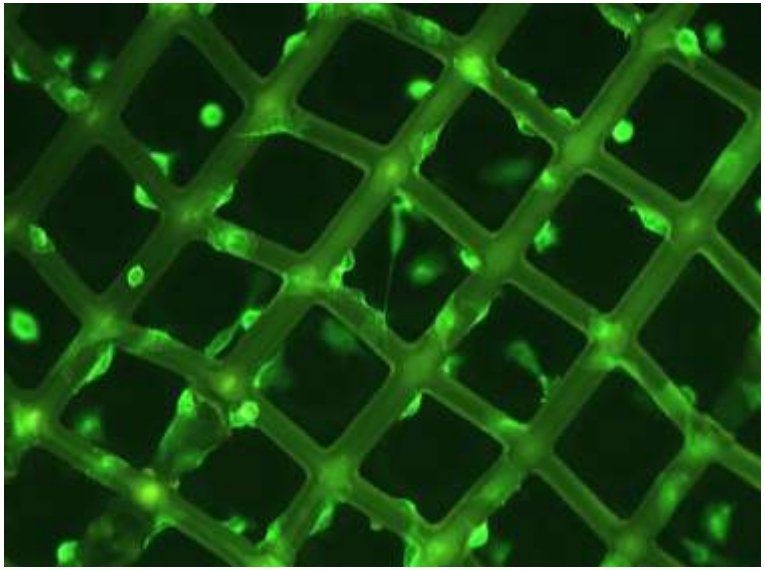

Fibroblast cells grown on a polymeric grid with 100 μm distance between lines

Spectroscopie d'un panache plasma

laser femtoseconde

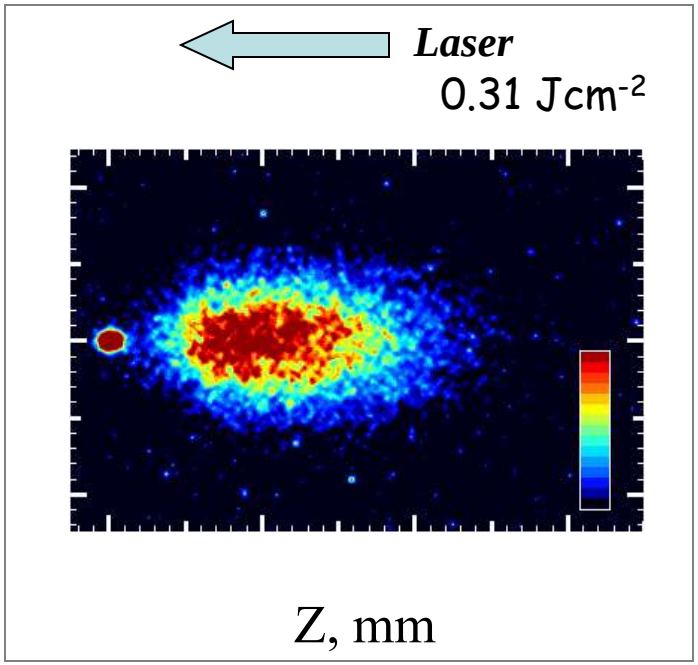

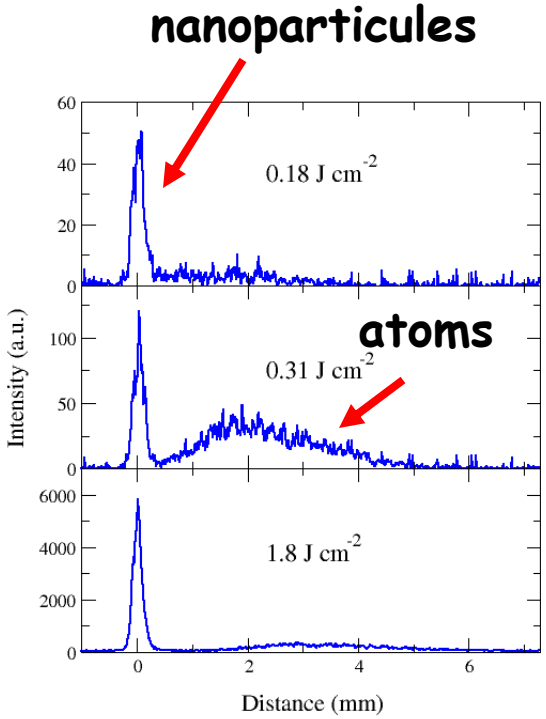

Expériences réalisées par (Grojo et al. LP3,Marseille)

t =400 ns Spot 35x35 µm², Cu

Formation de nano agrégats

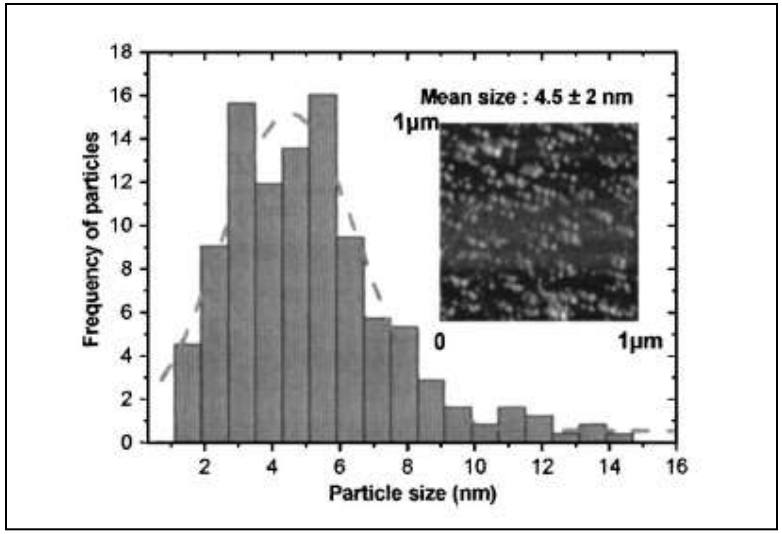

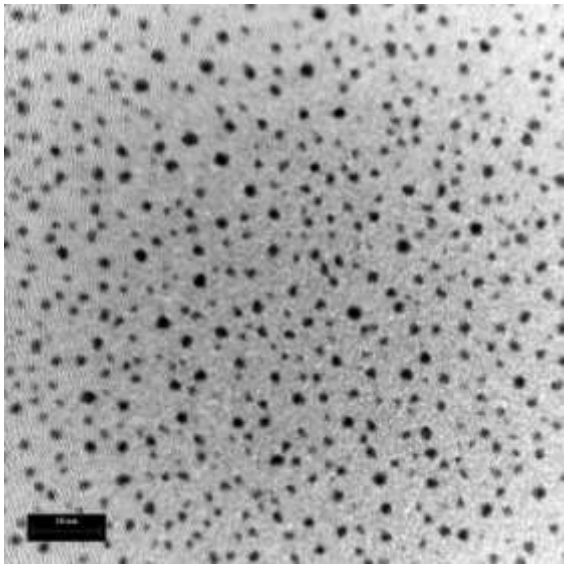

AFM

(Pereira et al.)

TEM

(Kabashin et al.)

Étude des mécanismes de la formation d'agrégats

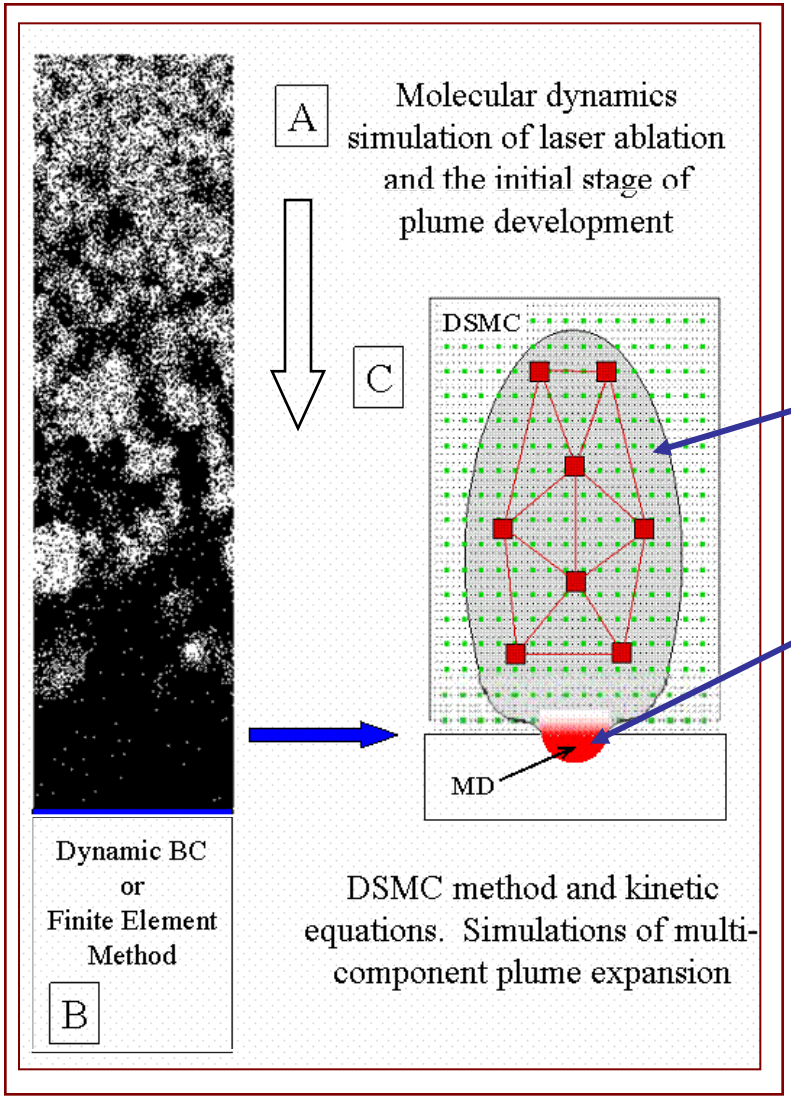

<u>Couplage:</u>

- Direct Simulation Monte Carlo

- Dynamique Moléculaire

Information détaillée

-*Continu du panache*

-*Distribution en taille des agrégats*

K. Gouriet, thèse (2008)

Simulation par Dynamique Moléculaire (MD)

=>distribution d'agrégats

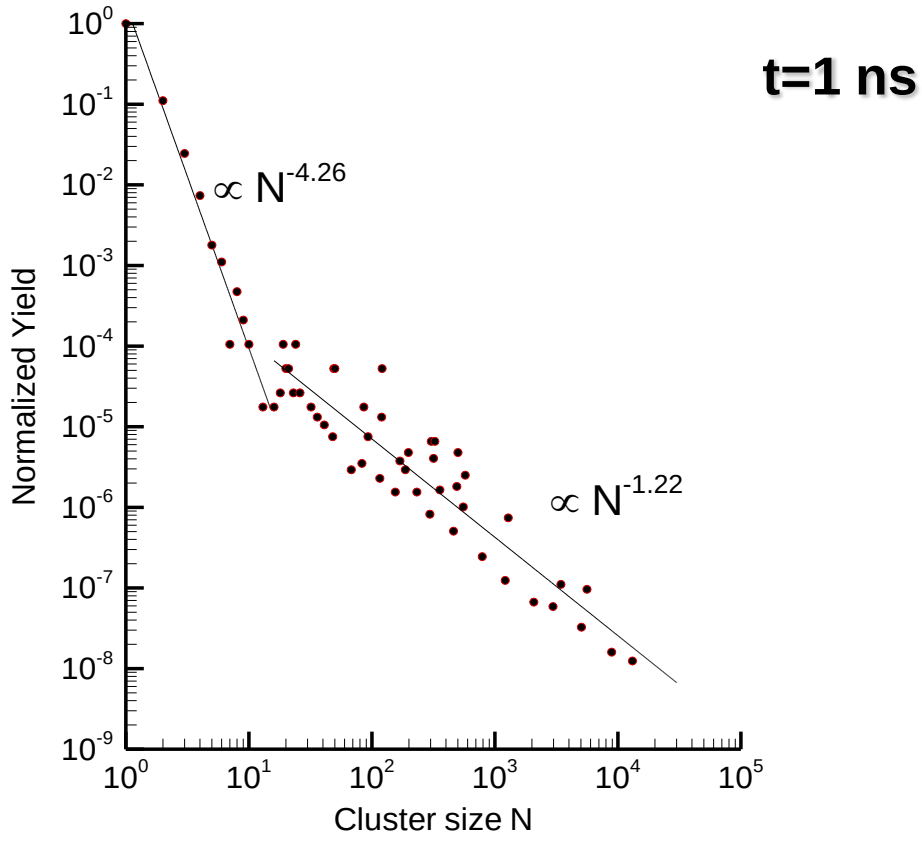

τ = 15 ps, F ~ 2 Fth, 40×10 nm, t =1 ns

Zhigilei et al. (Virginia University)

Target applications of mobile nanomaterials

Bioimaging

Optical imaging deals with visualization of biological objects or tissues in order to detect pathogens or follow the delivery of drugs etc: nanoparticles are uses as contrast agents

In vitro: Cellular imaging

In vivo: Cancer detection, drug delivery etc.

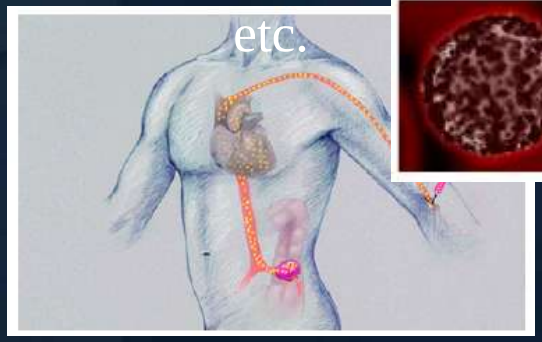

Light-induced therapies

Cancer therapy: nanoparticles are used as photosensitizers to produce local, targeted destruction of cancer cells

Photodynamic therapy

Light-induced hyperthermia

Diagnosis and Sensing

A. Diseases can be diagnosed through the (simultaneous) detection of a (set of) biomolecule(s) characteristic to a specific disease type and stage (biomarkers).

B. Each cell type has unique molecular signatures that differentiate healthy and sick tissues. Similarly, an infection can be diagnosed by detecting the distinctive molecular signature of the infecting agent

C. A nanoparticle can be functionalized in such a way that specifically targets a biomarker. Thus, the detection of the nanoparticle is linked to the detection of the biomarker, and to the diagnosis of a disease

D.

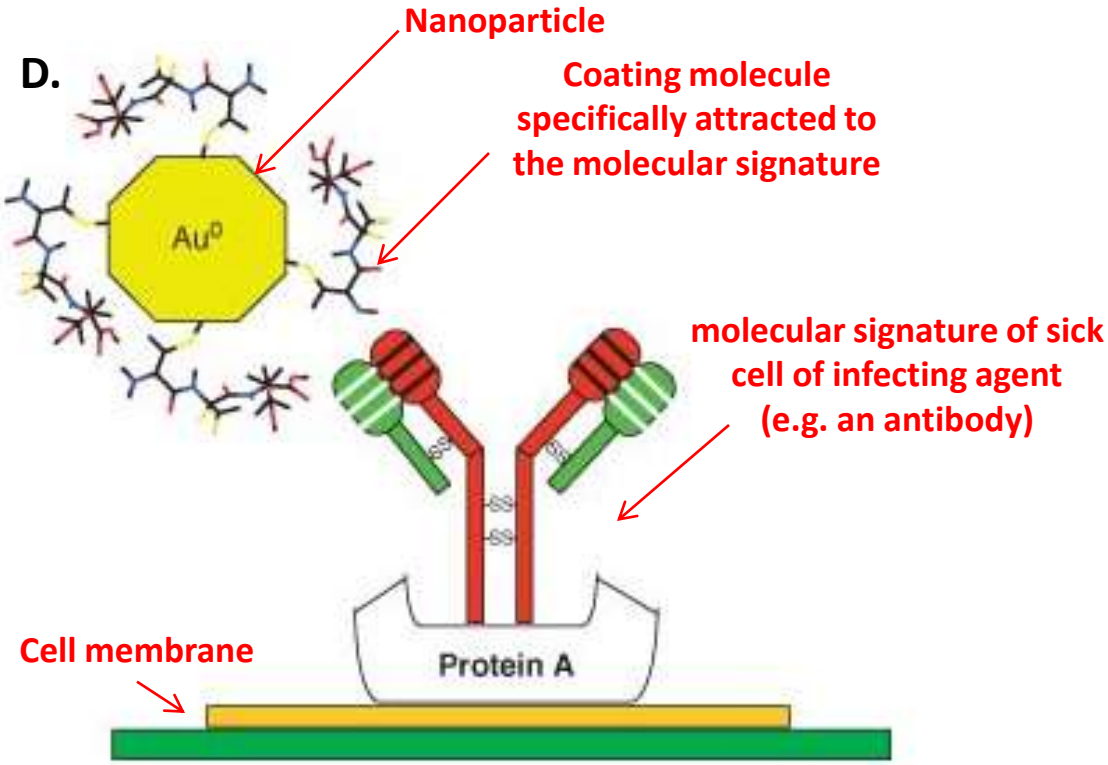

Huffman, Nanomedicine and Nanobiotechnology, Vol. 1, 1, 2009

Laser ablation of material from a solid target and production of nanoparticles/nanostructures

Production of nanoclusters by laser ablation and their subsequent cooling in ambient medium

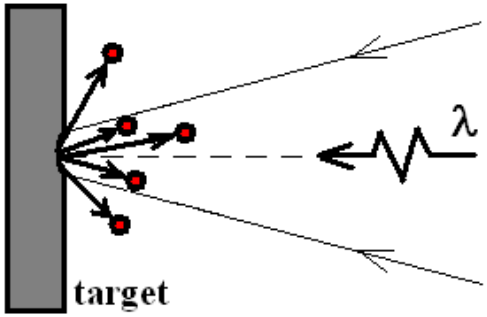

Gaseous ambience
Nanoclusters can be deposited on a substrate forming a nanostructured film

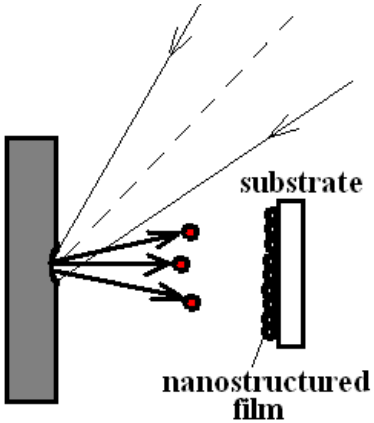

Aqueous ambience
Nanoclusters crystallize and form colloidal solution

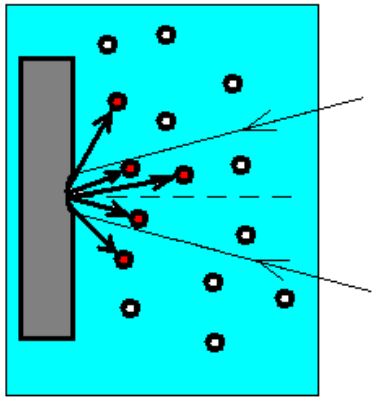

NPs produced in gaseous ambience

Silicon nanocrystal size : AFM

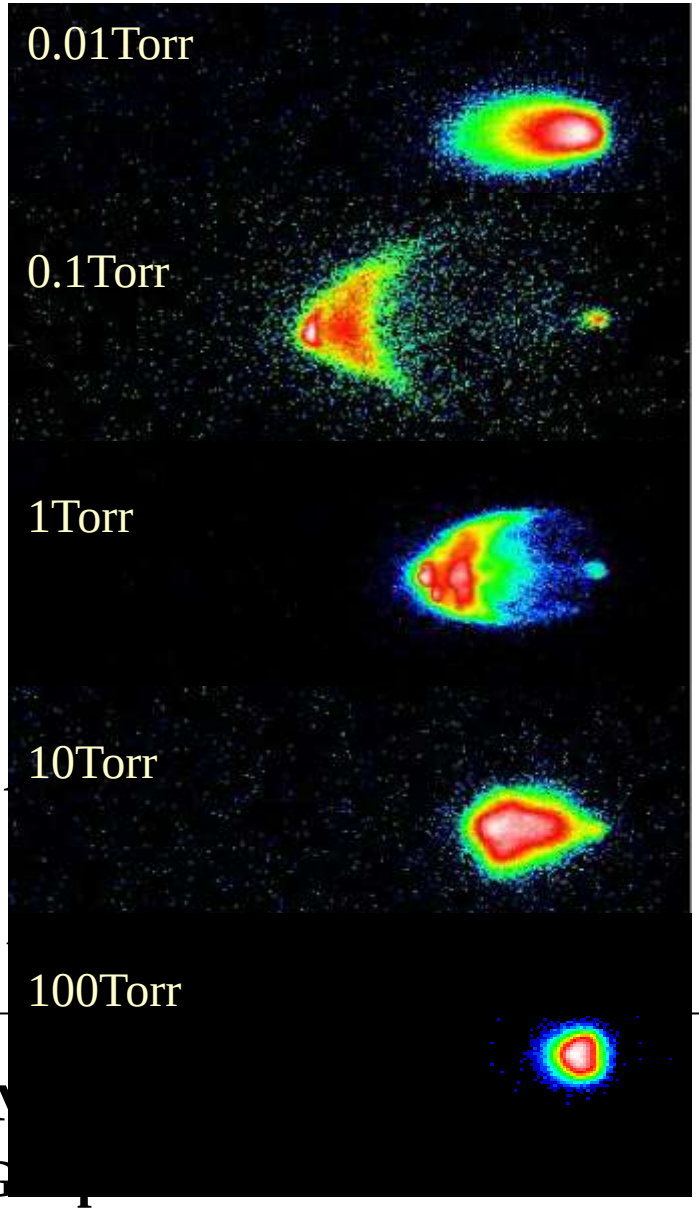

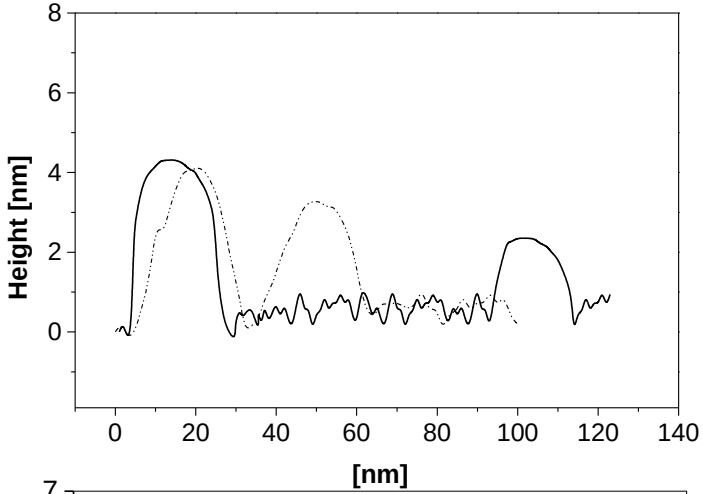

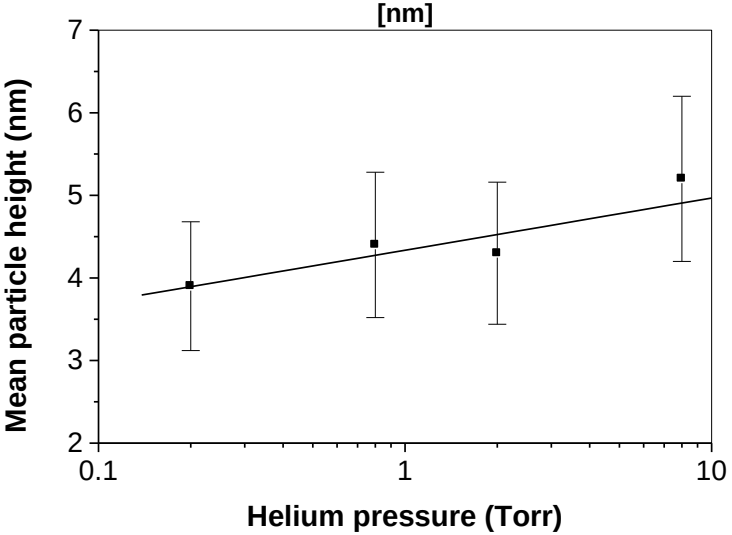

N (from height measurements)

G p → **Nanocrystal size decreases**

Photoluminescence of size selected nanoclusters

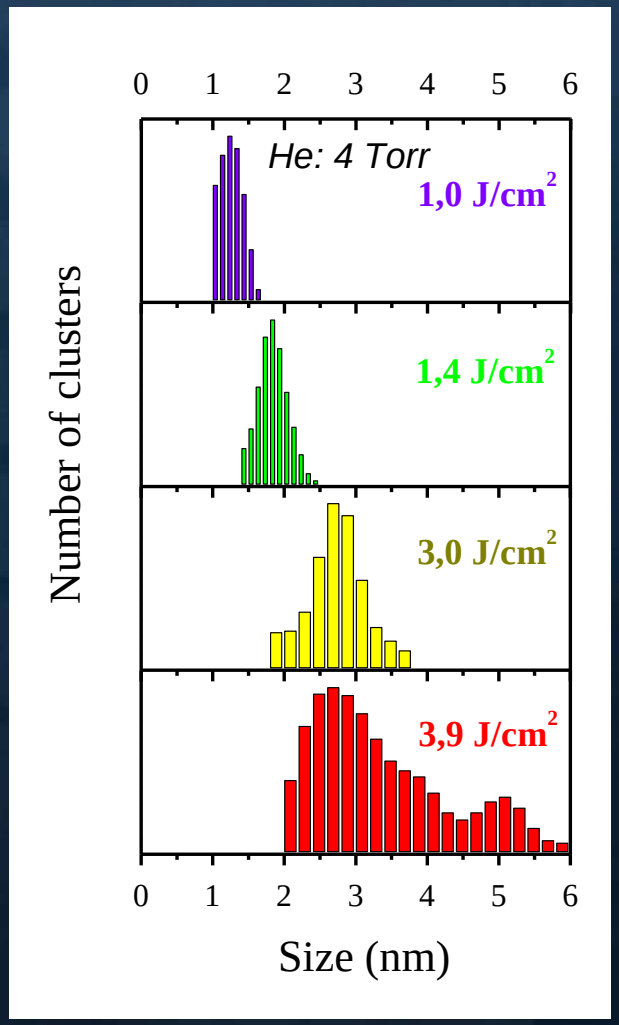

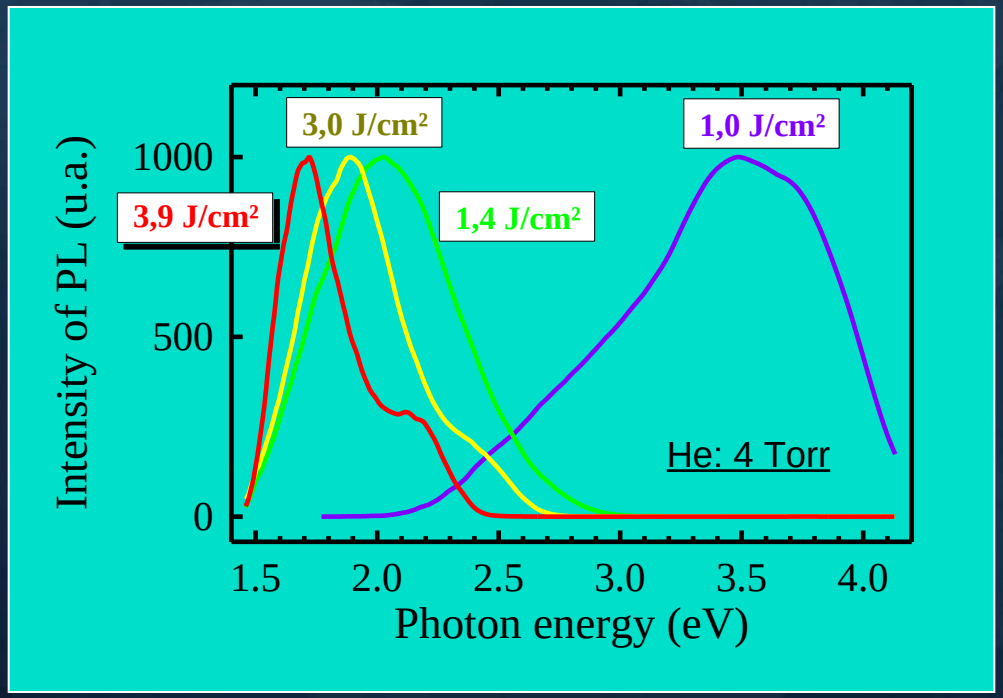

Silicon nanoclusters

Medical Imaging

A. Optical properties of nanoparticles depend greatly on its structure. Particularly, the color (wavelength) emitted by a quantum dot (a semiconductor nanoparticle) depends on its diameter.

B.

CdSe nanoparticle (QD) structure

Source: Laurence Livermore Laboratories

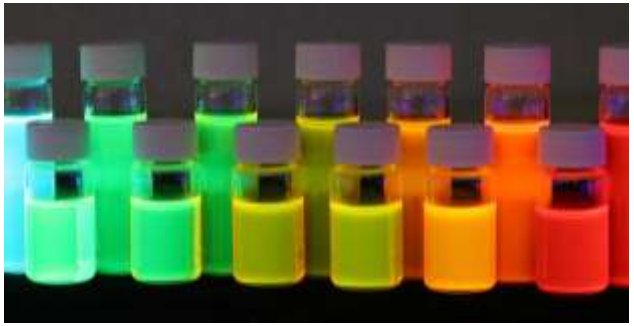

Solutions of CdSe QD's of different diameter

Source: Department of immunology, University of Toronto

C. The quantum dots (QD) can be injected to a subject, and then be detected by exciting them to emit light

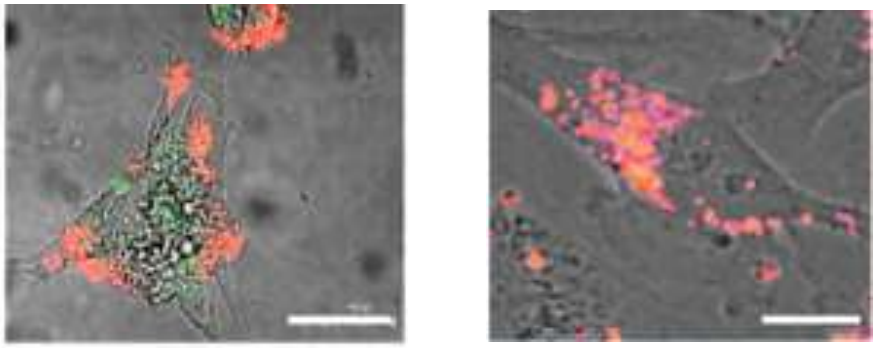

Imaging of QD's targeted on cellular structures

Nano Letters 2008., Vol. 8, pp3887-3892

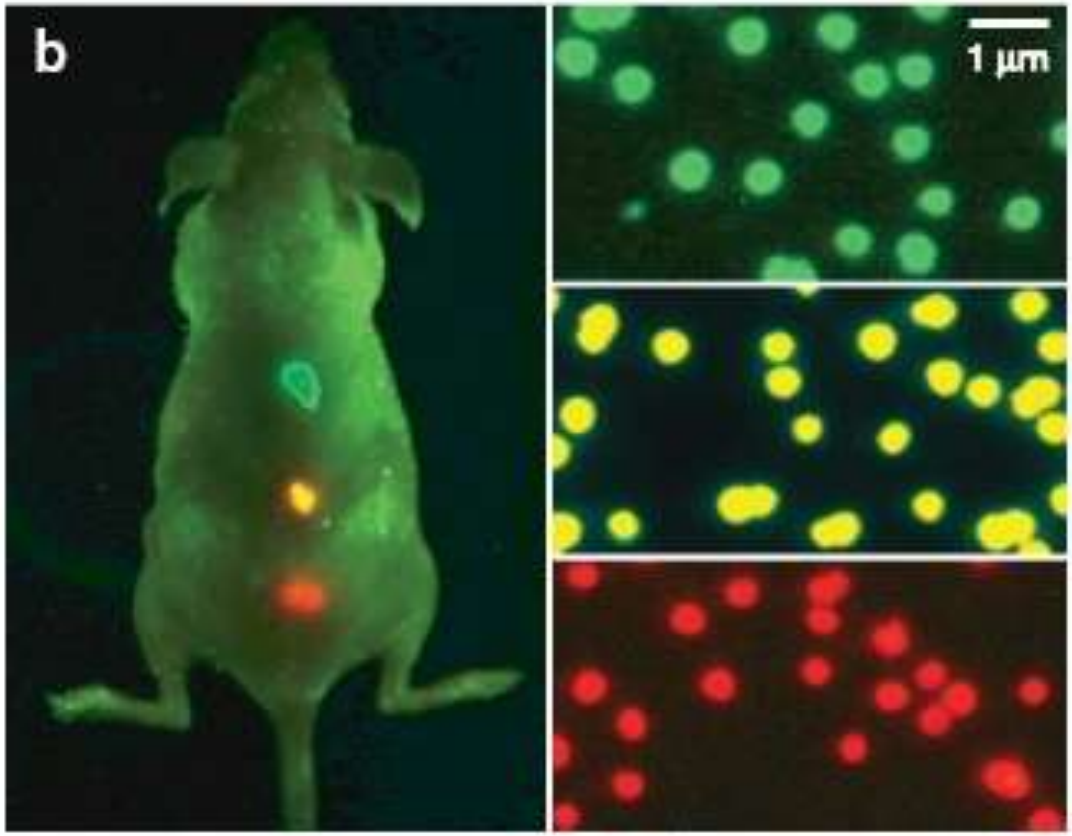

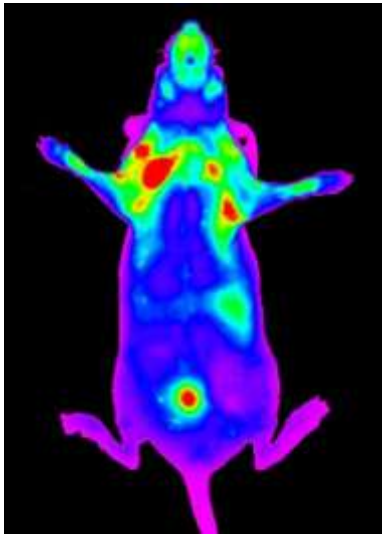

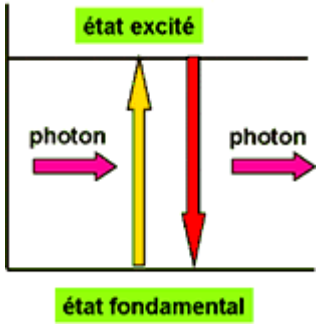

In vivo cancer targeting and imaging with semiconductor quantum dots

Gao et al., Nat Biotech **22**, 969 - 976 (2004)

NPs produced in aqueous ambience

Advantages of laser ablation-based nanofabrication compared to chemical methods

Disadvantage of chemical synthesis: contamination…….

In particular, chemical method for the fabrication of gold nanoparticles:

Reduction of chloroauric acid ($HAuCl_4$) with citrate in water

Control size by adding a stabilizing agent (thiol- (-SH) containing molecules.)

Contamination: impurities, Cl^- on surface, non-biocompatible surfactants…

Problems in imaging applications (especially in vivo)

Problems in field-enhanced applications (e.g., contaminants can provide false Raman signals)

Laser ablation in liquids: a way to avoid residual contamination???

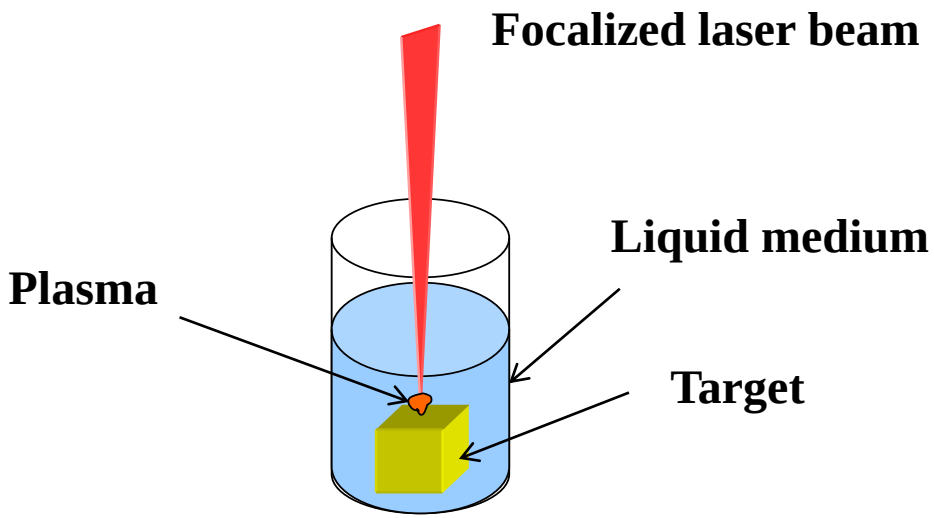

- Laser energy can be transmitted through a liquid to ablate a solid target: the nanomaterial is released to the solution

- The process can be performed without any dirty chemical products in clean liquid environment (deionized water, PBS solution): no contamination

Experiment

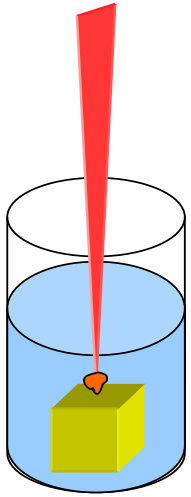

Ablation of gold: final colloidal solutions

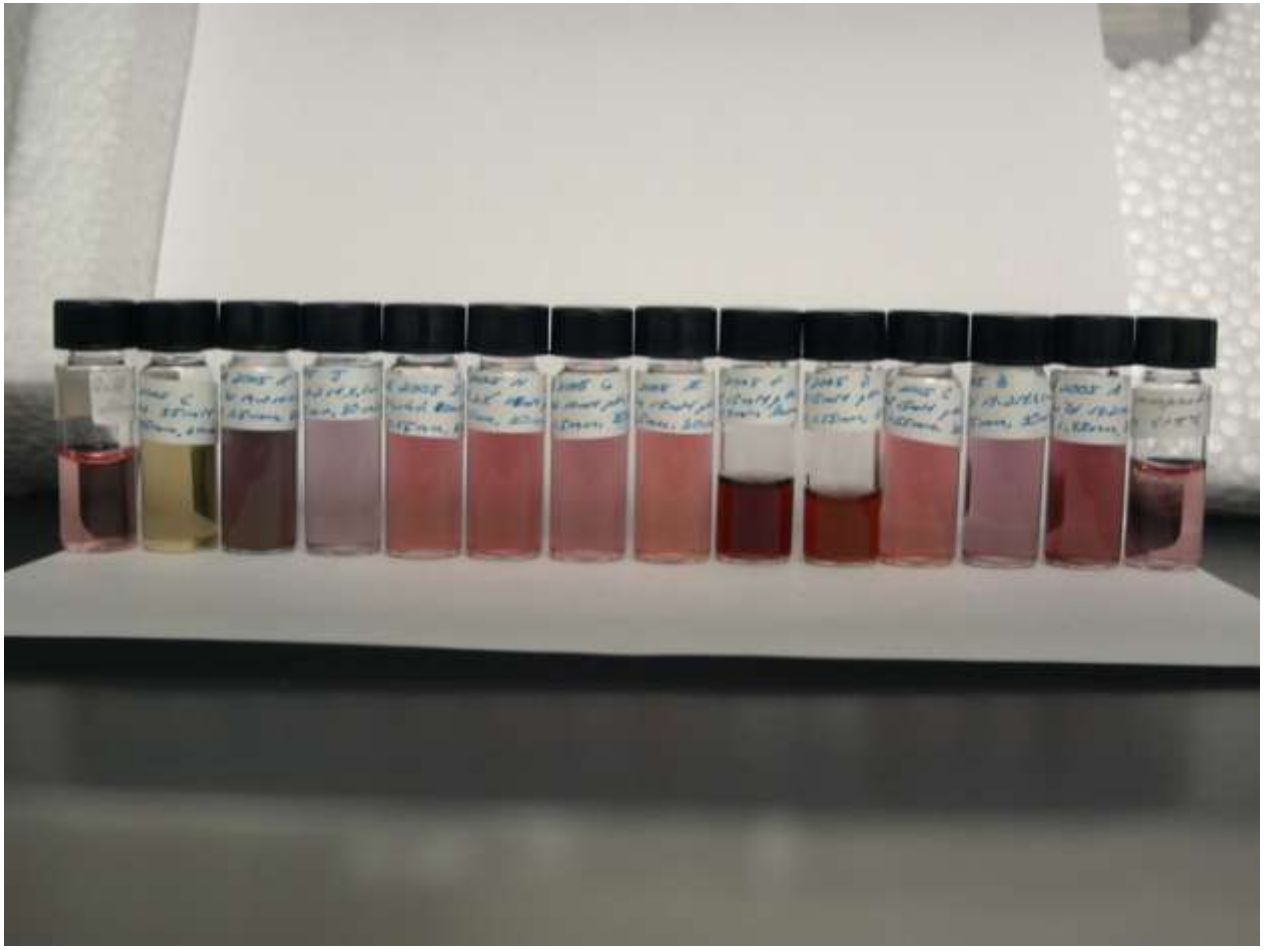

-Solution are ranging from deep wine red to pink and purple

- Color related to the size dependant surface plasmon resonance

Size distribution of Au nanoparticles prepared in distilled water

$F = 20F_0$ J/cm^2

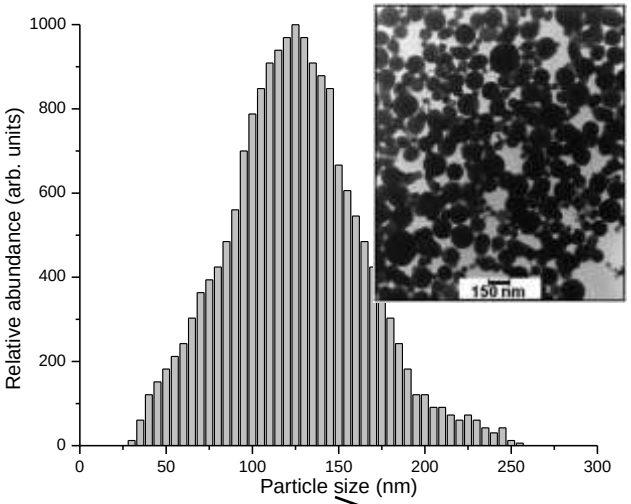

$F = 5F_0$ J/cm^2

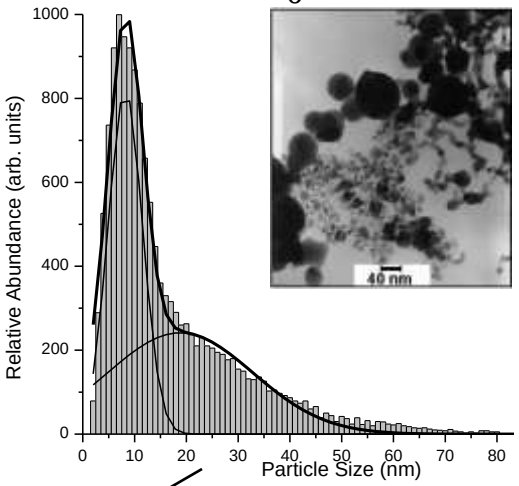

$F = F_0$ J/cm^2

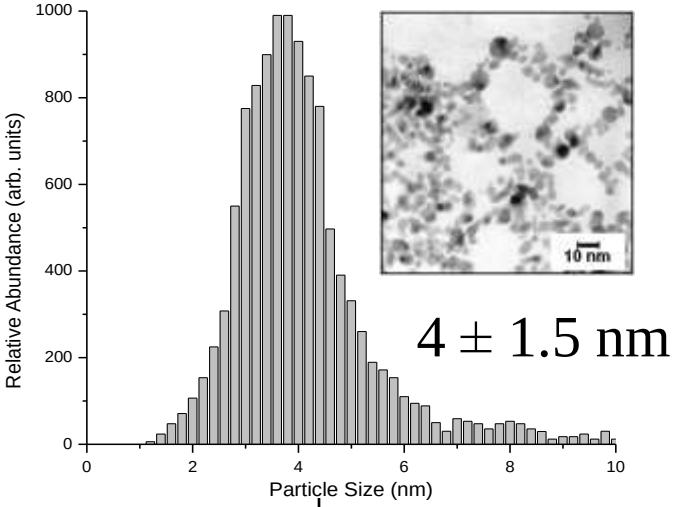

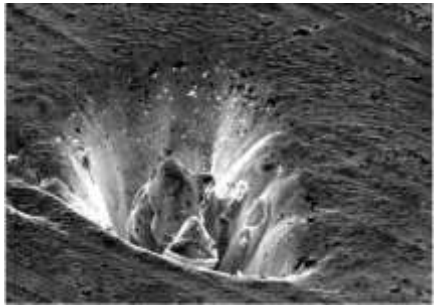

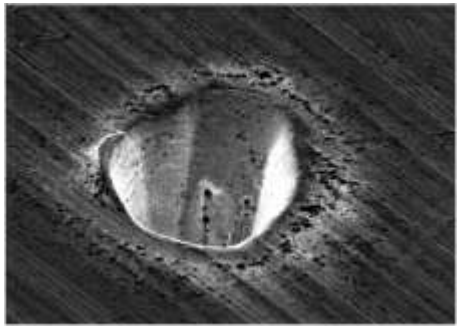

-Size and dispersion of nanoparticles can be controlled by laser fluence
- Shape of craters on target at high F suggests the presence of cavitation phenomena

A. V. Kabashin, M. Meunier, J. Appl. Phys. 94, 7941 (2003)

Ablation in biopolymers (dextran, PEG)

Dextran $(C_6H_{10}O_5)_n$

Influence of the concentration

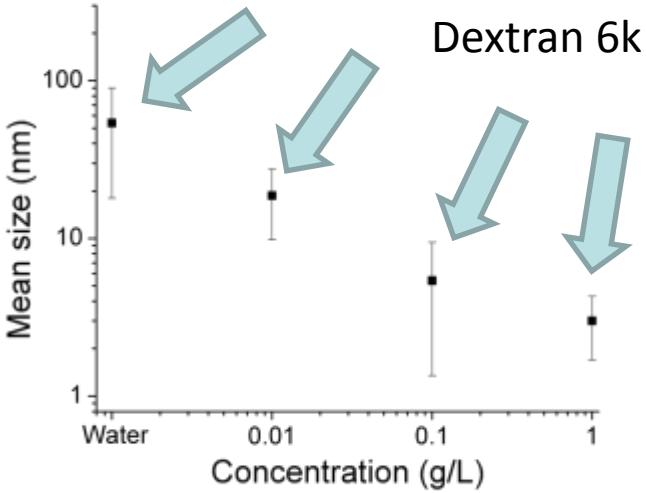

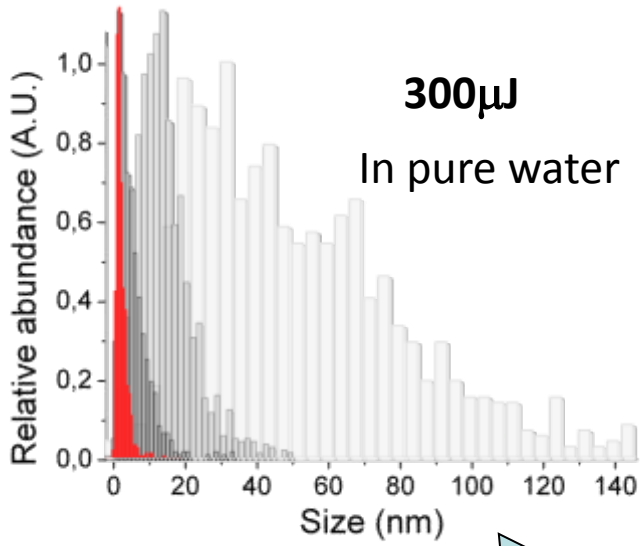

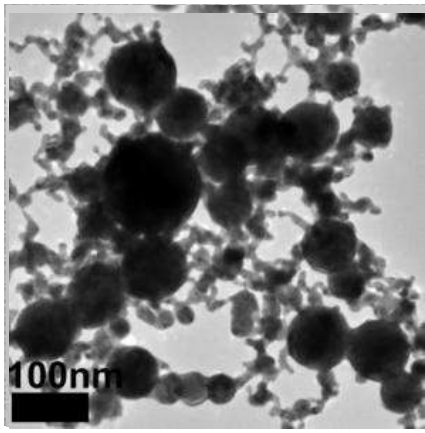

In water: Very dispersed population of nanoparticles

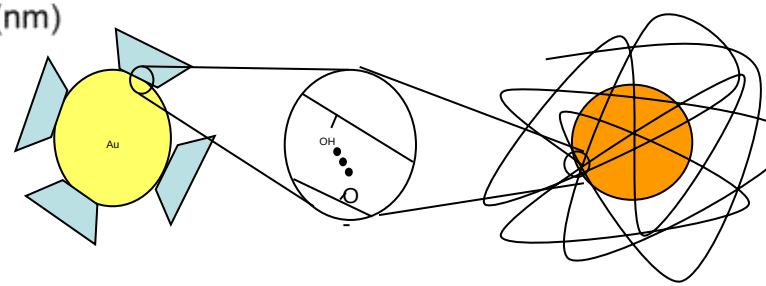

Dextran (MW=6000g/mol):

- ✓ Quenches the growth of the nanoparticles
- ✓ 2-4nm nanoparticles are produced (230-1850 atoms)
- ✓ Very fast dextran-gold interaction

Nanoparticles react with OH groups of biopolymers!!!

Gold Nanoparticles vs. Alzheimer

A. Alzheimer and other degenerative diseases are caused my the clustering of amyloidal beta (*Aβ*) protein.

Source: Berkeley Lab

B.

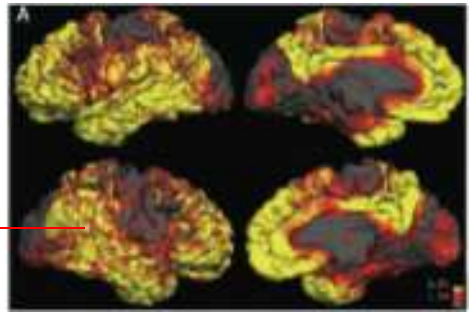

Alzheimer's brain

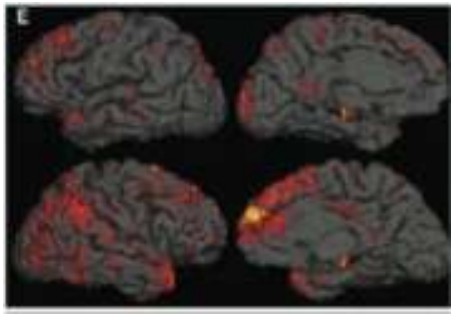

Healthy brain

C.

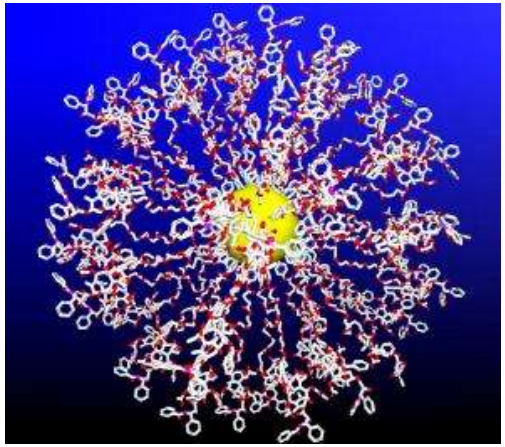

Functionalized nanoparticle

Source: www.internetchemistry.com

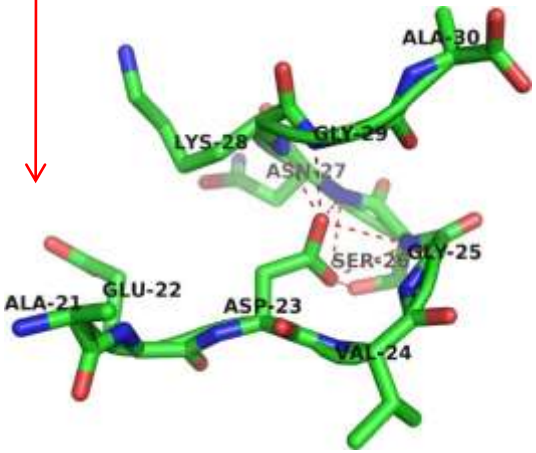

Chemical structure of Aβ-protein

Source: wwwthefutureofthings.com

D. Gold nanoparticles can be functionalized to specifically attach to aggregates of this protein (amyloidosis)

Gold Nanoparticles vs. Alzheimer

A. The functionalized gold nanoparticles selectively attach to the aggregate of amyloidal protein. The microwaves of certain frequency are irradiated on the sample. Resonance with the gold nanoparticles increases the local temperature and destroy the aggregate

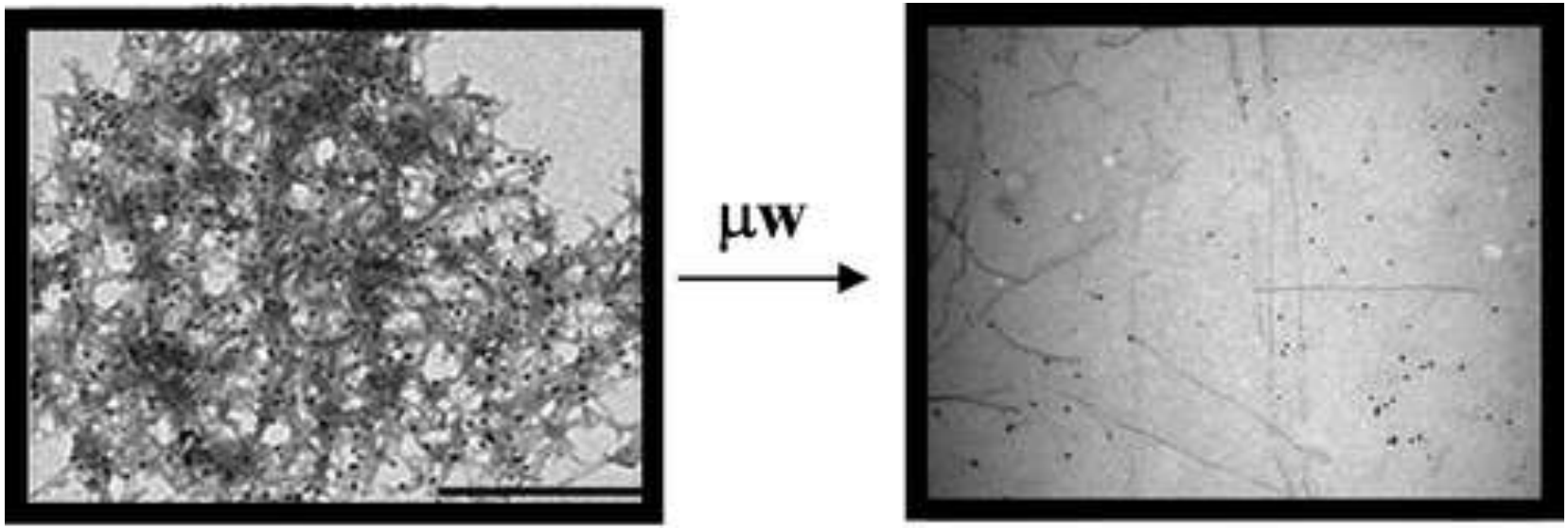

Before irradiation *After irradiation*

Nanoletters 2006, Vol. 6, pp.110-115

LIBS for biomedical applications

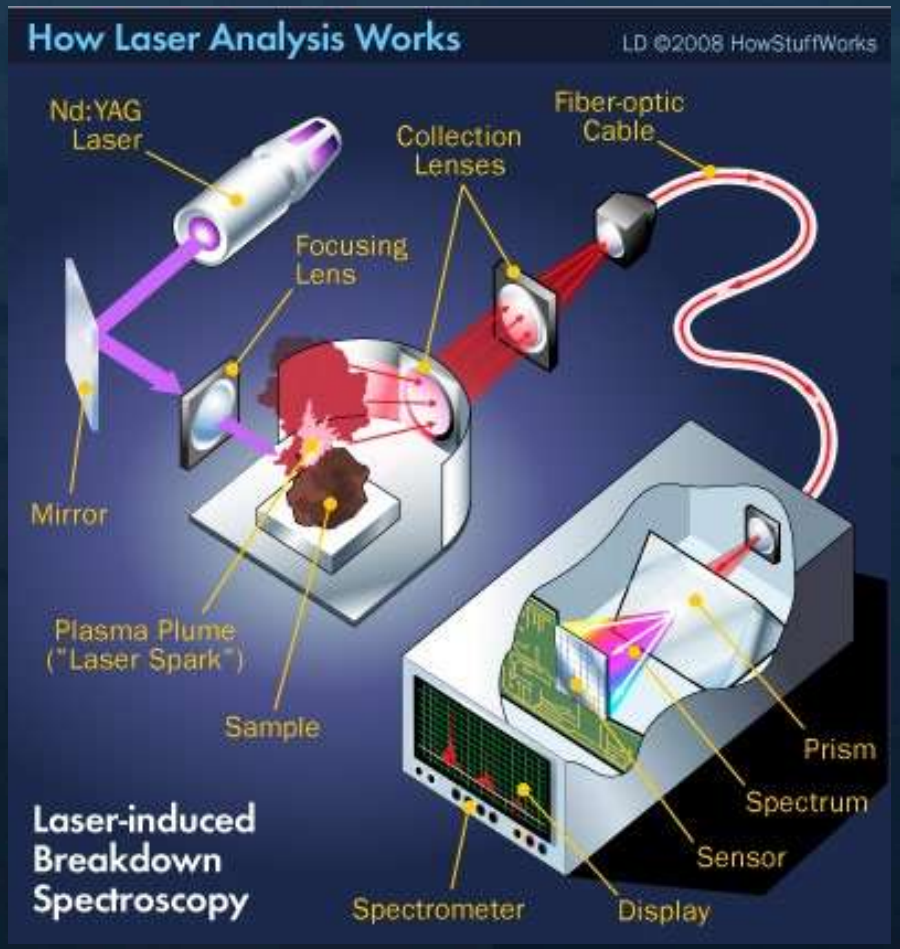

- *in vivo analysis of tissue for* real-time analysis
- real-time diagnosis of pathogen presence in human fluids (blood,urine, CSF, sputum)

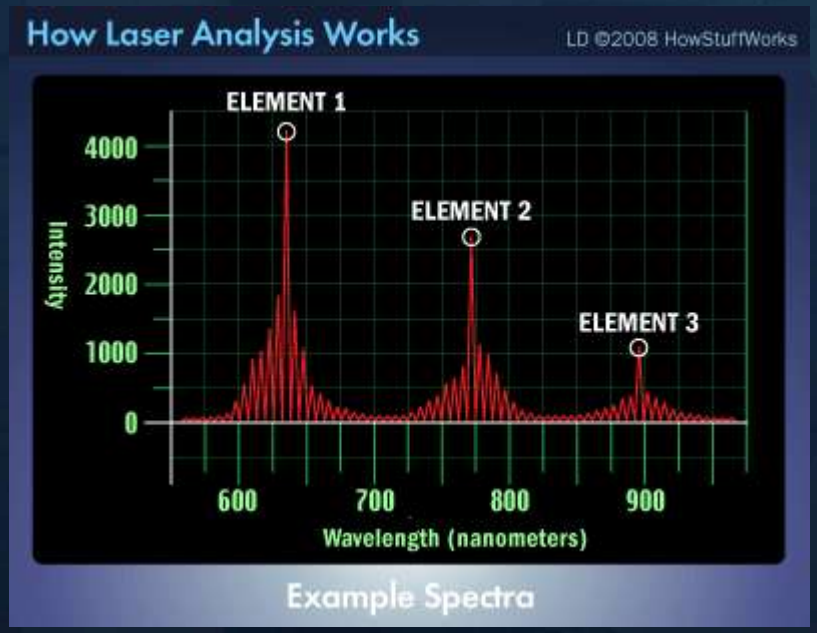

LIBS (Laser Induced Breakdown Spectroscopy)

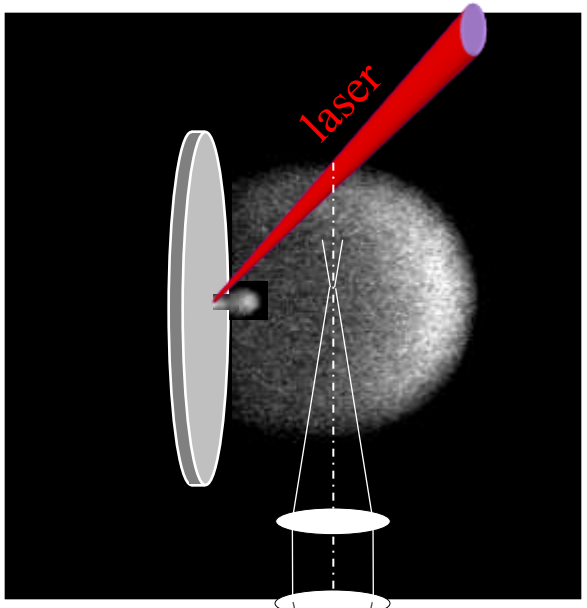

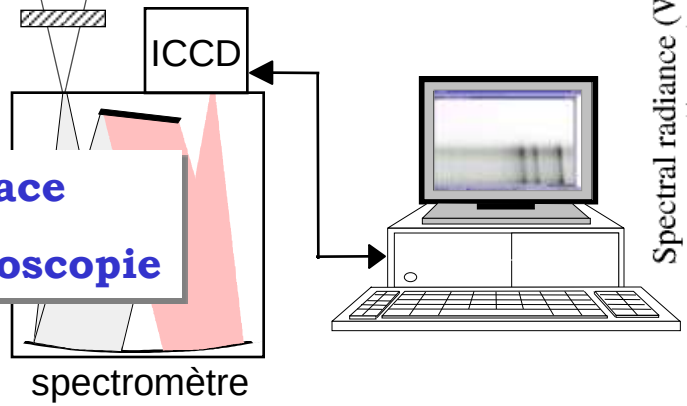

Time and space

Emission spectroscopie

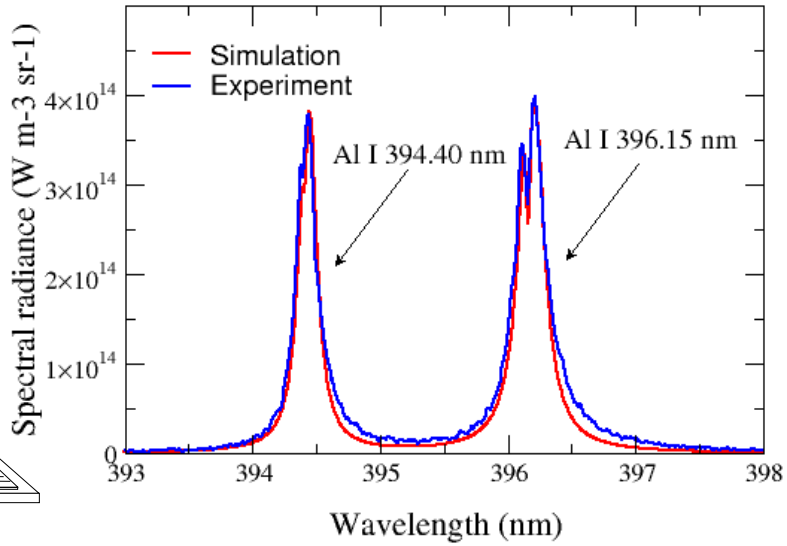

Laser-induced breakdown spectroscopy: a tool for real-time, *in vitro* and *in vivo* identification of carious teeth

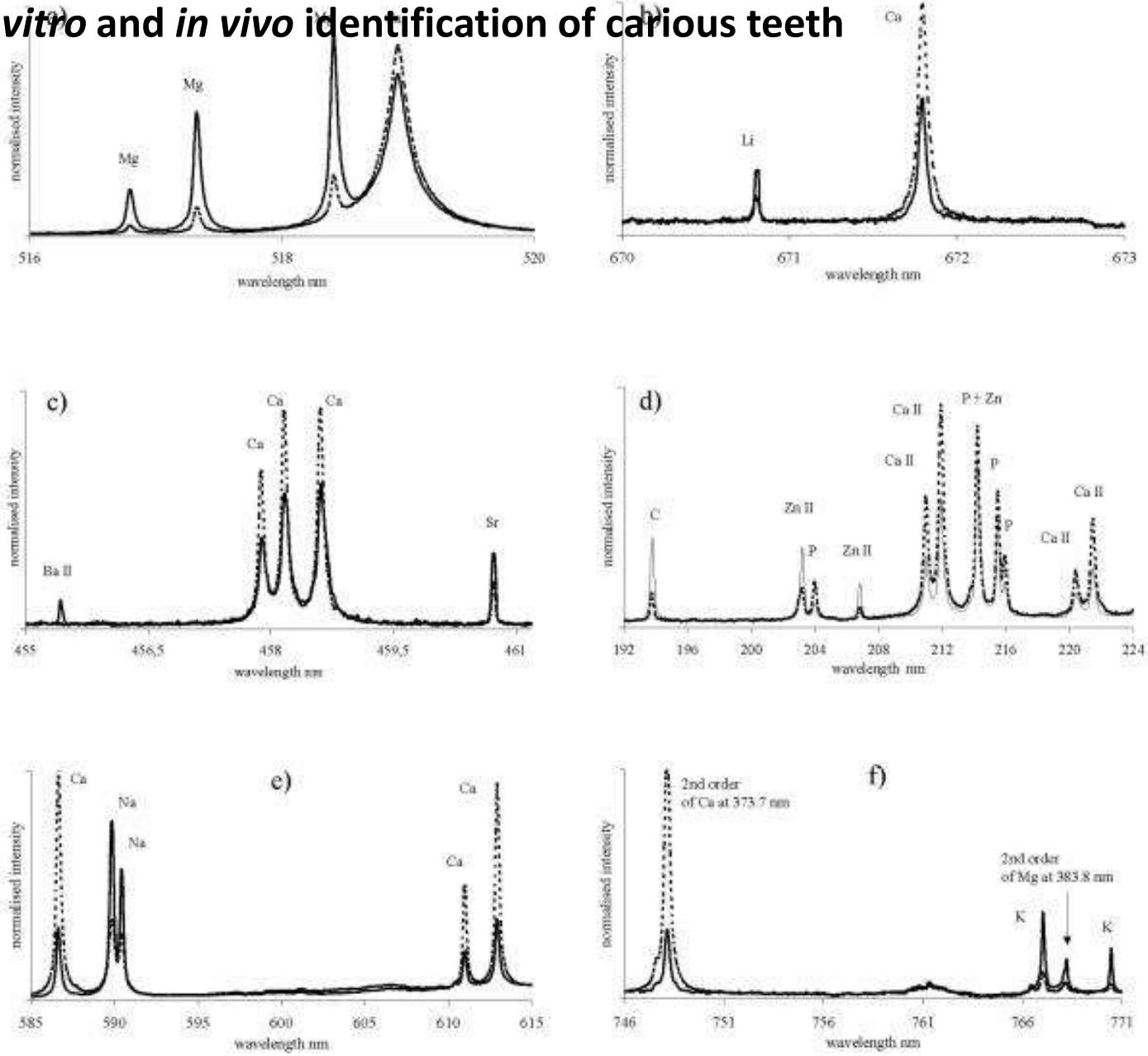

BMC Oral Health. 2001; 1: 1. Ota Samek,[1] Helmut H Telle,[2] and David CS Beddows

Sensitive Detection of Epithelial Ovarian Cancer Biomarkers Using Tag-Laser Induced Breakdown Spectroscopy

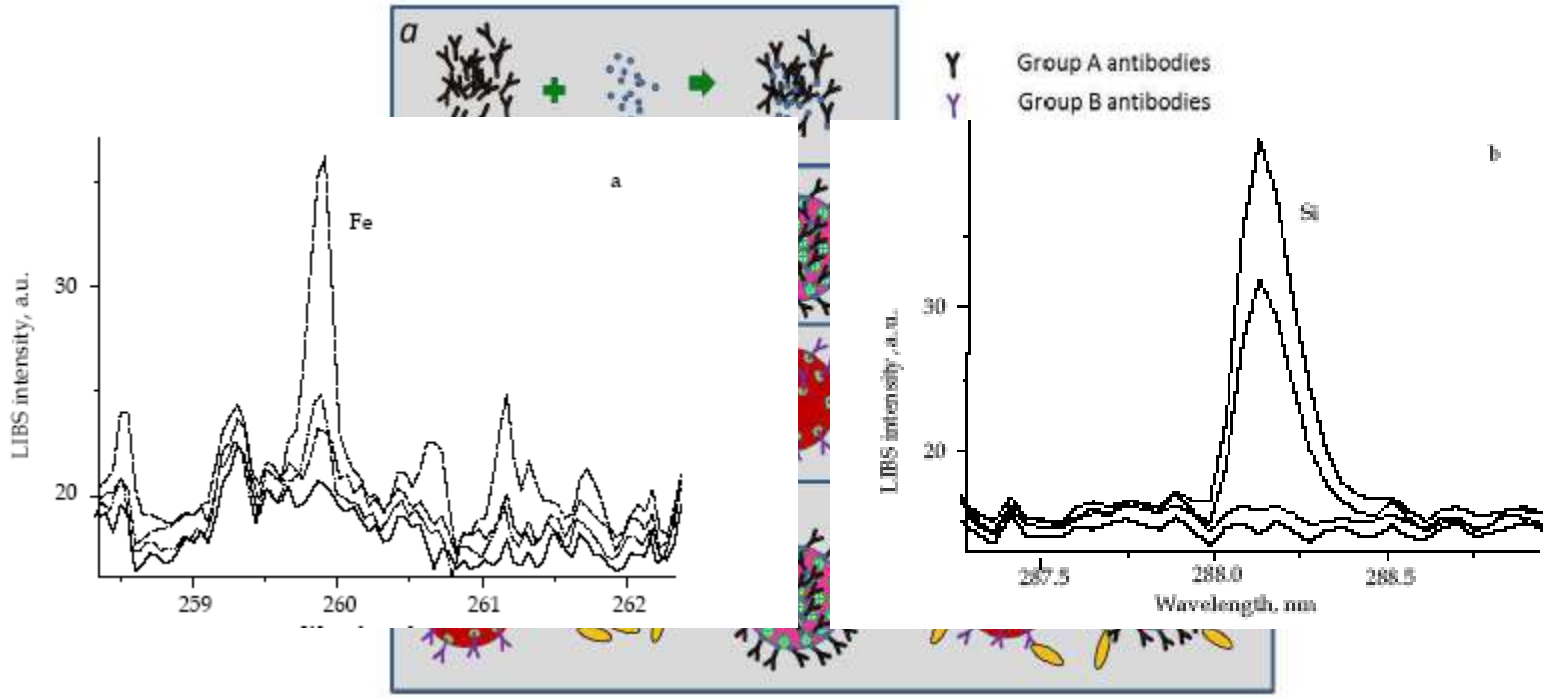

Yuri Markushin and Noureddine Melikechi*

Optical Science Center for Applied Research, Delaware State University, USA

X rays produced by laser plasmas

I = ~10^{16} à 10^{18} W/cm^2

$$T_{hot} \propto \left(I_{las}\lambda^2\right)^{1/3}$$

$$\eta \propto \left(I_{las}\lambda^2\right)^{3/4}$$

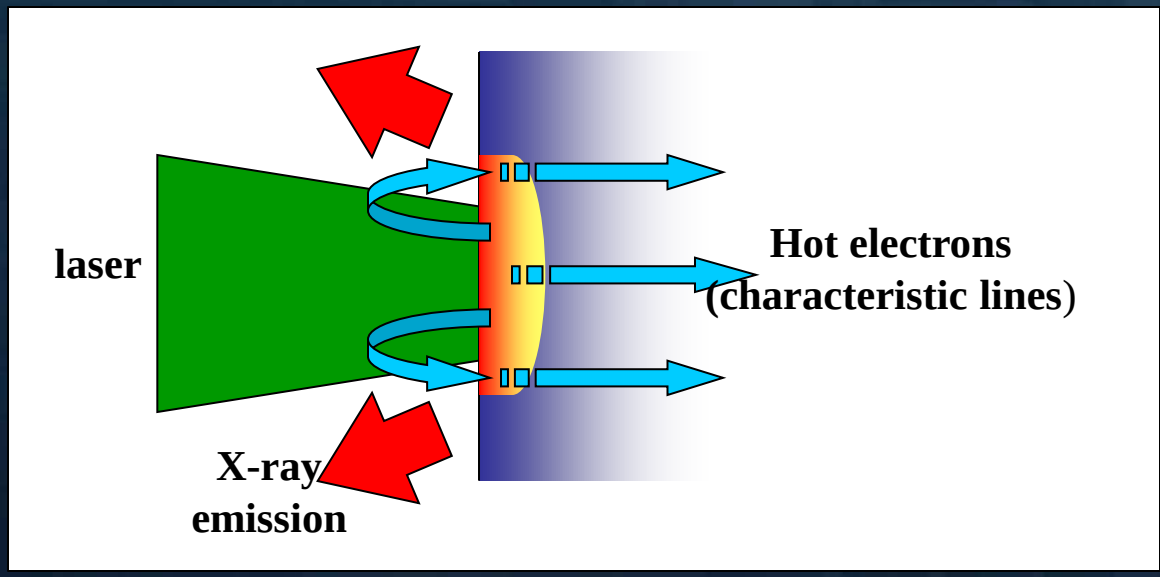

$$n_{c(\mathrm{cm}^{-3})} = 1{,}11.10^{21} / \lambda^2_{(\mu\mathrm{m})}$$

X-rays

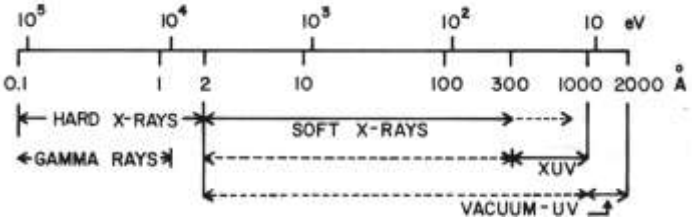

Laser-generated hot electrons produce x-rays by two dominant mechanisms

Kmetec, "MeV X-ray generation with a femtosecond laser," *Phys. Rev. Lett.* **68**, 1527 (1992)
Rousse, "Efficient Kα X-ray source from fs-laser-produced plasmas," *Phys. Rev. E* **50**, 2200 (1994)

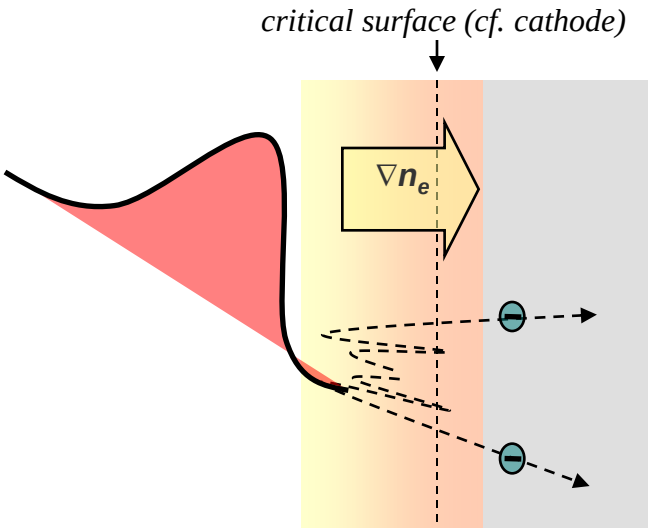

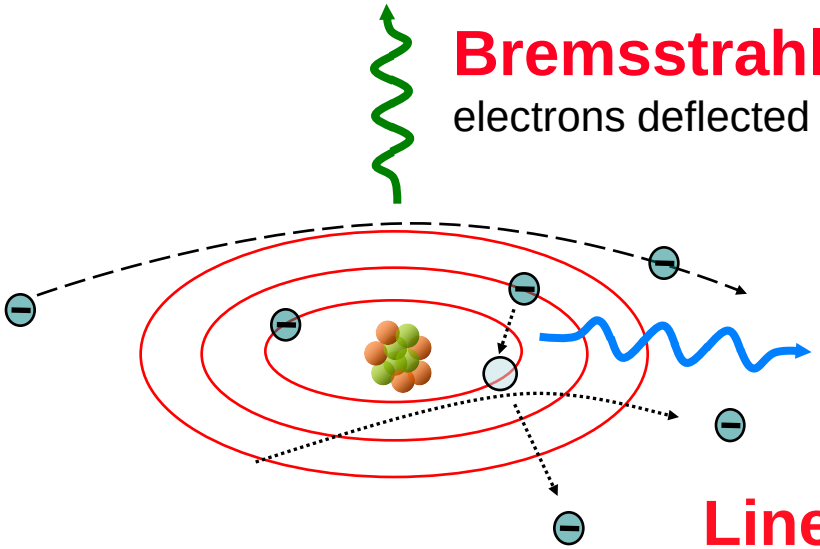

Bremsstrahlung:
electrons deflected by nucleus

conventional X-ray tube:

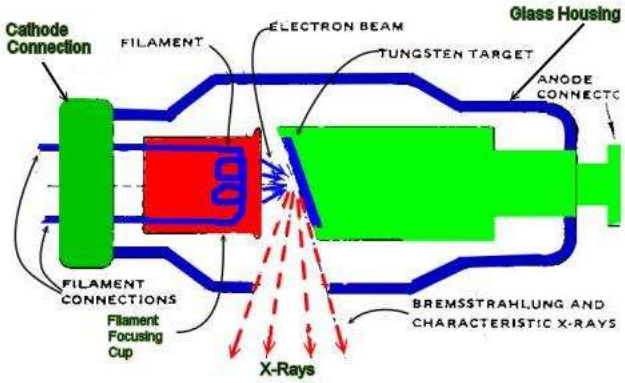

Line emission:
Fast electrons knock free core electrons from the inner shell

(typical recombination lifetimes: several fs)

Tightly focused fs lasers create the world's smallest hard x-ray source (~4 μm) for precision imaging

Hou *et al.*, *Appl. Phys. Lett.* **84**, 2259 (2004)

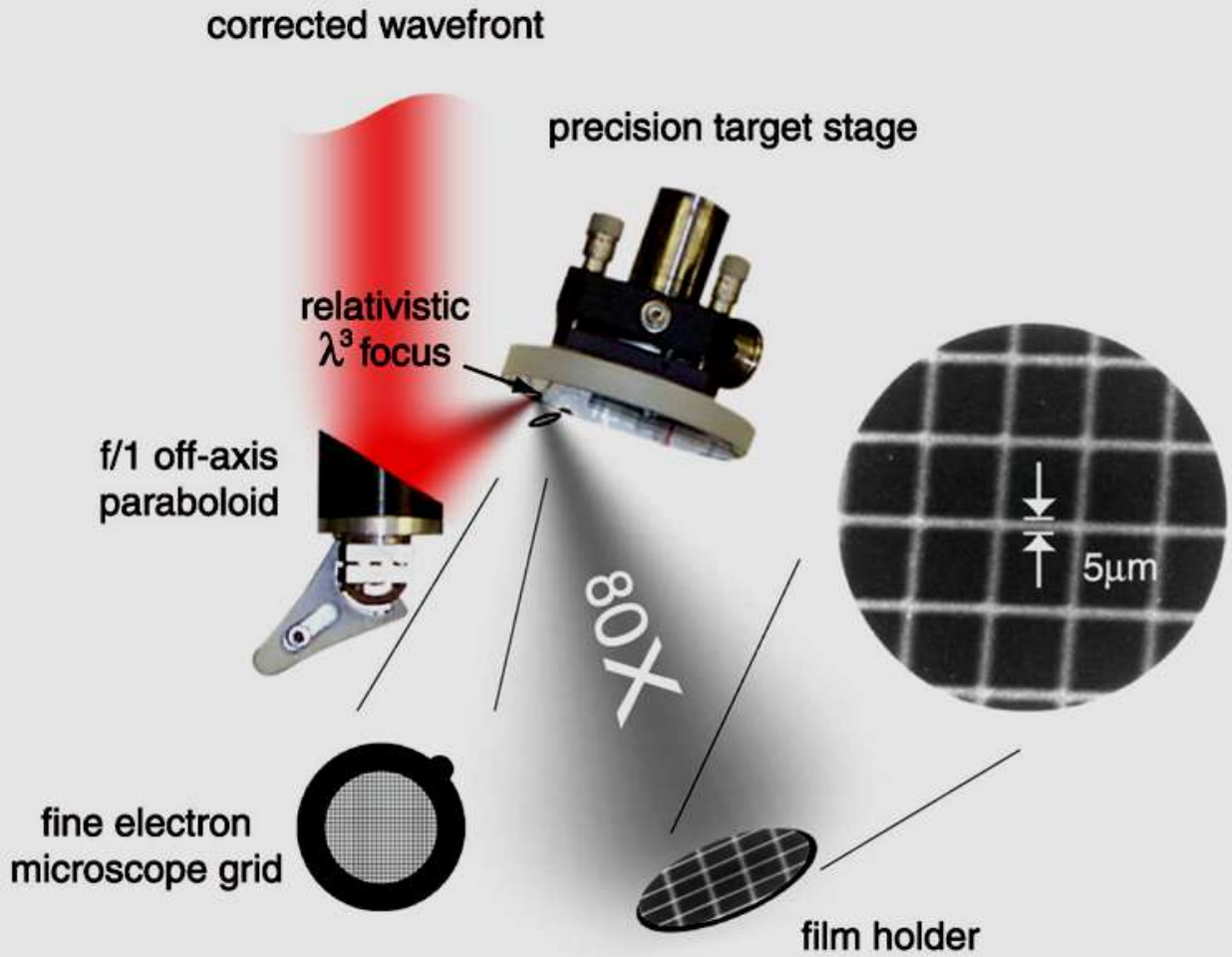

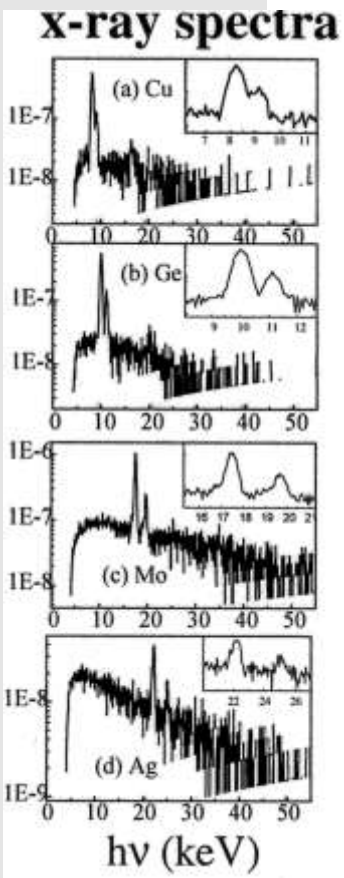

x-ray source size is ~ 4× larger than laser focus because of lateral heat transport*

*Bowes, *Opt. Lett.* **31**, 116 (2006)

2004: première démonstration d'imagerie avec contraste de phase avec une source X crée par laser

$$L_{coh} = \frac{2\lambda R_1}{\sigma}$$

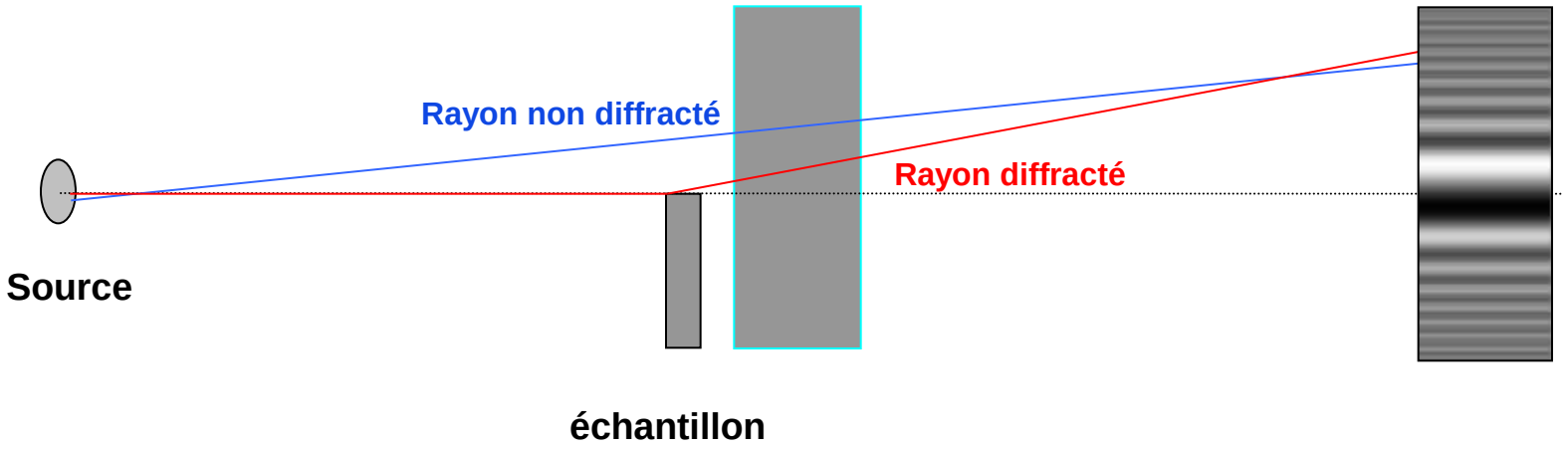

Absorption *vs.* contraste de phase

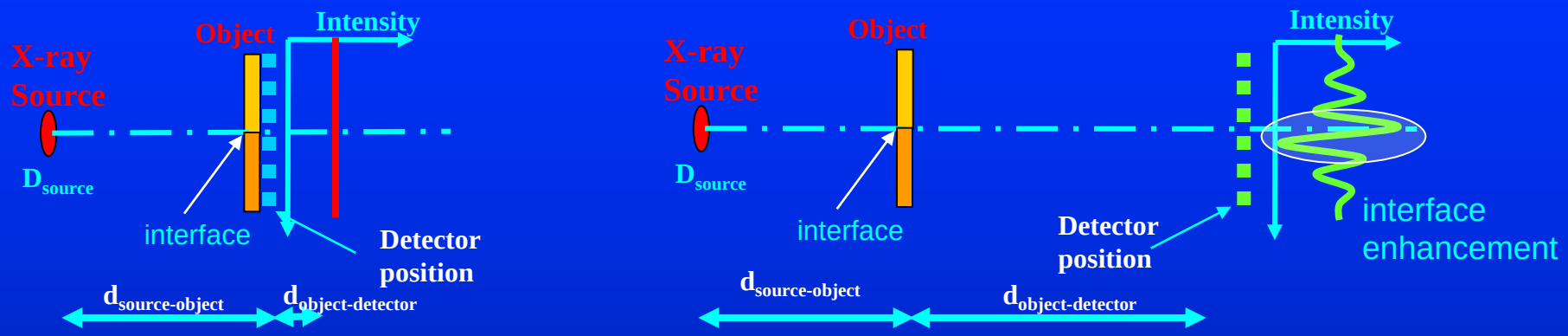

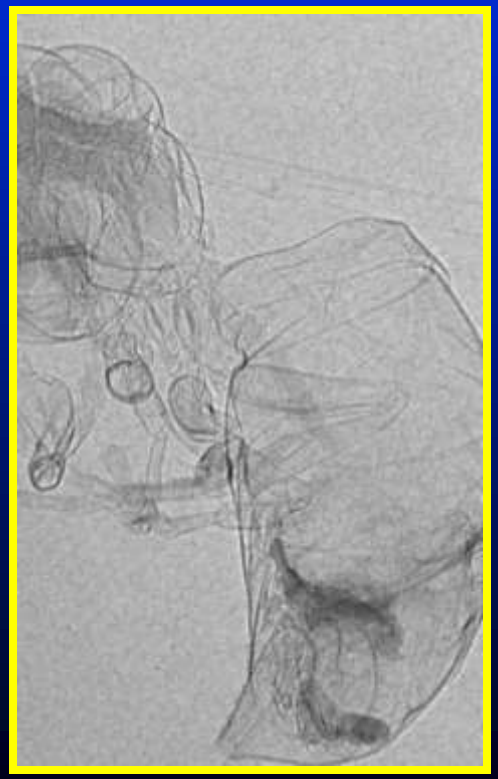

Fresnel Diffraction

R. Toth et al.,
Rev. Sci. Instrum. 76, 083701 (2005)

Imagerie par contraste de phase

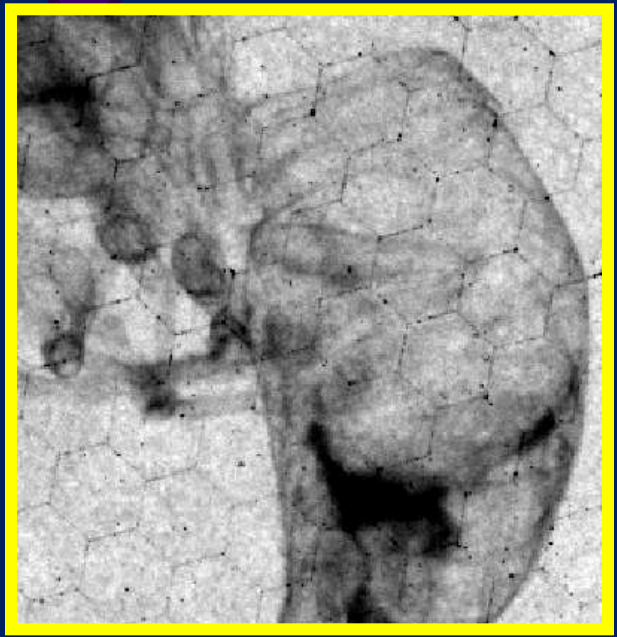

© INRS

- ***Meilleure résolution (5µm)***
- ***dose plus faible***

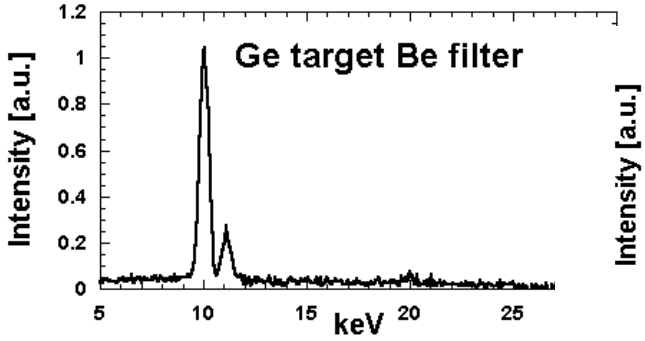

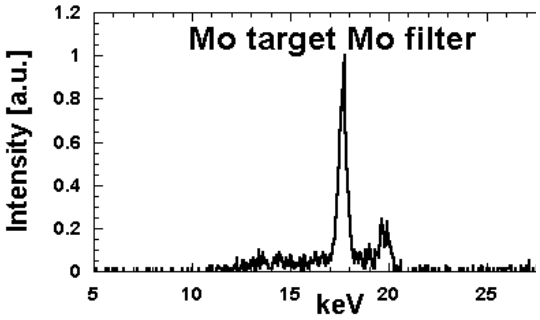

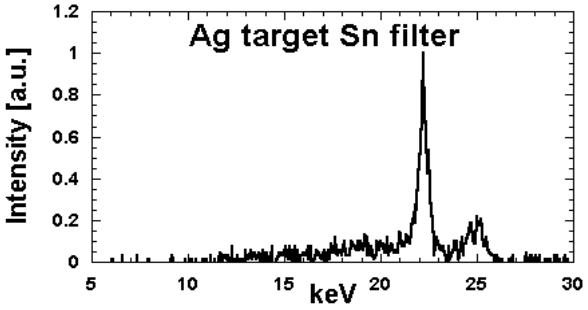

aux besoins de l'imagerie

R. Toth et al., Rev. Sci. Instru. 76, 083701 (2005)

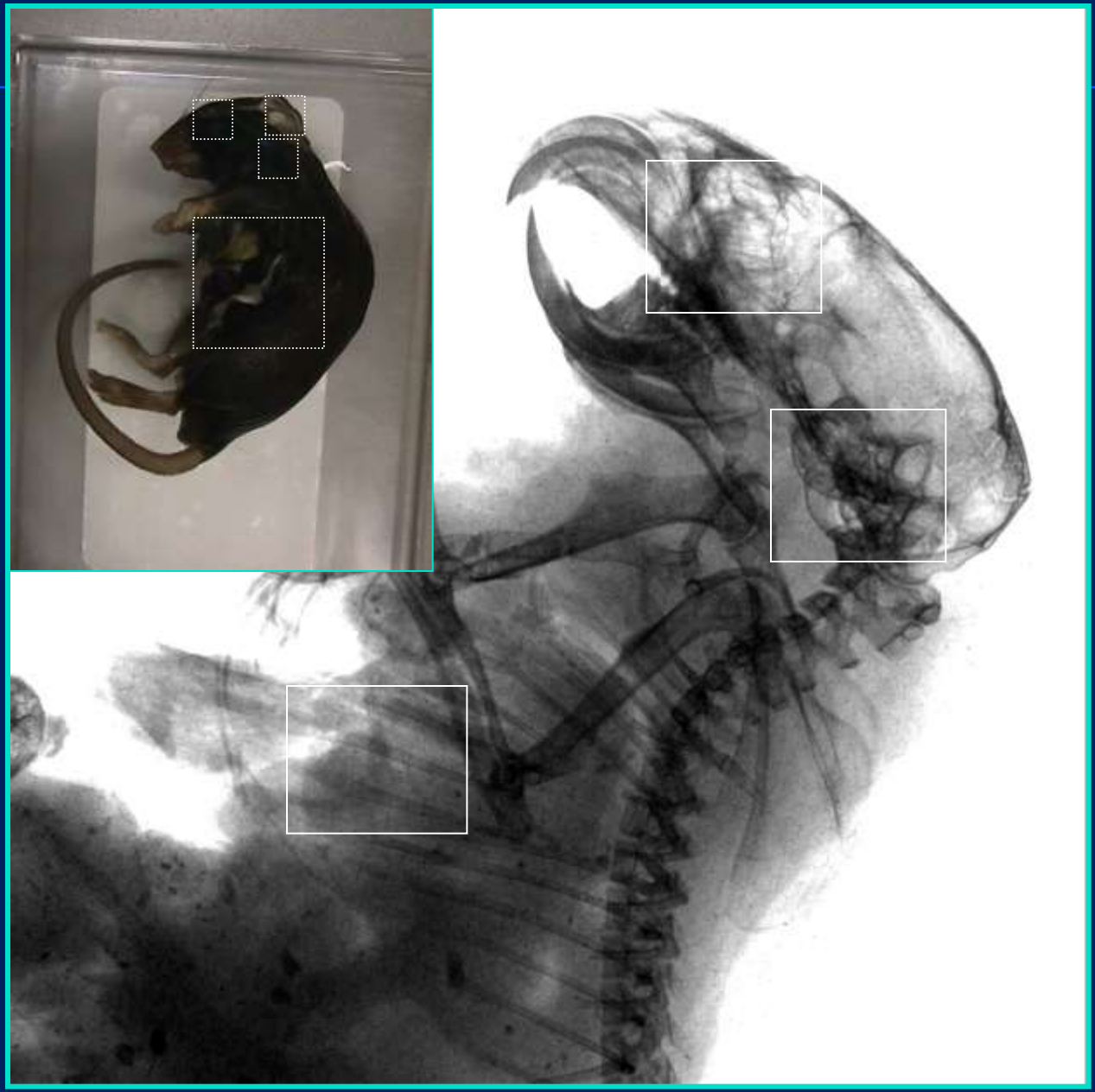

La référence mondiale : ALLS (INRS- Montréal) 200TW + Puissance moyenne 50W

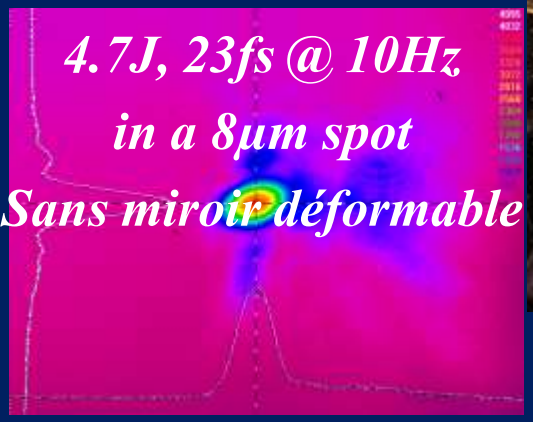

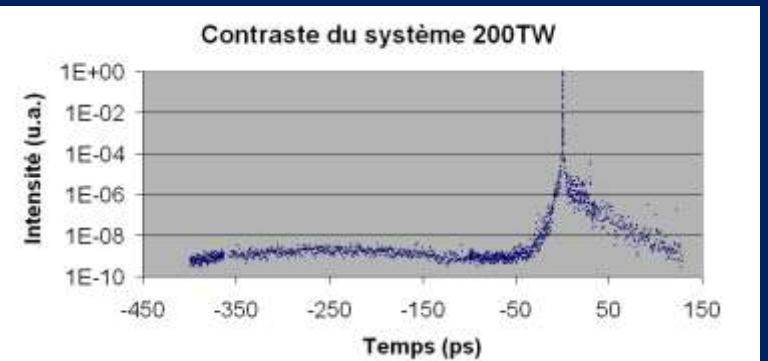

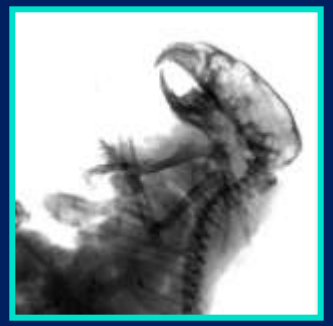

µCT

Scan duration avec 50W@10Hz (360 images)

2 min (mouse scan)

MeV Protons produced by laser

$I \geq 10^{19}$ W/cm^2

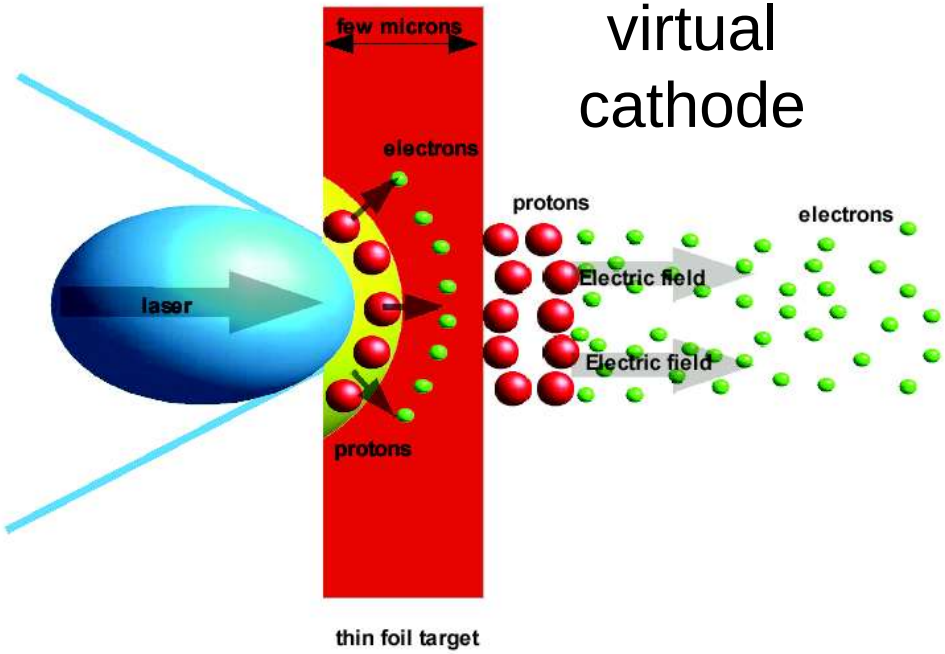

courtesy Prof. Dr. Oswald Willi, U. Düsseldorf

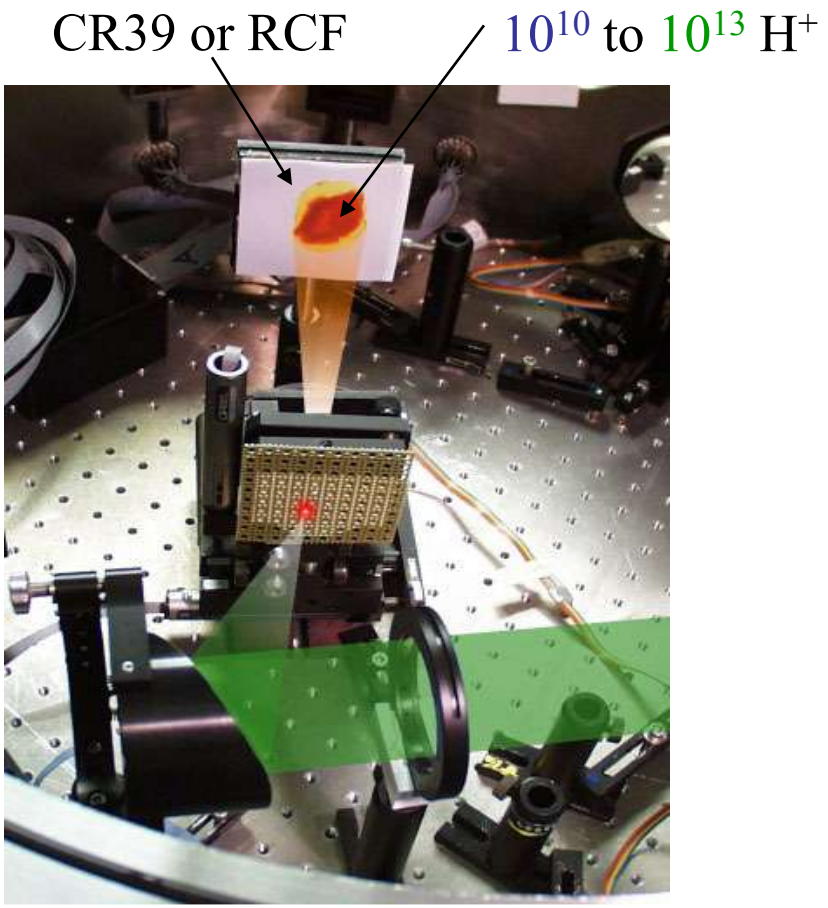

courtesy Prof. Don Umstadter, U. Nebraska-Lincoln

Target Normal Sheath Acceleration: hot electrons traversing target electrostatically accelerate impurity hydrogen ions on the rear surface

Protons de 10MeV (INRS)

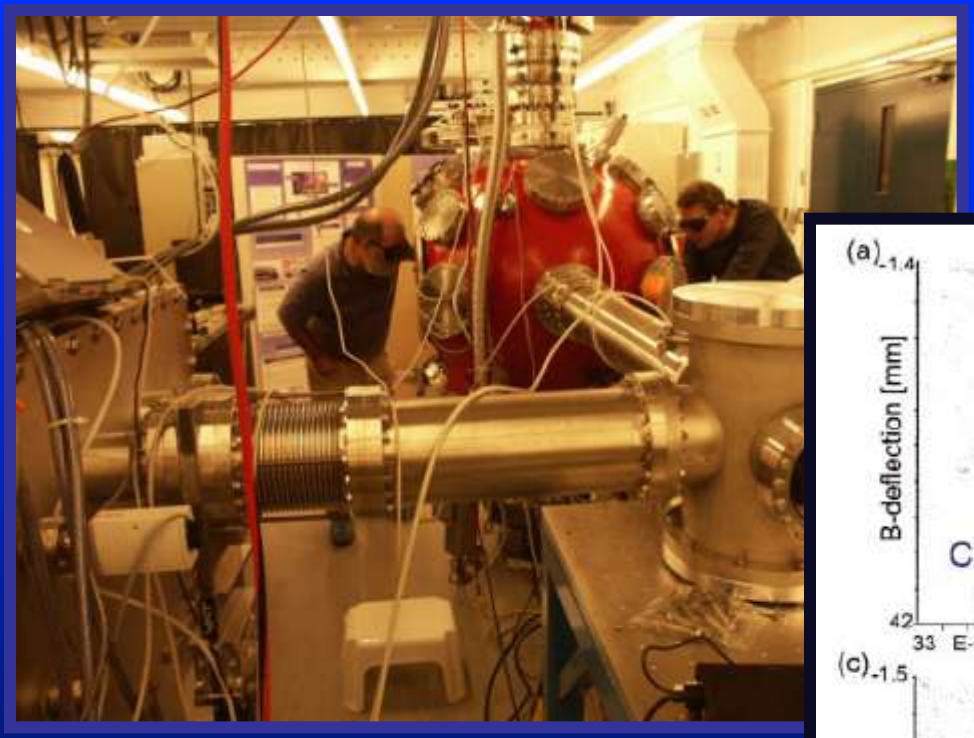

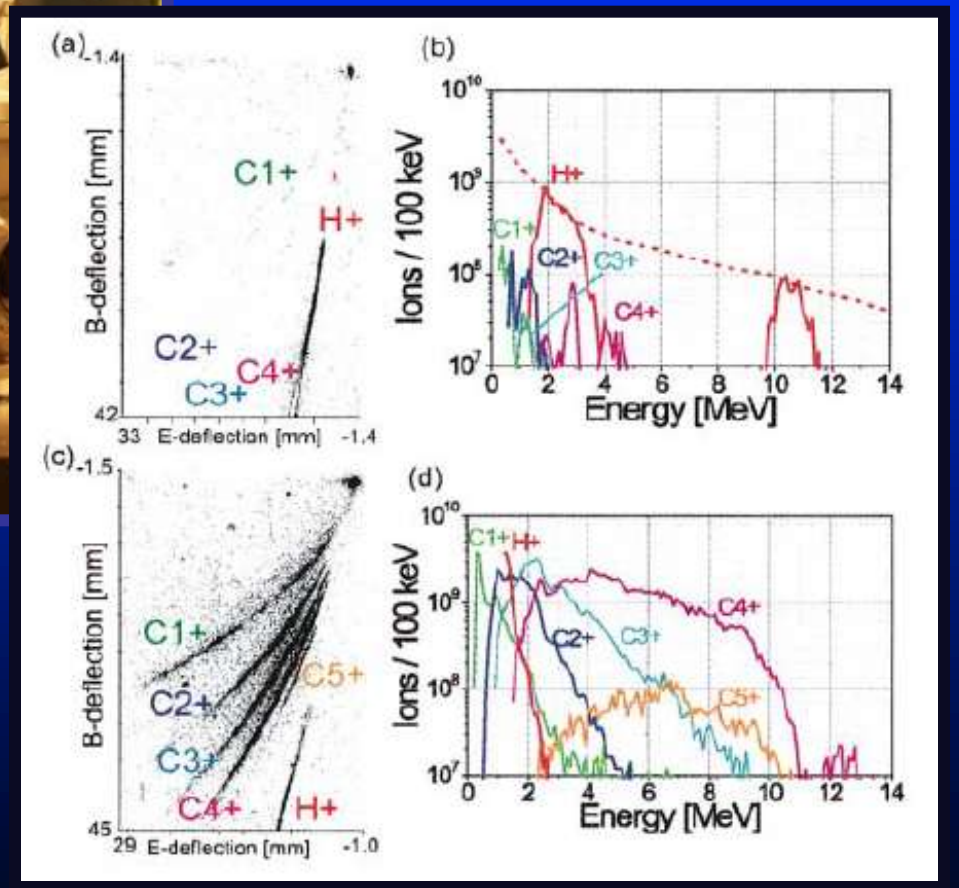

Protonthérapie par laser (projet SAPHIR)

Avantages des particules chargées ou hadrons (protons, ions) / Rayons X de la Radio-Thérapie

Le pic de Bragg!

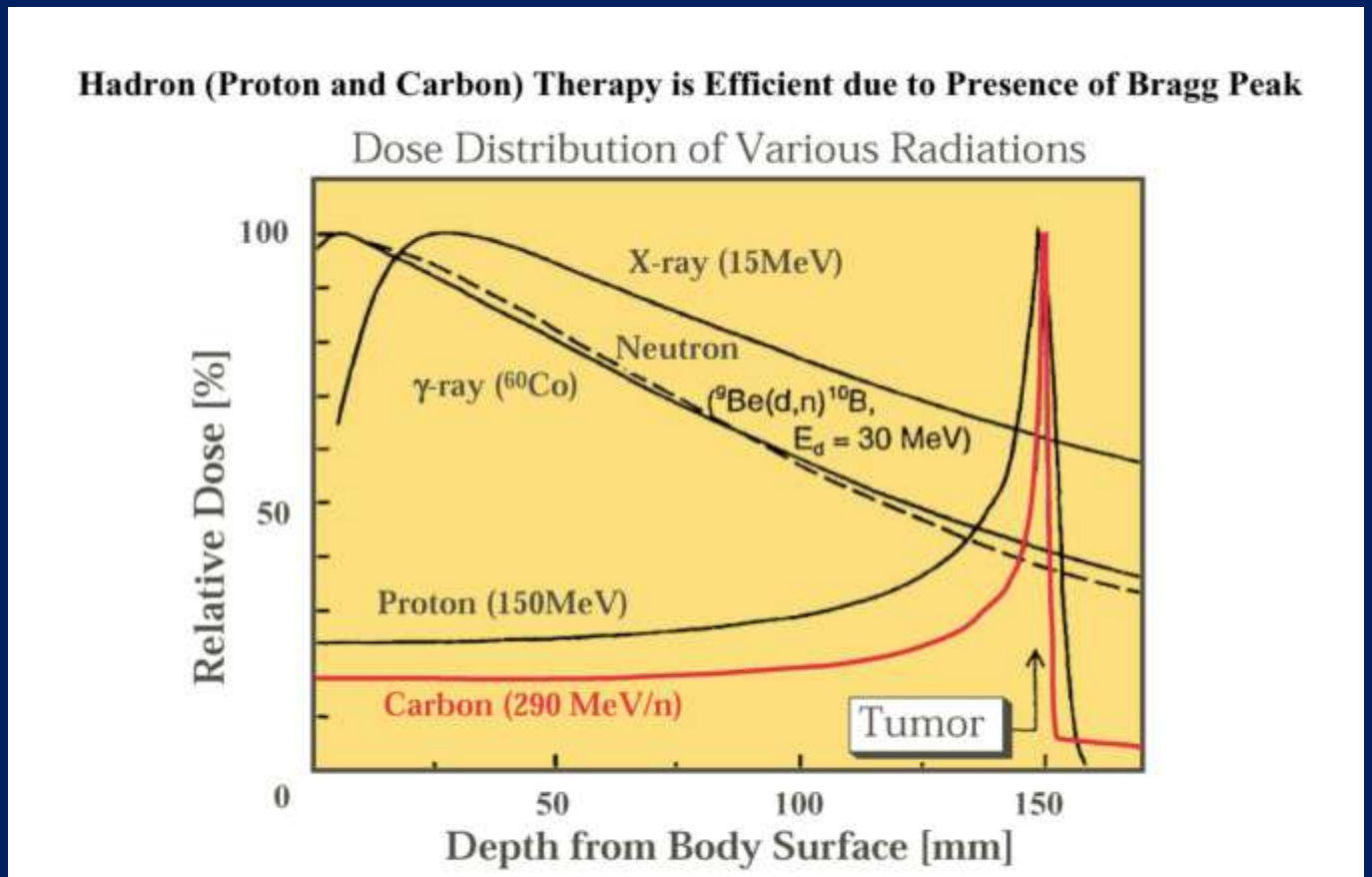

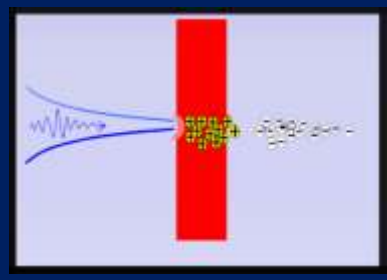

$\sim 10^{22}$ W/cm^2

La profondeur de pénétration dépend de l 'énergie incidente des protons:

la tumeur la plus superficielle = l 'œil 70 MeV
la plus profonde = la prostate 200 - 250 MeV

Exemple de dosimétrie prévisionnelle (photons vs protons)

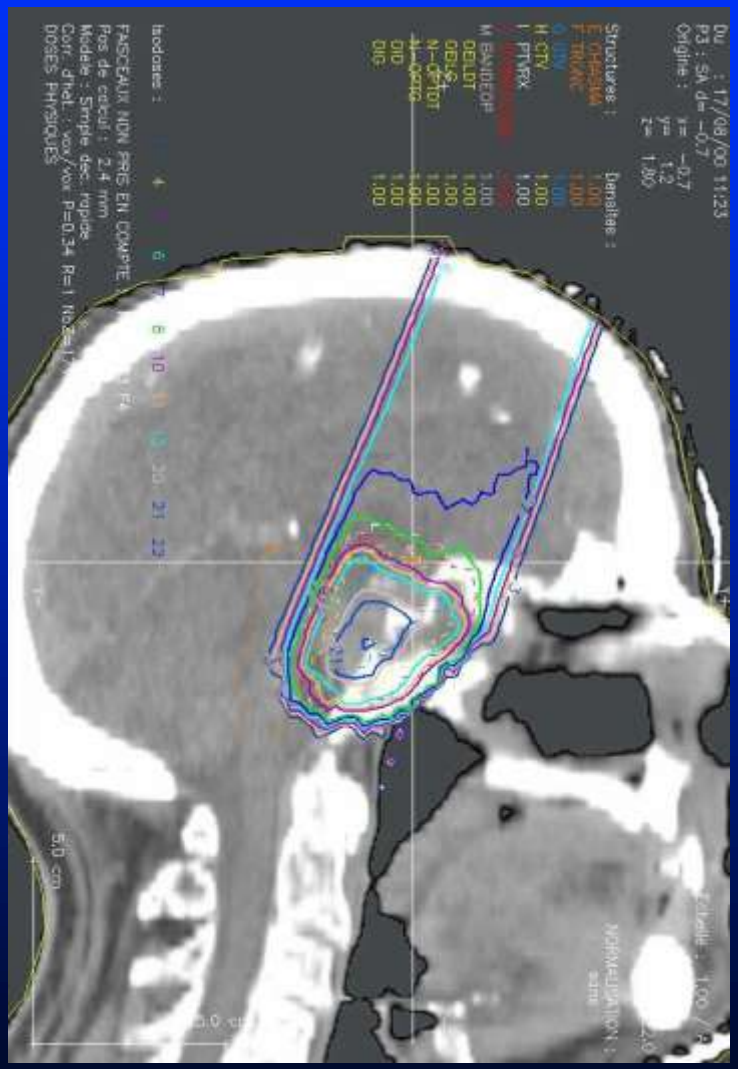

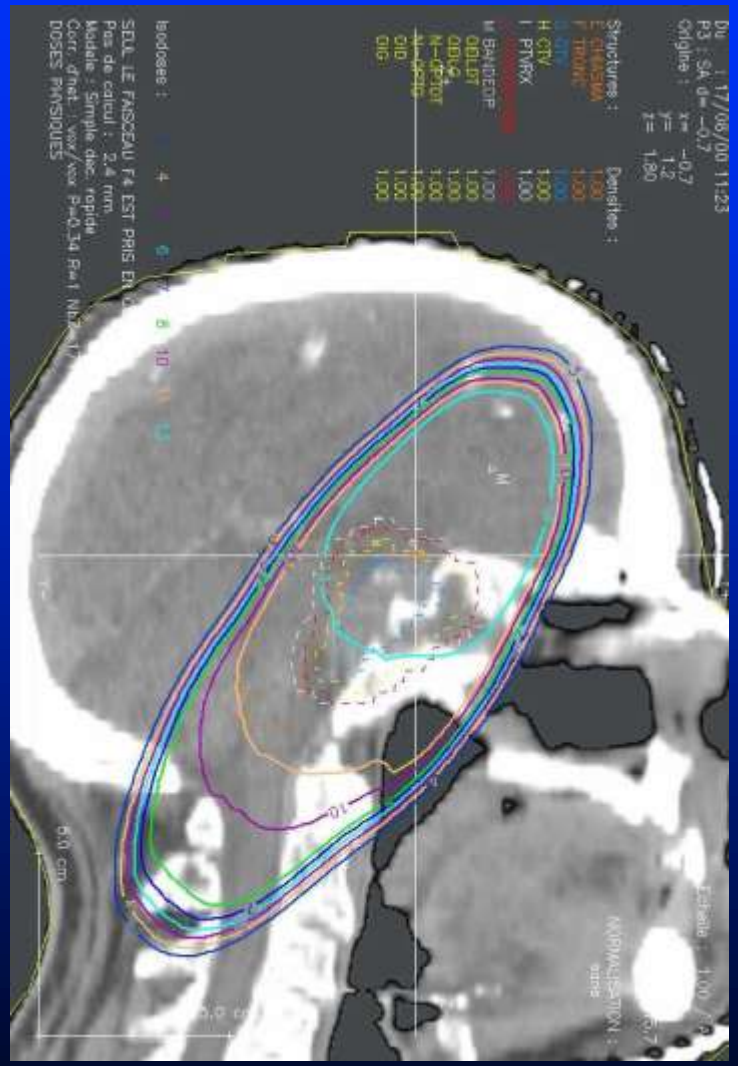

CPO

Les irradiations colatérales en radiothérapie et en protonthérapie

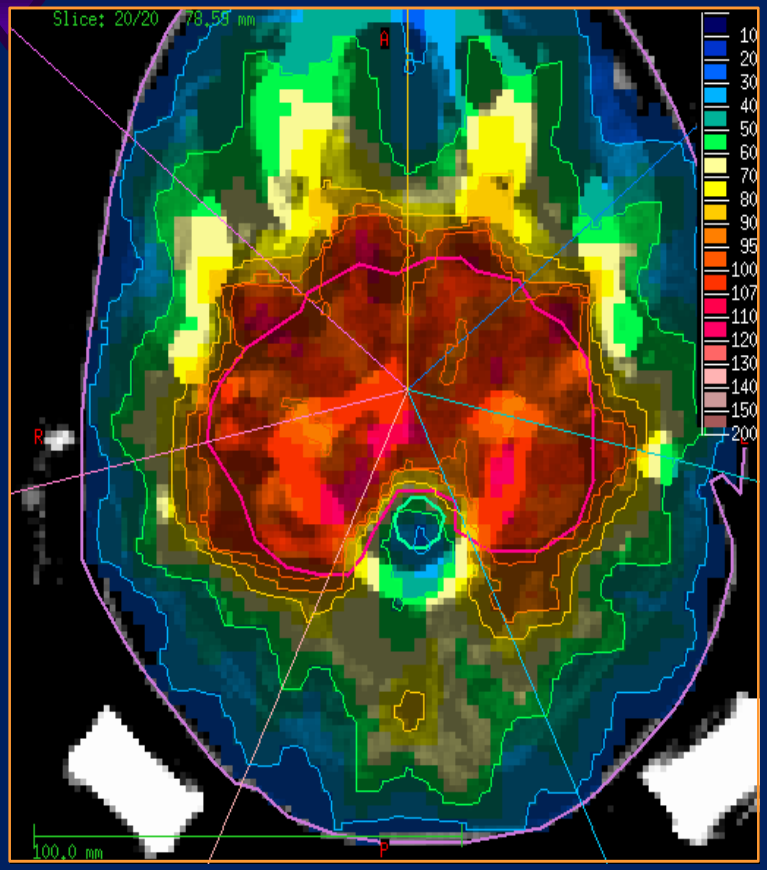

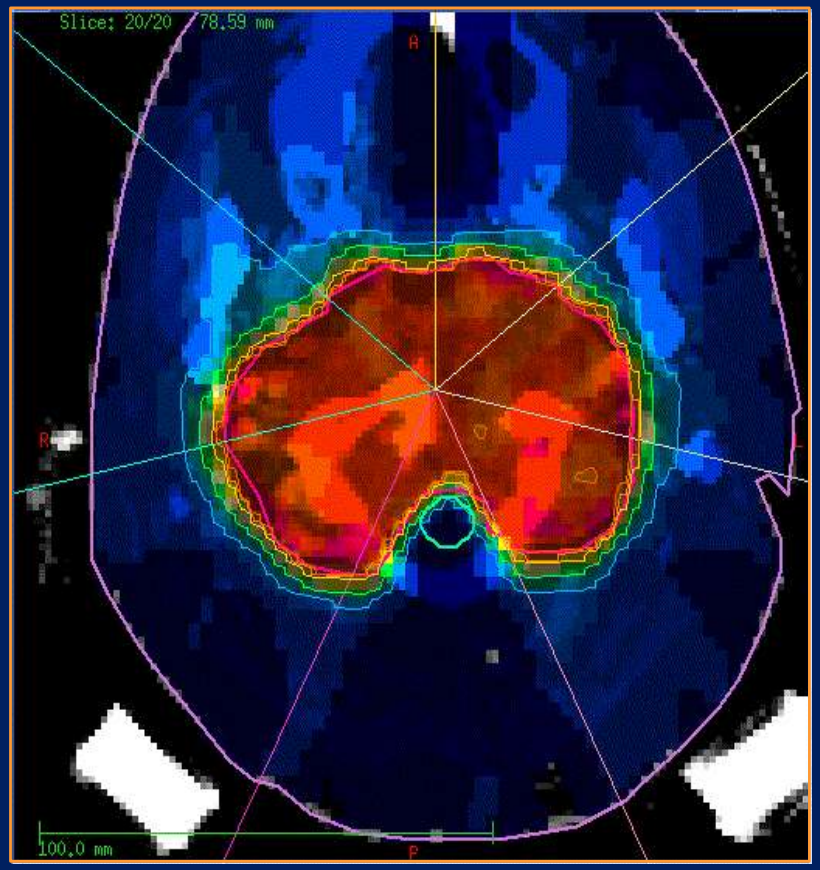

Comparaison de l'épargne de dose dans les tissus sains en protons (image de droite) par rapport aux photons (IMRT: *Intensity Modulated Radio-Therapy*, image de gauche)

***Avantage considérable* : pour le traitement de tumeurs localisées près d 'organes sensibles (œil, cerveau)**

Proton Therapy enables precise exposure of small tumors with minimal damage to surrounding healthy tissue ...

... but requires large, expensive facilities

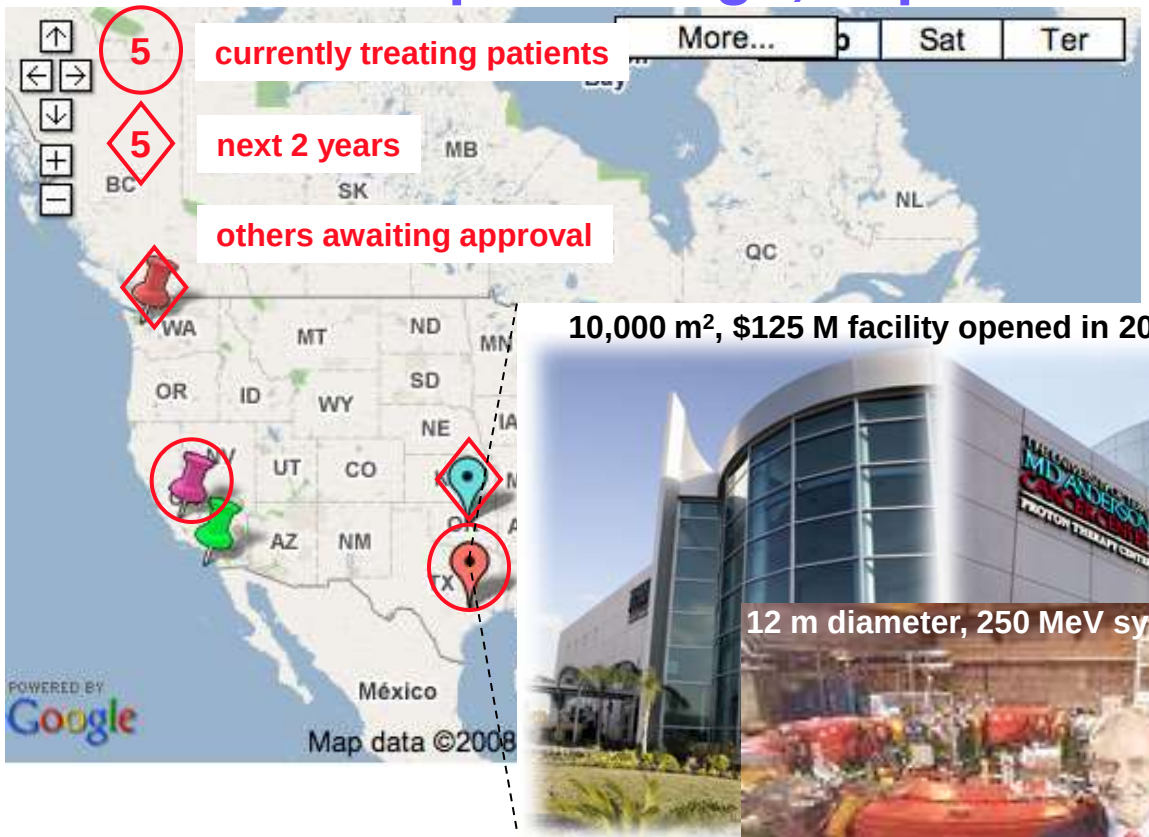

10,000 m², $125 M facility opened in 2006

"There are too few physicists in the world, and they are an incredibly important part of doing this... We have one of the largest physics departments in the world, with more than 50 medical physicists."

--- Dr. James D. Cox, head of Radiation Oncology at MD Anderson Cancer Center, Houston, Texas

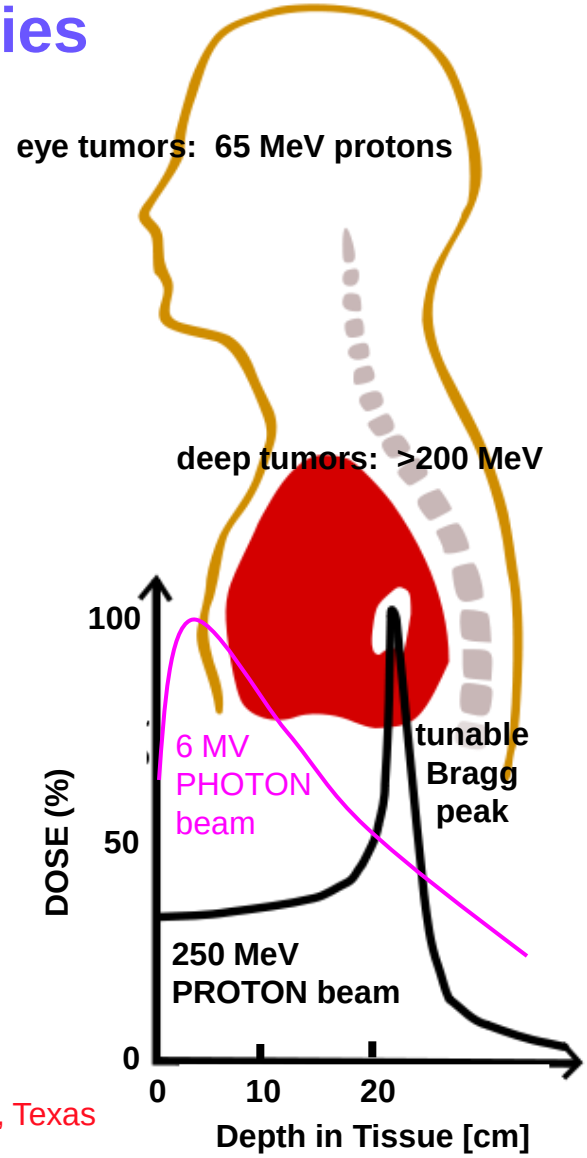

Laser proton therapy could be much smaller & cheaper:

Fourkal, *Med. Phys.* **29**, 2788 (2002)
Malka, *Med. Phys.* **31**, 1587 (2004)

On-site production of short-lived isotopes for medical imaging

Limitations to the widespread use of PET arise from the high costs of cyclotrons needed to produce the short-lived radionucleotides for PET scanning .... Few hospitals and universities are capable of maintaining such systems ... *- Wikipedia -*

Positron Emission Tomography

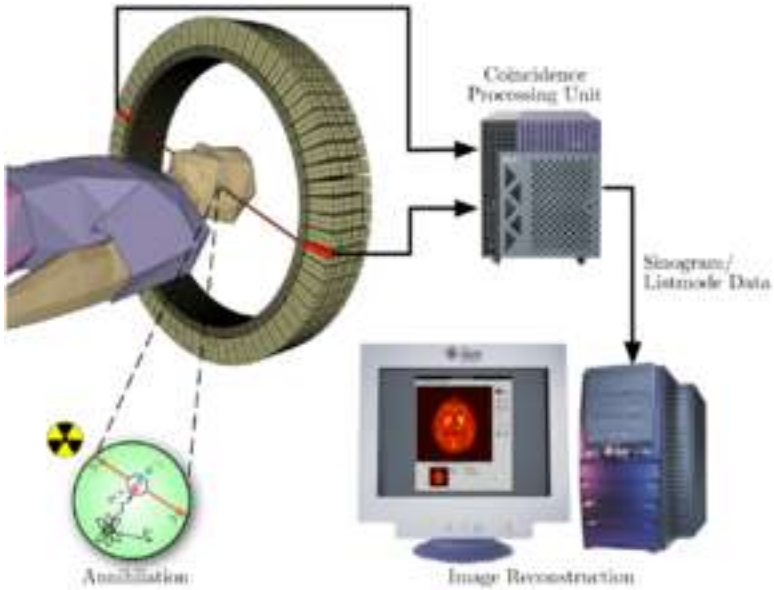

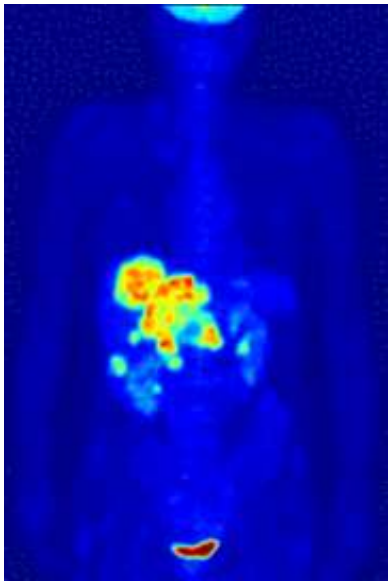

^{18}F PET scan of tumor

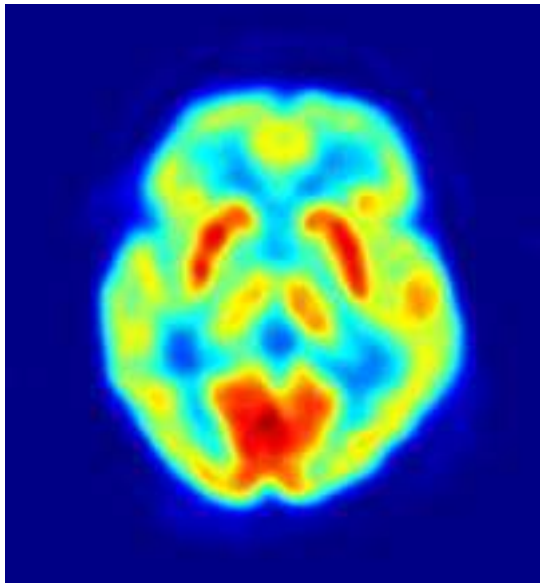

^{15}O PET scan of human brain

radiotracer	activation reaction	half-life	medical use
^{15}O	^{16}O $(\gamma,n)^{15}$O	2 minutes	neuro-imaging
^{11}C	^{12}C$(\gamma,n)^{11}$C	20 minutes	neuro-receptor-specific brain imaging
^{18}F	^{19}F$(\gamma,n)^{18}$F	110 minutes	clinical oncology

on-site production essential

Laser-generated quasi-mono-energetic electrons efficiently photo-activate materials of interest.

- **High Rep rate**
- **Low cost**
- **Compact**

Reed, "Efficient initiation of photonuclear reactions using quasi-monoenergetic electron beams from LWFA," *J. Appl. Phys.* **102**, 073103 (2007)

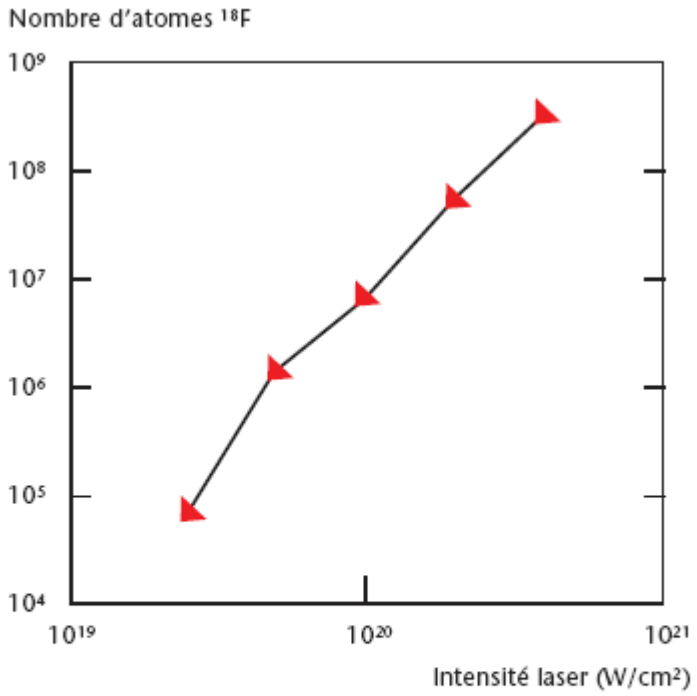

Figure 2
Calcul du nombre d'atomes de fluor 18 créés lors du ralentissement, dans une cible d'oxygène 18, d'un faisceau de protons accélérés par laser, à partir d'une cible de 2 µm d'épaisseur. Le nombre d'atomes d'isotope produits augmente proportionnellement à la puissance 2,7 de l'intensité laser sur cible, en accord qualitatif avec les mesures expérimentales.

[6] E. LEFEBVRE, E. D'HUMIÈRES, S. FRITZLER, V. MALKA, "Numerical simulation of isotope production for positron emission tomography with laser-accelerated ions", *Journal of Applied Physics*, **100**, 103308, p. 1-10 (2006).

Modèle animal

µCT +
contraste de phase
+ in vivo

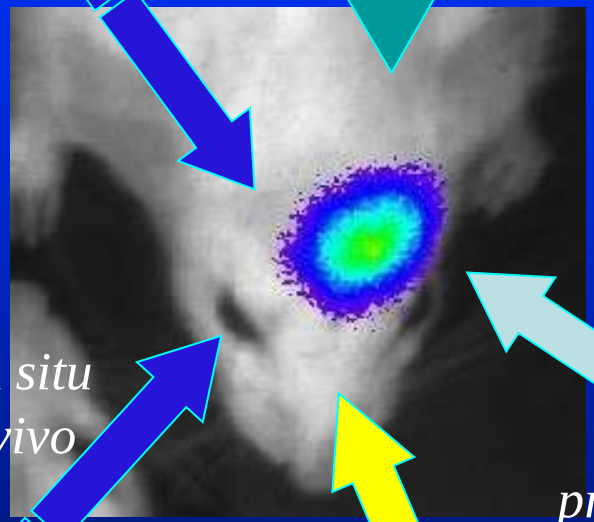

TEP in situ
+ in vivo

protons 50MeV

Radionuclide	Half-life
^{11}C	20.3 min
^{13}N	9.97 min
^{15}O	122 sec
^{18}F	109.8 min
^{62}Cu	9.74 min
^{64}Cu	12.7 hr
^{68}Ga	68.1 min
^{76}Br	16.1 hr
^{124}I	4.17 days

modèles de cancer

Comprendre le cancer
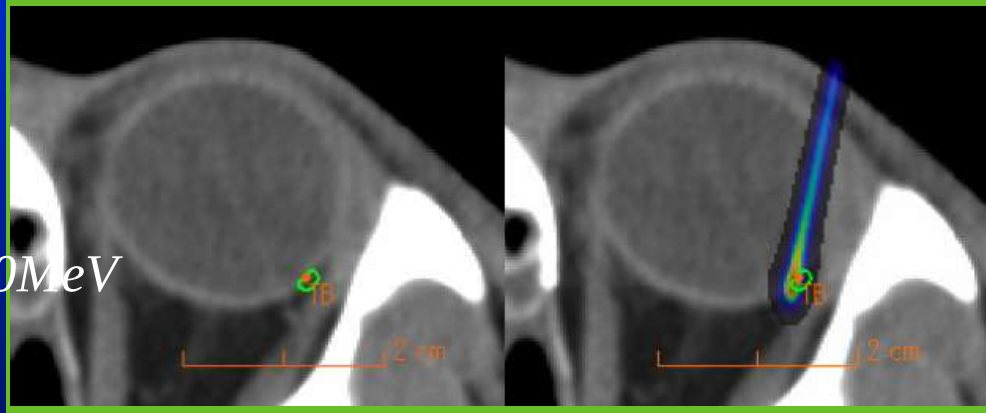
Préparer le traitement